QUANTUM MECHANICAL CALCULATION OF ETHYLENE HYDROGENATION ON NICKEL 111 SINGLE CRYSTAL SURFACE AND NICKEL NANOCLUSTERS

A THESIS SUBMITTED TO
THE GRADUATE SCHOOL OF NATURAL AND APPLIED SCIENCES
OF
MIDDLE EAST TECHNICAL UNIVERSITY

BY

ASLI SAYAR

IN PARTIAL FULFILLMENT OF THE REQUIREMENTS
FOR
THE DEGREE OF MASTER OF SCIENCE
IN
CHEMICAL ENGINEERING

SEPTEMBER 2005

Approval of the Graduate School of Natural and Applied Sciences

Prof. Dr. Canan ÖZGEN
Director

I certify that this thesis satisfies all the requirements as a thesis for the degree of Master of Science

Prof. Dr. Nurcan BAÇ
Head of Department

This is to certify that we have read this thesis and that in our opinion it is fully adequate, in scope and quality, as a thesis for the degree of Master of Science

Prof. Dr. Işık Önal
Supervisor

Examining Committee Members

Prof. Dr. İnci EROĞLU	(METU, CHE)	
Prof. Dr. Işık ÖNAL	(METU, CHE)	
Prof. Dr. Suzan KINCAL	(METU, CHE)	
Prof. Dr. Saim ÖZKAR	(METU, CHEM)	
Prof. Dr. Şinasi ELLİALTIOĞLU	(METU, PHYS)	

I hereby declare that all information in this document has been obtained and presented in accordance with academic rules and ethical conduct. I also declare that, as required by these rules and conduct, I have fully cited and referenced all material and results that are not original to this work.

Name, Last name: ASLI SAYAR

Signature:

ABSTRACT

QUANTUM MECHANICAL CALCULATION OF ETHYLENE HYDROGENATION ON NICKEL 111 SINGLE CRYSTAL SURFACE AND NICKEL NANOCLUSTERS

Sayar, Aslı

M.S., Department of Chemical Engineering

Supervisor: Prof. Dr. Işık Önal

September 2005, 170 pages

Ethylene hydrogenation on Ni(111); equilibrium geometry calculations for Ni_2 dimer, Ni_{13} and Ni_{55} nanoclusters; and ethylene adsorption on Ni(100), Ni(111), Ni_2, and Ni_{13} were studied quantum mechanically by means of energetic and kinetic differences.

Ethylene hydrogenation on Ni(111) was simulated by use of DFT/B3LYP/6-31G** formalism. The reaction mechanism was mainly composed of three elementary steps. Firstly, ethylene adsorption on bare Ni(111) surface was performed. Second step and third step were the formation of ethane from adsorbed ethylene by use of two types of hydrogen atom, bulk and surface. During the hydrogenation reaction of ethylene on Ni(111), bulk hydrogen atom, representing for hydrogen atoms emerging from the bulk of Ni metal, was determined to be rather reactive than surface hydrogen atom, as suggested by experimental findings.

Small Ni clusters, Ni_2 and Ni_{13}, were investigated by means of DFT/B3LYP/modified-6-31G**. Equilibrium geometry calculations resulted in Ni_2 binding energy of 1.078eV/atom, showing good agreement with experimental value. Ni_{13} was found to have a structure of icosahedral, suggested experimentally, and binding energy of 2.70eV/atom. Ni_{55} was, also, studied by semi-empirical PM3 formalism, resulting in expected icosahedral structure.

Finally, DFT/B3LYP/6-31G** investigation of ethylene adsorption was performed on Ni(111), Ni(100) and Ni_{13} surfaces which were selected according to their nickel atom coordination numbers of 9, 8 and 6, respectively. Comparison of adsorption energies of -18.00kcal/mol, -31.4kcal/mol and -43.42kcal/mol, respectively, indicated that the change in energies for ethylene adsorption on different nickel surfaces was directly proportional to coordination number of the nickel atoms constructing the surfaces.

KEYWORDS: DFT, ethylene hydrogenation, Ni_2, Ni_{13}, Ni_{55}, Ni(111)

ÖZ

NİKEL 111 YÜZEYİ ÜZERİNDE ETİLEN HİDROJENASYONUNUN VE NİKEL NANOKÜMELERİNİN KUANTUM MEKANİKSEL OLARAK İNCELENMESİ

Sayar, Aslı

Yüksek Lisans, Kimya Mühendisliği Bölümü

Tez Yöneticisi: Prof. Dr. Işık Önal

Eylül 2005, 170 sayfa

Etilenin Ni(111) yüzeyi üzerine hidrojenasyonu; Ni_2 molekülünün, Ni_{13} ve Ni_{55} nanokümelerinin denge geometrisi hesapları ile etilenin Ni(100), Ni(111), Ni_2 ve Ni_{13} üzerine adsorpsiyonu, enerjitik ve kinetik farklar açısından kuantum mekaniksel olarak incelenmiştir.

Ni(111) yüzeyi üzerinde gerçekleşen etilen hidrojenasyonu DFT/B3LYP/ 6-31G** metodu kullanılarak araştırılmıştır. Bu hidrojenasyon asıl olarak üç adımdan oluşmaktadır. Birinci adımda, etilenin boş Ni(111) yüzeyine adsorpsiyonu gerçekleştirilmiştir. İkinci ve üçüncü adımlar, iki tip hidrojen atomu kullanarak. adsorbe olmuş etilenden etan oluşturulmasıdır. İlki, yığın Ni metali içinden yüzeye çıkan hidrojen atomlarını tanımlayan yığın hidrojeni ve diğeri de yüzey hidrojenidir. Yüzey etileninin, daha sonra yüzey etil grubunun, yüzey hidrojen atomlarıyla reaksiyonları, bu yüzey moleküllerinin yığın hidrojen atomlarıyla reaksiyonlarından çok daha fazla bir aktivasyon bariyerine ihtiyaç duymaktadır. Bu durumda, etilen hidrojenasyonu sırasında, yığın hidrojen

atomlarının yüzey hidrojenlerinden çok daha aktif oldukları teorik olarak bulunmuştur.

DFT/B3LYP/(modifiye edilmiş)6-31G** metodu ile küçük nikel kümeleri olan Ni_2 ve Ni_{13} üzerine de çalışılmıştır. Denge geometrisi hesabıyla bulunan nikel molekülünün 1,078eV/atom olan bağlanma enerjisi deneysel çalışmalarla uyum içindedir. Ni_{13} nanokümesinin geometrisinin deneysel olarak da tespit edilmiş olan şemsiye modeli "icosahedral" olduğu ve bağlanma enerjisinin 2,70eV/atom olduğu bulunmuştur. Yarı-empirik metodlarla incelenen Ni_{55} kümesinde denge geometrisi deneysel sonuçlarda olduğu gibi "icosahedral" olmuştur.

Son olarak, sırasıyla kendi yüzey atomlarının koordinasyon sayıları olan 9, 8 ve 6'ya göre seçilen Ni(111), Ni(100) ve Ni_{13} yüzeyleri üzerinde etilen adsorpsiyonu gerçekleştirilmiştir. DFT/B3LYP/6-31G** metoduyla hesaplanan, sırasıyla, -18.00kcal/mol, -31.4kcal/mol ve -43.42kcal/mol olan adsorpsiyon enerjilerinin kıyaslanması sonucunda, farklı yüzeylerde gerçekleşen etilen adsorpsiyonun enerjisindeki değişimin yüzeydeki nikel atomlarının koordinasyon sayılarıyla doğru orantılı olduğu tespit edilmiştir.

Anahtar kelimeler: DFT, etilen hidrojenasyonu, Ni_2, Ni_{13}, Ni_{55}, Ni(111)

ACKNOWLEDGEMENTS

I would like to express my sincere appreciation to my supervisor Prof. Dr. Işık Önal for his guidance, valuable discussions and comments through out this study.

I wish to thank my family for their greatest support and encouragement.

I would like to thank to Mustafa Öztürk for his extreme patience and his continuous moral support.

Special thanks to Sezen Soyer for her greatest encouragement and her valuable friendship.

I also want to extend my thanks to all my friends, especially, Alper Uzun, Deniz Gürhan, Hakan Olcay and Hande Kaya for motivating and supporting me during this study.

TABLE OF CONTENTS

LIST OF TABLES

LIST OF FIGURES

CHAPTER 1

INTRODUCTION

1.1 Nanotechnology

During the past ten to fifteen years, powerful, new capabilities for manipulating, assembling, and characterizing matter at extremely small scales (upto 100nm) have been developed, thereby opening the broad new field of nanoscience. Nanotechnology is the application of nanoscience to the creation and utilization of new materials, devices, and systems through the control of matter at the level of supramolecular structures, molecules, and atoms. The ability to work at the ultra-small dimensions of individual objects is expected to result in novel electronic, chemical, physical, and biological properties and phenomena.

Many scientists and technologists believe that nanoscience will provide the basis for an industrial revolution in the 21st century that will have an impact on the health, wealth, and security of the world's people as significant as the combined influence of antibiotics, integrated circuits, and human made polymers. Already, impressive examples demonstrate the potential impact of nanotechnology:

- Nanostructured catalysts
- Ink jet systems (nanoparticle pigments)
- Carbon nanotubes been shown to be ten times as strong as steel with one sixth of the weight and to exhibit semiconducting properties similar to silicon on the nanometer scale (reinforced materials, probes, connectors/transistors)

- Nanoparticle-reinforced polymers, with lightweight and strong mechanical strength, which improve fuel efficiencies and increase safety for transportation vehicles
- Molecular switches that could potentially improve computer storage capacity by a million times
- Chemical and bio-detectors
- Nanostructured silicates and polymers which are used as effective contaminant scavengers for a cleaner environment.
- New drugs made of nanoparticle powder have nearly ten times the bioavailability and faster response times compared with conventional drugs.
- Thermal barriers
- Patterning of nanoporous surface texturing at the interface between medical implants and their biological substrates has provided a powerful new way to encourage tissue integration.
- Giant magnetoresistance in nanocrystalline materials - Information recording layers or hard disk heads -
- Systems on a chip (Ex: NASA thin film batteries, nanopixel sensors for low power consumption)
- New generation of lasers -high hardness cutting tools-
- Nanolayers with selective optical barriers; filters; cosmetics; infrared low observable; special windows; Hard coatings
- Dispersions with optoelectronic properties, high reactivity
- Chemical-mechanical polishing with nanoparticle slurries

As a result, nanotechnology will be a strategic branch of science and engineering for the 21st century and will fundamentally restructure the technologies currently used in manufacturing, medicine, defense, energy production, environmental management, transportation, communication, computation, and education. (OMNI, 2004 and Roco et al., 2005)

1.2 Nanotechnology in Catalysis

The catalysis is the central field of nanoscience and nanotechnology. There are two types of catalysts that carry out chemical reactions with high rates and selectivity. Enzymes are nature's catalysts, and many of them are composed of inorganic nanoclusters surrounded by high-molecular-weight proteins. These catalysts help the human body to function and are responsible for the growth of plants. They usually operate at room temperature and in aqueous solution. Synthetic catalysts, either heterogeneous or homogeneous, are often metal nanoclusters that are used in the chemical technologies to carry out reactions with high turnover and selectivity. (Grunes et al., 2003)

Especially, monodisperse metal nanoclusters with diameters smaller than 10 nm in general exhibit unique physical and chemical properties as compared to their counterparts that are composed of particles. Studies of size-dependent properties of small metal clusters are important for developing fundamental understanding of the transition from atomic to bulk properties. Nanoparticles have been used for years in the field of catalysis. The basic reason for producing nanoparticle-based catalysts was to improve the active surface to the total metal volume ratio. It also appeared that the catalytic properties changed qualitatively with change of the metal particle size. This change was not surprising in retrospect since electronic properties are strongly dependent on particle size as they approach the atomic scale.

Both enzyme and synthetic catalysts are usually nanoclusters in size and thus the fields of catalysis science and technologies are also nanoscience and nanotechnologies. The evolution of the field of catalysis is strongly coupled to the development of nanoscience and nanotechnology at the present. (Grunes et al, 2003)

1.3 Review of Computational Chemistry

Chemistry is the science dealing with construction, transformation and properties of molecules. Theoretical chemistry is the subfield where mathematical methods are combined with fundamental laws of physics to study processes of chemical relevance (Jensen, 1998). As a science becomes more exact, it inevitably moves toward more precise mathematical descriptions (Clark, 1985).

Chemistry traditionally has been an experimental science-no molecule could be investigated until it had been synthesized or was found in nature. In contrast, computational chemistry requires no preparations, no separation techniques, and no spectrometers or any physical measurements; it does not even require a chemical laboratory. Through the combined use of ever faster computers and increasingly sophisticated programs, a scientific revolution is taking place. It is now possible, and in fact quite easy, to study unknown molecules, reactive intermediates, reaction transition states, and even species that cannot exist by computational means. Many chemical facts can now be obtained more accurately by computer than by experiment. Experience demonstrates that results obtained by adequate calculations can be trusted, and need not always require experimental verification. (Clark, 1985)

Molecules are traditionally considered as being composed of atoms or in a more general sense, a collection of charged particles, positive nuclei and negative

electrons. The only important physical force for chemical phenomena is the coulombic interaction between these charged particles. Given a set of nuclei and electrons, theoretical chemistry can attempt to calculate things such as: (Jensen, 1998)

1. The geometrical arrangements of the nuclei that correspond to stable molecules.

2. Their relative energies (heat of reaction, heat of adsorption etc)

3. Their physical properties (dipole moment, polarizability, NMR coupling constants etc.)

4. Molecular structures (bond lengths, bond angles etc.)

There are two modeling techniques of particular utility. The first is *molecular mechanics (force field)*, which utilizes empirical force fields to model the forces acting between nuclei and the second is *quantum mechanical* calculations.

Experiments are rarely done on single molecules; rather they are performed on macroscopic samples with perhaps 10^{23} molecules. The link between the properties of a single molecule or a small collection of molecules and the macroscopic observable is statistical mechanics. Briefly, macroscopic properties, such as temperature, heat capacities, entropies etc., are the net effect of a very large number of molecules having a certain distribution of energies. If all the possible energy states can be determined for an individual molecule or a small collection of molecules, statistical mechanics can be used for calculating macroscopic properties. (Jensen, 1998)

Computational quantum chemistry is leading to new, theoretically based methods for the prediction of thermodynamic properties and phase behavior of interest to engineers. Quantum chemistry calculations, computer simulation and theory have now developed to the point that they are useful tools for predicting

thermodynamic properties and phase behavior of some substances to an accuracy useful in engineering calculations. Quantum mechanics leads to obtaining the intermolecular potential energy surface for the interaction between a pair of molecules and using this potential to calculate second virial coefficients and, in simulation, to determine vapor-liquid phase behavior. (Sandler, 2003)

Klauda et al., 2004 claimed that molecular simulations have been used to predict a broad range of physical and thermodynamic properties, including protein-folding dynamics, gas transport properties in nanostructures and phase behavior. Quantum mechanics can be used to develop the intermolecular potentials necessary to accurately calculate properties from simulation.

1.4 Quantum Mechanical Applications to Catalysis

Understanding chemisorption is the first step for the rationalization of reactions on surfaces. Most of the reactions on surfaces take place between adsorbed species (Langmuir-Hinshelwood mechanism). The heats of reaction and the activation energies are modified by the adsorption. However, in another class of reactions (Eley-Rideal mechanism) one reactant remains in the gas phase and interacts with adsorbed species. As the catalyst is supposed to modify the reactivity, one would like to find active substrates that deeply perturb the adsorbate. When adsorbates are strongly bound to the surface, they are distorted and they may cleave. However, large binding energies are not always the clue for surface reactivity. Intermediates should not be too stabilized to be able to react. The products of the reaction should be able to desorb and regenerate vacant sites. Already many theoretical investigations of surface mechanisms have been performed. A better understanding of chemisorption however will allow control of the different steps of catalytic activity. (Minot and Markovits, 1998)

1.5 Quantum Mechanical Applications to Nanotechnology

The major research objectives in molecular nanotechnology are the design, modeling, and fabrication of molecular machines and molecular devices. While the ultimate objective must clearly be economical fabrication, present capabilities preclude the manufacture of any but the most rudimentary molecular structures. The design and modeling of molecular machines is, however, quite feasible with present technology. More to the point, such modeling is a cheap and easy way to explore the truly wide range of molecular machines that are possible, allowing the rapid evaluation and elimination of obvious dead ends and the retention and more intensive analysis of more promising designs. While it can be debated exactly how long it will take to develop a broadly based molecular manufacturing capability, it is clear that the right computational support will substantially reduce the development time. (Merkle, 1991)

Chemical calculations that can predict the structures, energies and other properties of known or unknown molecules have often been heralded as important new tools in chemical research. There is, however, a fundamental difference between calculations, which are quantum mechanical and molecular mechanics (force field), and experimental techniques: calculations can just as easily be performed for compounds that have never been made, or even cannot exist under real conditions. (Clark, 1985) This opportunity really provides to make nanotechnological researches without using any experiments at the first stage. That is, with appropriate molecular CAD software, molecular modeling software (including available computational chemistry packages, e.g., molecular mechanics, semi-empirical and ab initio programs) and related tools, one can plan the development of molecular manufacturing systems on a computer. (Merkle, 1991)

Today, the most acceptable computational methods are quantum mechanical methods especially density functional theory (DFT) and *ab initio* calculations.

While empirical force fields are sufficiently accurate to model the behavior of chemically stable stiff structures interacting with other chemically stable stiff structures, they do not provide sufficient accuracy to deal with chemical transitions. Thus, if someone wishes to model the manufacture of a molecular part then he must use higher order DFT or ab initio techniques. These techniques impose severe constraints on the number of atoms that can be modeled (perhaps one or two dozen heavy atoms, depending on the hardware, software, and specific type of modeling being attempted), but can provide an accuracy sufficient to analyze the chemical reactions that must necessarily take place during the synthesis of large, atomically precise structures. More generally, higher order quantum mechanical techniques are sufficient to analyze the addition or removal of a small number of atoms from a specific site on a work piece. (Merkle, 1991)

Molecular dynamics by means of computational experiments can literally provide information about the position of each individual atom over time, information which would usually be inaccessible in a physical experiment. Of course, the major advantage of computational experiments over physical experiments in the current context is the simple fact that physical experiments aren't possible for molecular machines that researchers can not make with today's technology. By using computational models derived from the wealth of experimental data that is available today, description of the behavior of proposed systems planned to be built in the future can be made. If one deliberately designs systems that are sufficiently robust they will work regardless of the small errors that must be incurred in the modeling process. Systems which will not be able to be built for some years can be designed today, and yet one still has reasonable confidence that they will work. By fully utilizing the experience that has been developed in the rapid design and development of complex systems, the development time for molecular manufacturing systems can be dramatically reduced. It is possible to debate how long it will be before an achievement of a

robust molecular manufacturing capability. However, it is very clear that researchers will get there sooner if they develop and make intelligent use of molecular design tools and computational models. These will provide to design and to check the blueprints for the new molecular manufacturing technologies seen on the horizon, and to chart a more rapid and more certain path to their development. (Merkle, 1991)

1.6 Scope of Thesis

As mentioned in the previous parts, nanotechnology in catalysis field in conjunction with quantum chemistry becomes important with today's computer technology. Crystal structural materials at the nanoscale, generally the diameter smaller than 100 Å, show explicitly new characteristics comparing to the materials made by micro and macro scale particles. Hence, nanosized materials bring innovations in catalysis field. That is, nanoclusters have potentials of being catalysts which show higher activity and selectivity than the bulk catalyst (Pool, 1990). The statement could be explained by the high percentage of catalyst atoms being on the nanocluster surface and by the different orientation of the nanocluster atoms from those of mass.

Ethylene hydrogenation on Ni catalyst has been chosen as a model reaction to study the effect on the reaction mechanism of important single crystal surfaces such as Ni(111) and that of small Ni clusters such as, Ni_{13} and Ni_{55}. It can be expressed that ethylene hydrogenation became a basis for hydrocarbon hydrogenation kinetics on transition metals (Zaera, 1990) during the last decades. Ethylene, C_2H_4, which is the smallest molecule of alkenes group, can undergo hydrogenation, dehydrogenation, and H-D exchange reactions. Its simplicity and reactivity have served as a model to interpret the surface chemistry of hydrocarbons, especially, on transition metals. Hence, nickel, one

of the major transition metal catalyst using for ethylene hydrogenation, was chosen. Its 111 plane single crystal surface was preferred since there have been smart experimental studies about ethylene hydrogenation on that surface and to the best of our knowledge, there are no theoretical investigations on this particular ethylene hydrogenation mechanism. In addition, this mechanism involves a radical intermediate, i.e., ethyl radical, which could not be observed by experimental methods. By the help of quantum mechanics, the most probable elementary step for the conversion of ethyl radical to ethane could be found.

Overall, the ultimate scopes of this thesis have been to make a quantum mechanical investigation of ethylene hydrogenation reaction over Ni(111); to calculate equilibrium geometry structures of Ni_2 dimer, Ni_{13} and Ni_{55} nanoclusters; and to observe ethylene adsorption over single crystal surfaces and Ni_{13} cluster by means of their energetic and kinetic differences.

CHAPTER 2

LITERATURE SURVEY

2.1 Nickel as Catalyst

Nickel is a transition metal in group VIII of the Periodic Table following iron and cobalt. Its atomic number is 28, and its outer shell of electrons has a $4s^2 3d^8$ configuration. Crystals are face centered cubic (fcc). It is hard, malleable, ductile and to an extent ferromagnetic (up to 360°C). Nickel is highly resistant to atmospheric corrosion and resists most acids, but is attacked by oxidizing acids such as nitric acid. (AZoM, 2005)

As a catalyst, following are few important industrial uses; D-glucose to sorbitol, nitriles & nitro groups to amines, nitro-aromatic to anilines, reductive alkylation and amination, polymerization, carbonyl compounds hydrogenation, aldehydes, ketones, pyridine hydrogenation, aromatic ring hydrogenation, Alkynes to alkanes hydrogenation and dehydrogenation (Gorwara, 2005). For example, in the food sector, one of the most important reactions is the hydrogenation which is the process of converting oils to fats. Margarine is the product made by hydrogenating oils. As a conclusion, nickel is one of the famous transition metal used for hydrogenation and dehydrogenation reactions. Hence, kinetics of the hydrogenation of ethylene on a nickel catalyst has an engineering importance.

2.2 Ethylene Adsorption on Ni(111)

The adsorption of ethylene is one of the simplest of hydrocarbon adsorptions on transition metals in order to examine catalytic activity which can be connected

with the surface topology (Beeck, 1950; Gwathmey and Cunningham, 1958; and Bertolini and Rousseau, 1979). Because of this fact, its adsorption on nickel catalyst is widely investigated, especially, by experimental methods in terms of temperature effects, adsorption sites, and surface structure for over 30 years.

Various studies employing surface technologies such as UPS and Thermal Desorption Spectroscopy studies (Demuth and Eastman, 1974; Demuth (a), 1978; Zhu and White, 1989), LEED and Auger spectroscopy studies (Cattania et al., 1979); High Resolution Electron Energy Loss Spectroscopy studies (Lehwald and Ibach, 1979); Temperature Programmed Static Secondary Ion Mass Spectroscopy studies (Zhu and White, 1989) have suggested that ethylene adsorbs molecularly on Ni(111) up to 200 K under UHV conditions where upon heating, ethylene decomposes into acetylene and atomic hydrogen.

Two different bonding are possible for ethylene adsorption to describe ethylene-surface interaction to metal surfaces, π-bonded or di-σ bonded ethylene. LEED, Auger and thermal desorption studies by Demuth and Eastman (1974), three different ultraviolet photoelectron spectroscopy (UPS) spectra analysis by Demuth (1978(a), 1978(b) and 1979) have resulted in the chemisorption of ethylene on Ni(111) as a π-adsorbed species and significant rehybridization have not occur upon chemisorptions. But, high resolution electron energy loss spectroscopy (EELS) at 150 K on flat and stepped Ni(111) surface by Lehwald and Ibach (1979) and more recently, the near edge x-ray-absorption fine-structure (NEXAFS) spectra of ethylene on Ni(111) by Carr et al. (1985) and Sham and Carr (1986) have illustrated that di-σ configuration is formed for ethylene whose C-C axis is determined as parallel to the surface. Similarly, Cooper and Raval in 1995, studied the adsorption of ethylene on Ni(111) at 110 K using reflection absorption infrared spectroscopy. Bao et al. (1994, 1995) determined the adsorption modes of both acetylene and ethylene on Ni(111) by

scanned-energy-mode photoelectron diffraction. They concluded that C-C axis of ethylene remains parallel to the surface with the di-σadsorption mode.

Density functional studies of both acetylene and ethylene on Ni(111) was studied by Fahmi and van Santen (1997). They used cluster model (Ni_4 and Ni_{14}) and performed quasi-relativistic spin-unrestricted frozen-core calculations with Vosko-Wilk-Nusair local spin density approximation. They reported adsorbed ethylene geometrical properties and heat of adsorption.

Sellers and Gislason (1999) have presented the adsorption/desorption of hydrogen molecule, carbon monoxide, ethylene, acetylene and ethane on fcc (111) surfaces of Ni, Pd and Pt from statistical mechanical point of view.

2.3 Ethylene Hydrogenation on Ni(111)

Over a century, mechanisms for ethylene hydrogenation on different transition metal surfaces have been investigated. First suggestion on ethylene hydrogenation on different transition metals was suggested by Horiuti and Polanyi in 1934. According to their mechanism, as shown in the following Table 2.1, first, ethylene is adsorbed by two surface metal atom, formed two σ bonds with the underlying metal substrate (di-σ bonded ethylene). Secondly, hydrogen molecule is adsorbed and dissociated on the metal surface. Then, one of the surface hydrogen atoms reacts with one of the carbon of adsorbed ethylene molecule to form surface ethyl. Then, the other surface hydrogen atom reacts with ethyl radical bound on the metal surface and ethane desorbs from the catalyst surface. This mechanism has been widely accepted to explain stepwise hydrogenation of hydrocarbons.

Table 2.1 Horiuti-Polanyi mechanism for ethylene hydrogenation on transition metal surfaces

$2M + CH_2{=}CH_2$	➞	$MCH_2\text{-}CH_2M$
$2M + H_2$	➞	$2MH$
$MCH_2\text{-}CH_2M + MH$	➞	$2M + MCH_2\text{-}CH_3$
$MCH_2\text{-}CH_3 + MH$	➞	2M + CH3-CH3

(M is referred as surface site)

Recently, Horiuti-Polanyi mechanism has become very questionable on Ni(111) surface. Significant studies by, Demuth and Eastman (1974); Dalmai-Imelik and Massardier (1977); Demuth (b) (1978); Klimesch and Henzler (1979); Lehward and Ibach (1979); Benninghoven et al. (1980); Hasse et al. (1983); and Daley et al. (1994) showed that a co-adsorbed layer of ethylene and H on Ni(111), formed by exposure to 10^{-4} Torr of ethylene and hydrogen molecule in an UHV environment, does not react to form ethane. Recent surface science experimental investigations by Daley et al. (1994) and Haug et al. (2001) showed that surface bound hydrogen atom has no effect on ethylene hydrogenation at the first stage. That is, both acetylene and ethylene hydrogenation on Ni(111) surface occurs only by bulk hydrogen atom which are moving out from the bulk metal to the surface. Moreover, the presence of those historically called bulk hydrogen atoms does not change ethylene-nickel interaction.

There are two forms of hydrogen atoms on Ni(111). One form is surface bound hydrogen atom, which is formed by the dissociative chemisorption of gas molecule of hydrogen (Christmann and Schober, 1974; Christmann and Behm, 1979; Winkler and Rendulic, 1982). Each surface hydrogen atoms, produced on Ni(111) bound at fcc or hcp threefold site (Figure 2.1) with about 62.0 kcal/mol to 67.0 kcal/mol adsorption energy, experimentally reported by Eley (1950); Lapujoulade and Neil (1972); Christmann and Schober (1974); Christmann and

Behm (1979) and theoretically shown by Yang and Whitten (1993); Klinke II and Broadbelt (1999); Greeley and Mavrikakis (2003).

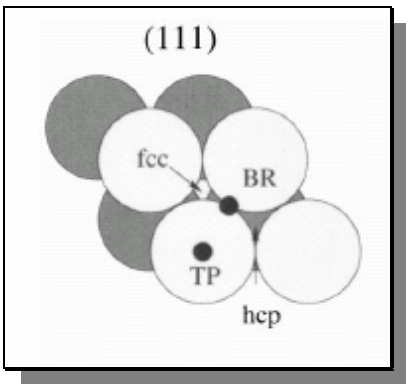

Figure 2.1 Representation of sites on Ni(111) surface: Top (TP); Bridge (BR); Face Centered Cubic (fcc); and Hexagonal Close Packed (hcp) (Kress and Hafner, 2000)

The other form of hydrogen atom is bulk hydrogen which is bound at interstitial octahedral sites below the surface by about 48 kcal/mol and they move upon out the surface, at temperatures above 180 K (Johnson et al., 1991; Maynard et al., 1991). As illustrated in Figure 2.2, during their emergence on the surface, they surmount 9.0 kcal/mol of activation barrier at the bulk-surface interface resulting in an increase in their potential energy by the same amount, that is, they have 39.0 kcal/mol (48.0 -9.0 kcal/mol) potential energy. Hence, an emerging bulk hydrogen atom is 24.0 kcal/mol (64.0 - 39.0 kcal/mol) more energetic then a surface bound hydrogen atom. By the light of this fact, Ceyer and co-workers (Daley et al. 1994, Johnson et al., 1992; Haug et al., 2001; Ceyer, 2001; Bürgi et al., 2002) reported that emerging bulk hydrogen uses its energy to react with adsorbate hydrocarbon molecule on Ni(111) to form ethane whereas surface-

bound hydrogen atom is unreactive. Bürgi et al. (2002) explained that there are reaction-channels open to bulk H and closed to surface bound H.

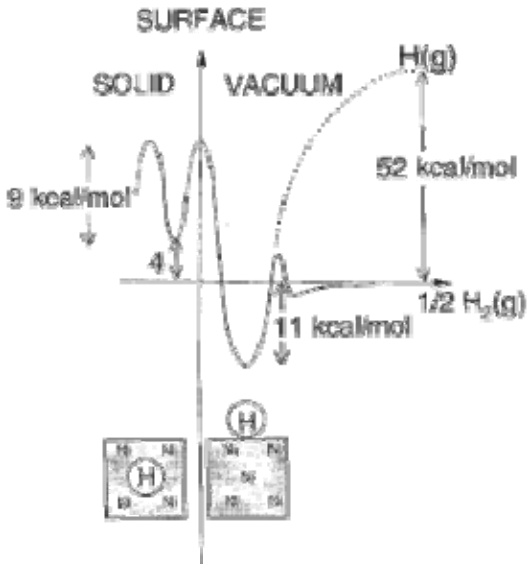

Figure 2.2 Potential energy diagram for hydrogen-Ni system: Left-hand side represent a H atom beneath the surface; Right-hand side a H atom or a H_2 molecule at or away from the surface. (Ceyer, 2001)

Daley et al. (1994) performed the investigation of the reactivity of both surface-bound and bulk hydrogen atoms with adsorbed ethylene by smart experiments. First, they observed bulk hydrogen effects on ethylene hydrogenation. They used a small diameter; thick walled metal tube whose end is sealed off with a thin disk of Ni with faces of (111) is connected to a source of a high pressure of hydrogen molecule and is placed in a vacuum chamber. A beam of atomic H was directed at a Ni(111) held at 130 K, this yielded up to an equivalent of 10 ML of H absorbed in the bulk metal but also left a monolayer of H bound to the surface. In order to remove those surface-bound hydrogen atoms, a 144 kcal/mol Xe beam with a 40^o incident angle was directed to the surface which caused collision-induced recombinative desorption while leaving the bulk H

unperturbed (Johnson et al., 1992). Then, the crystal at 80 K was exposed to a beam of ethylene to form an adsorbed layer. By using high-resolution electron spectroscopy (HREEL), they confirmed the presence of adsorbed ethylene and bulk hydrogen. They also reported that the bulk H did not change the C_2H_4-Ni interaction by comparing the vibrational spectrums of adsorbed ethylene with bulk H (Daley et al., 1994) and without bulk H (Lehwald and Ibach, 1979; Ibach and Mills, 1982; Hammer et al., 1986). The crystal heated at a rate of 2K/s. At 180 K, emergence of bulk H atoms on the surface started as reported by Johnson et al., 1991; and Maynard et al., 1991 and up to 65% of ethylene was hydrogenated to ethane.

Daley and co-workers (1994), also, observed hydrogenation activity of surface-bound H atom to compare with that of emerging bulk hydrogen atom. They exposed first ethylene, then H_2 molecule to the Ni(111) surface at 80 K. The crystal temperature was raised but no ethane formation was observed.

Haug et al. (2001) explained that the identity of second H atom to form surface bound ethyl to gas phase ethane molecule was unknown. They underlined that there was no evidence for or against the role of surface-bound H; therefore, both bulk hydrogen atom and surface hydrogen atom could hydrogenate C_2H_5.

As a result, against the Horiuti-Polanyi mechanism, Ceyer and co-workers (Daley et al. (1994), Johnson et al., 1992; Haug et al., 2001; Ceyer, 2001; Bürgi et al., 2002) experimental studies illustrated that ethylene hydrogenation mechanism on Ni(111) should have following reaction steps:

$$2M + CH_2{=}CH_2 \rightarrow MCH_2\text{-}CH_2M$$

$$MCH_2\text{-}CH_2M + H_{bulk} \rightarrow M + MCH_2\text{-}CH_3$$

$$MCH_2\text{-}CH_3 + H_{bulk}/\ H_{surface} \rightarrow M + CH3\text{-}CH3$$

2.4 Ni_2 Dimer and Nickel Nanoclusters

The most commonly used experimental tools for probing the structure of supported clusters, such as transmission electron microscopy and x-ray diffraction, are not applicable to small clusters. Another important experimental technique for determining cluster structure is the chemical probe method. In this method, the chemisorptions of weakly bound molecules to clusters is used to probe the arrangement of the clusters' surface atoms, from which it is often possible to infer overall cluster structure. Recent work report experiments using chemical reactions as probes of various structural features of metal clusters (Parks et. al 1991, 1994, and 1995; Pellarin et. al 1994). These studies reveal an evolutionary process taking place for the clusters as the cluster size increases and reaches the bulk limit. For example, for fcc materials, it appears that the fcc structure seems to be attained for clusters of very large size, while smaller clusters tend to exhibit geometries based on the icosahedral (IC) structures. Chemical probe experiments with ammonia (Parks et al. 1991) and nitrogen (Parks et al. 1994, 1995) adsorption on neutral nickel gas clusters with different sizes ranging from 3 to 120 atoms have demonstrated that nickel clusters in the size range from 10 to 28 atoms, and from 49 to roughly 200 atoms form primarily with icosahedral packing. Here, the term icosahedral clusters refers to multilayer structures with shell closings at magic numbered - 13, 55, 147, 309, etc. - atoms, clusters derived from these species by adding or removing atoms (Ho et. al., 1993). Nayak et al. (1997), also, have determined the IC structure of Ni_{13} experimentally. However, the experimental difficulties encountered in the characterization of small metal clusters, on the one hand, and their technological importance; on the other hand, stimulate the need for theoretical calculations which would predict cluster properties.

In theoretical literature, Raghavan et al. (1989) and later Stave and DePristo (1992) have studied nickel nanoclusters containing 4 to 23 atoms by use of CEM

(Corrected Effective Medium) theory and have determined IC structure as optimum structure for nickel nanoclusters including Ni_{13}. They have also reported binding energies and bond lengths of the clusters. Castro et al. (1997) studied small nickel clusters of up to five atoms with all-electron density functional calculations using both local and generalized gradient approximations. A more recent DFT study on nickel nanoclusters have been presented by Calleja et al. (1999). They have used the method of *ab initio* to show Ni_2 and Ni_{13} nanoclusters and especially in Ni_2 clusters; the results were in good agreement with available experimental data in terms of total energy and bond distance.

Although, molecular mechanics potentials give less correct results than quantum mechanics density functional theory, the "mechanical" molecular model describe molecular structures and properties in as practical a manner as possible. There are certain people who work with this molecular mechanics method for nickel nanoclusters. Lathiotakis et al. (1996) have used TB – MD method for nickel nanoclusters containing 2 to 55 atoms where IC structure for both Ni_{13} and Ni_{55} was also confirmed. Luo (2002) adopted the TB approximation and MD technique to compute the energies and structural properties of nickel clusters containing 4–55 atoms and obtained an IC structure for Ni_{13} as well.

Grigoryan and Springborg (2003) reported a study conducted by use of classical mechanical method calculations involving clusters with up to 150 nickel atoms. For total energy calculations, they used the embedded-atom method, and for structure optimization *Aufbaul Abbau* method was utilized where they concluded that IC structure for nickel clusters was the most optimum structure.

CHAPTER 3

METHODOLOGY OF THEORETICAL INVESTIGATIONS

This part was included in order to make the theoretical approach more comprehensive. First, computational chemistry, especially quantum mechanics, was briefly described in terms of semi-empirical and first principles methods. Then, the general concept of the calculations were summarized by giving definitions of most important keywords; molecular orbitals, self-consistent field techniques, etc. which were used frequently in quantum mechanical calculations. Finally, our methodology was explained in terms of the model used to describe the surface, our computational method, kind of basis set and keywords used. During calculations, two different program and computer configuration were used; SPARTAN program on normal PC and PQS program on 4-processor workstation procured by TÜBİTAK (The Scientific and Technical Research Council of Turkey).

3.1 Computational Chemistry Methods

Modern chemistry is divided into two calculations field: molecular mechanics and quantum mechanics.

3.1.1 Molecular Mechanics Calculations

The most accurate modeling of chemical systems is via quantum mechanical methods that are based on predictions of the sub-atomic electronic structure. But quantum mechanical methods can be exceedingly computationally expensive, rendering study of some complex systems impractical. Quantum mechanical can

also provide detail or a degree of accuracy that is unnecessary for the application and which could be traded-off for a faster calculation.

Classical atomistic simulation offers less precise, but often more practical, approach. The mechanical molecular model was developed out of a need to describe molecular structures and properties in as practical a manner as possible. It takes the atom as its fundamental unit, discarding the electronic detail, and assumes these atoms can be described by relatively simple equations, just as the prediction of the collision of billiard balls by the laws of Newtonian mechanics. (Accelrys II, 2005; CMM, 2004)

Therefore, Molecular Mechanics, or force field, calculations are based on a simple classical-mechanical model of molecular structure. The model nature of the calculations should be emphasized. There is very little physical significance in the parameters and energies in molecular mechanics calculations. Molecular mechanics treats the molecule as an array of atoms governed by a set of classical-mechanical potential functions. (Clark, 1985)

The range of applicability of molecular mechanics includes:

- Molecules containing thousands of atoms.
- Organics, oligonucleotides, peptides, and saccharides (metallo-organics and inorganics in some cases).
- Vacuum, implicit, or explicit solvent environments.
- Ground state only.
- Thermodynamic and kinetic (via molecular dynamics) properties.

The great computational speed of molecular mechanics allows for its use in procedures such as molecular dynamics, conformational energy searching, and docking that require large numbers of energy evaluations.

Molecular mechanics methods are based on the following principles: (CMM, 2004)

- Nuclei and electrons are lumped into atom-like particles.
- Atom-like particles are spherical (radii obtained from measurements or theory) and have a net charge (obtained from theory).
- Interactions are based on springs and classical potentials.
- Interactions must be preassigned to specific sets of atoms.
- Interactions determine the spatial distribution of atom-like particles and their energies.

3.1.2 Quantum Mechanics

Molecules and materials are made up of atoms. Atoms can be described as a nucleus of protons and neutrons surrounded by a cloud of electrons. It is the structure and interactions of these electrons that determine most chemical properties. (Godby, 2004)

Quantum Mechanical modeling methods predict the behavior of electrons. They are thus the most fundamental and accurate theoretical tool available to predict materials and molecular properties. In theory, quantum mechanical methods enable completely accurate prediction of any property; there are some important classes of property (notably reactivity, electronic, magnetic, and optical behavior) that can only be modeled using QM methods, because they are

determined by electronic behavior that cannot be approximated well using other methods (such as atomistic simulation). (Godby, 2004)

Hence, the development of computational quantum mechanics is leading to a new paradigm in the prediction of thermodynamic properties and phase behavior. In the most direct and computationally intense form, computational quantum mechanics can provide the information needed to construct the multidimensional interaction potential surface between molecules, and this can be used in computer simulation to predict thermodynamic properties and phase equilibria. (Sandler, 2003)

3.1.2.1 Mathematical Background for Quantum Mechanics

Classical mechanics is concerned with the trajectories of particles which theoretically can be calculated from knowledge of the initial conditions and the structure of the Hamilton H, or the sum of a kinetic - energy contribution T and potential-energy function V.

$$H = T + V \tag{3.1}$$

However, the existence of the atom can not be explained classically, but rather by the wave properties of the electron bounded to the nucleus. For this reason Schrödinger suggested to replace the classical kinetic and potential energy functions of (3.1) with linear operators $\hat{T}$ and $\hat{V}$ set up a wave equation of the form

$$\hat{H}\Psi = E\Psi \tag{3.2}$$

Where E is the energy of the system, H is a Hamiltonian (a mathematical operation) and electrons are considered as wave-like particles whose "waviness" is mathematically represented by a set of wavefunctions Ψ obtained by solving Schrodinger's equation.

The Schroedinger equation plays the role of Newton's laws and conservation of energy in classical mechanics that is, it predicts the future behavior of a dynamic system and the probability of events or outcome. (GSU, 2003)

Schrodinger's equation addresses the following questions (CMM, 2005):

- Where are the electrons and nuclei of a molecule in space? That is, configuration, conformation, size, shape, etc.
- Under a given set of conditions, what are their energies? That is, heat of formation, conformational stability, chemical reactivity, spectral properties, etc.

The Schroedinger equation is unsolvable for any chemical system more complex than a hydrogen atom. Fortunately, various approximations can be made that enable its solution, although even such approximations result in extremely complex computations for all but the simplest systems. This has meant that long computing times have been required for meaningful calculations, and the size of the system which can be studied has been limited. (Accelrys I, 2005)

The quantum-mechanical Hamilton in Schrodinger's equation (3.2) is

$$\hat{H} = \hat{T} + \hat{V} \tag{3.3}$$

For one electron system such as the hydrogen atom, with the electron centered on the atomic nucleus, kinetic and potential energy operators are

$$\hat{T} = -\frac{h}{8\pi^2 m}\nabla^2 \tag{3.4}$$

$$\hat{V} = -\frac{Ze^2}{r} \tag{3.5}$$

where m is the mass of the electron, r is the distance of the electron from the nucleus, Z is the atomic number, and e is the unit of the electronic charge, and in equation (3.3) the Laplacian ∇^2 is in cartesian coordinates.

In Schrodinger's equation (3.2), each particle is represented by a wave function Ψ (position, time) such as $\Psi^* \Psi$ = the probability of finding the particle at that position at that time. The wavefunction properties are as follows (GSU, 2003):

- Containing all the measurable information about the particle.
- $\Psi^* \Psi$ summed over all space = 1; if particle exists, probability of finding it somewhere must be one.
- Being continuous
- Allowing energy calculations via the Schrödinger equation.
- Establishment of the probability distribution in three dimensions.
- It permits calculation of most probable value (expectation value) of a given variable.
- For a free particle is a sine wave, implying a precisely determined momentum and totally uncertain position (uncertainty principle).

Additional information and assumptions needed for solving Schrödinger equation was given in Appendix A of this thesis.

3.1.2.2 Semi-Empirical Methods

Semi-empirical approximations simplify the solution of the Schrödinger equation by substituting some elements of the calculation with parameters that have been derived from experimental data or the results of first principles calculations. The result is that semi-empirical methods are much less

computationally demanding than first principles methods, but also less accurate. A limitation is that they cannot be applied to systems that are radically different from those used in the 'parameterization' procedure. (Accelrys I, 2005)

However, these methods do provide practical and fast solutions to tasks from geometry optimization (i.e., predicting the shape of molecules) and transition state search (used in studying chemical reactions) to vibrational frequency calculations (important for comparisons with experiment) and the evaluation of many chemical and physical properties. Moreover, *they allow researchers to calculate and obtain good starting geometries* and transition states before DFT refinement, to calculate properties and spectra of DFT-optimized structures, and to perform quick potential energy scans or prescreening of large databases. (Accelrys I, 2005)

In this study, especially for the calculations of nickel nanoclusters, semi-empirical quantum chemical methods using the MNDO-PM3 formalism is employed in order to investigate geometry optimization. Following section contains the summary of this formalism.

Ab initio quantum chemical methods are limited in their practical applicability because of their heavy demands of CPU-time and storage space on disk or in the computer memory. Because in ab initio methods such as the Hartree-Fock method the two-electron, multi-center integrals are solved explicitly. In semi-empirical methods these integrals are neglected or parameterized, and only valence shell electrons are considered. The Hamiltonian operator takes the form:

$$\hat{H}_{val} = \sum_{i=1}^{N_v}\left(-\frac{1}{2}V_i^2 + V(i)\right) + \sum_{i=1}^{N_v-1}\sum_{j=i+1}^{N_v}\frac{1}{r_{ij}} = \sum_{i=1}^{N_v}\hat{H}_{val}^{core}(i) + \sum_{i=1}^{N_v-1}\sum_{j=i+1}^{N_v}\frac{1}{r_{ij}} \qquad (3.6)$$

where N_v is the total number of valence electrons in the molecule, V(i) is the potential energy of the i^{th} electron in the field of nuclei and inner-shell electrons, and

$$\hat{H}_{val}^{core}(i) = -\frac{1}{2}V_i^2 + V(i) \tag{3.7}$$

The semi-empirical methods that are currently included in both the Spartan software are the **MNDO** (modified neglect of diatomic overlap), **AM1** (Austin model 1), and **PM3** (parametric method number 3) methods. These methods employ Slater-type orbitals (**STOs**) as basis set functions

$$f = Nr^{n-1}e^{-\zeta r}Y_i^m(\theta\phi) \tag{3.8}$$

and make the following simplifying approximation

$$\int\int \frac{f_z(1)\times f_y(1)\times f_m(2)\times f_n(2)}{r_{12}} d\upsilon_1 d\upsilon_2 = \delta_{zy}\delta_{mn}(zy \mid mn) \tag{3.9}$$

where $\delta_{zy} = 1$ if z = y or if z ≠ y and the functions f_z and f_y are on the same atom. In all other cases $\delta_{zy} = 0$. Likewise, $\delta_{mn} = 1$ if m = n or if m ≠ n and the functions f_m and f_n are on the same atom, and $\delta_{zy} = 0$ in all other cases. The notation (zy|mn) refers to the two-electron interaction integral.

$$\int\int \frac{f_z(1)\times f_y(1)\times f_m(2)\times f_n(2)}{r_{12}} d\upsilon_1 d\upsilon_2 = (zy \mid mn) \tag{3.10}$$

The F_{yy} terms in the secular determinant are

$$F_{yy} = U_{yy} - \sum_{B\neq A} C_B(yy \mid s_B s_B) + \sum_{z}^{A} P_{zz}\left[(yy \mid zz) - 1/2(yz \mid yz)\right] + \sum_{B\neq A}\sum_{P}^{B}\sum_{q}^{B} P_{pq}(yy \mid pq) \tag{3.11}$$

where the core integral U_{yy} is

$$U_{yy} = \left\langle f_y \mid -\frac{1}{2}V^2 + V_A \mid f_y \right\rangle \tag{3.12}$$

The orbitals f_z and f_y are centered on atom **A**, and orbitals f_p and f_q are centered on atom **B**. The second term in 3.11 is an approximation of the integral $< f_y \mid V_B \mid f_y >$. C_B is the **core charge** on atom **B**, i.e. atomic number of atom **B** minus the number of inner-shell electrons, and $(yy|s_B s_B)$ is a two-electron, two-center interaction integral. The s_B orbital is the valence s orbital on atom **B**. P_{zz} and P_{pq} are called **density matrix elements** and are defined as

$$P_{zz} \equiv 2\sum_{j=1}^{N_v/2} c_{zj}^* c_{zj} \quad \text{and} \quad P_{pq} \equiv 2\sum_{j=1}^{N_v/2} c_{pj}^* c_{,qj} \tag{3.13}$$

for closed-shell configurations. There are two types of off-diagonal elements F_{zy} in the secular determinant. The element in which the f_z and f_y orbitals are on the **same** atom constitutes one type and is labeled F_{zy}^{AA}. The other type of off-diagonal element has the $f_z$and f_p orbitals on **different** atoms and is labeled F_{zP}^{AB}.

$$F_{zy}^{AA} = -\sum_{B\neq A} C_B(zy \mid s_B s_B) + 1/2 P_{zz}\left[3(zy \mid zy) - (zz \mid yy)\right] + \sum_{B\neq A}\sum_{P}^{B}\sum_{q}^{B} P_{pq}(zy \mid pq) \tag{3.14}$$

$$F_{zp}^{AB} = 1/2\left[\beta_Z + \beta_P\right]S_{zp} - 1/2\sum_{y}^{A}\sum_{q}^{B} P_{yq}(zy \mid pq) \tag{3.15}$$

S_{zp} is the overlap integral $< f_z \mid f_p >$ and it is solved exactly. The total energy of the molecule, E_{total}, is the sum of the total valence electronic energy, E_{el}, and the energy of repulsion between the cores on atoms **A** and **B**.

$$E_{total} = E_{el} + \sum_{B>A}\sum_{A}\left[C_A C_B(s_A s_A \mid s_B s_B) + f_{AB}\right] \tag{3.16}$$

The one-center, two-electron interaction integrals (zz|yy) and (zy|zy) in eqs 3.11 and 3.14 are evaluated by a procedure that involves the fitting of the theoretical energies of the atoms to spectroscopic data. The values of these one-center, two-

electron interaction integrals and the internuclear distances are used to compute the two-center, two-electron interaction integrals (zy|pq) in eqs 3.11, 3.14, and 3.15. The atomic parameters ζ (the **orbital parameter**, eq2), U_{yy}, β_z, β_p, α_A, and α_B are evaluated by a nonlinear least-squares optimization procedure. This procedure involves the selection of a number of molecules that contain elements for which these atomic parameters are to be optimized. Only molecules for which the enthalpy of formation, molecular geometry, and dipole moment are experimentally known are chosen. Initial guesses for the parameters are used to calculate the enthalpies of formation, geometric variables, and dipole moments of these molecules. The calculated and experimental values are compared, a new set of values for the parameters are chosen, and the enthalpies of formation, geometric variables, and dipole moments are recalculated. This iterative process is continued until the squares of the weighted differences between the calculated and experimental values of the enthalpies of formation, geometric variables, and dipole moments are minimized. The optimized values of the atomic parameters ζ, U_{yy}, β_z, β_p, α_A, and α_B for each element are stored in the software. These values are accessed and used to calculate the F_{yy} and F_{zy} terms in the secular determinant each time that a calculation is performed. (Brouwer, 2004; Nutt, 2003)

3.1.2.3 First Principles Methods

First principles methods, such as Density Functional Theory (DFT) and Hartree-Fock, require only the positions and atomic numbers of each atom as input in the calculation. A pre-defined methodology, containing no adjustable parameters, approximates a solution to the Schrödinger equation. These methods work for every element in the periodic table, and a vast literature demonstrates their accuracy. Hartree-Fock methods work by solving the Schrödinger equation for each electron in the system. (Accelrys I, 2005)

Density Functional Theory is based on functions that describe the electron density. This theory describes how the ground state electron density and total energy can be obtained by solving a set of one-electron Schrödinger equations (the Kohn-Sham equations) instead of the complicated many electron Schrödinger equation. (Hammer and Nørskov, 2000)

As with other quantum mechanical methods, the results of these calculations usually include the position of all of the atoms concerned, the forces on them, the electronic structure (i.e., a description of the 'electron cloud'), and the energy of the system. From these basic facts, and how they develop over time, most other key properties can be derived. (Accelrys I, 2005)

In the density functional theory, the energy is not written in terms of the many-electron wavefunction as is conventional in quantum chemistry, but as a functional of the electron density. Kohn and Sham proposed that the total energy of an n-electron system can be written without approximations as:

$$E_{el} = -\tfrac{1}{2}\sum_i \int \phi_i(\vec{r}_1)\nabla^2\phi_i(\vec{r}_i)d\vec{r}_1 + \sum_A \int \frac{Z_A}{\left|\vec{R}_A - \vec{r}_1\right|}\rho(\vec{r}_i)d\vec{r}_1 + \tfrac{1}{2}\int \frac{\rho(\vec{r}_1)\rho(\vec{r}_2)}{\left|\vec{r}_1 - \vec{r}_2\right|}d\vec{r}_1 d\vec{r}_2 + E_{xc} \qquad (3.17)$$

The first term in equation 3.17 represents the kinetic energy of n non-interacting electrons with the same density $\rho(\vec{r}_1) = \sum_i \phi_i(\vec{r}_1)\phi_i(\vec{r}_1)$ as the actual system of interacting electrons. The second term accounts for the electron-nucleus attraction and the third term for the Coulomb interaction between the two charge distributions $\rho(\vec{r}_1)$ and $\rho(\vec{r}_2)$. The last term contains the exchange-correlation energy and can be expressed in terms of the spherically averaged exchange-correlation hole functions $\overrightarrow{\rho_x^{\gamma\gamma'}}(\vec{r}_1, s)$ as:

$$E_{xc} = \sum_{\gamma}\sum_{\gamma'} -4\pi/2 \int \frac{\vec{\rho}_1{}^{\gamma}(\vec{r}_1)\vec{\rho}_1{}^{\gamma\gamma'}(\vec{r}_1, s)}{s} d\vec{r}_1 s^2 ds \qquad (3.18)$$

where the spin indices γ and γ` both run over a α-spin as well β-spin and $s = \left|\vec{r}_1 - \vec{r}_2\right|$ the one electron orbitals, $\left\{\phi_i(\vec{r}_1); i = 1,...,n\right\}$ of equation 3.17 are solutions to the set of one-electron Kohn-Sham equations:

$$\left[-1/2\nabla^2 + \sum_A \frac{Z_A}{\left|\vec{R}_A - \vec{r}_1\right|} + \int \rho(\vec{r}_2) + V_{xc} \right] \phi_i(\vec{r}_1) = h_{KS}\phi_i(\vec{r}_1) = \varepsilon_i \phi_i(\vec{r}_1) \qquad (3.19)$$

where the exchange-correlation potential V_{xc} is given as the functional derivative of E_{xc} with respect to the density:

$$V_{xc}[\rho] = \delta E_{xc}[\rho] / \delta\rho \qquad (3.20)$$

the hole function $\overrightarrow{\rho_x}^{\gamma\gamma'}(\vec{r}_1, s)$ contains all information about exchange and correlation between the interacting electrons as well as the influence of correlation on the kinetic energy. The interpretation of $\overrightarrow{\rho_x}^{\gamma\gamma'}(\vec{r}_1, s)$ is that an electron at $\vec{r}_1$ to a larger or smaller extend will exclude the other electrons from approaching within a distance s. the extend of exclusion or screening increases with the magnitude of $\overrightarrow{\rho_x}^{\gamma\gamma'}(\vec{r}_1, s)$. The intricate function $\overrightarrow{\rho_x}^{\gamma\gamma'}(\vec{r}_1, s)$, can in practice only be obtained from an exact solution to the Schrödinger equation of our n-electron system. The set of one electron Kohn-Sham equations is a consequence of limited value for exact solutions to many-electron systems. They

form, however, the starting point for an approximate treatment in which $\overrightarrow{\rho_x}^{\gamma\gamma'}(\vec{r}_1,s)$ is replaced by model hole functions. The form of the exact hole function $\overrightarrow{\rho_x}^{\gamma\gamma'}(\vec{r}_1,s)$ is not known in detail. Nevertheless, a number of properties of $\overrightarrow{\rho_x}^{\gamma\gamma'}(\vec{r}_1,s)$ can be deduced from general considerations. It can readily be shown that the spherically averaged (Coulomb) hole-correlation functions $\overrightarrow{\rho_x}^{\gamma\gamma'}(\vec{r}_1,s)$ have the following properties:

$$4\pi\int \vec{\rho}_x{}^{\gamma\gamma`}(\vec{r}_1,s)_1 s^2 ds = 0 \qquad \text{when } \gamma \neq \gamma` \qquad (3.21a)$$

whereas the corresponding (Fermi) functions $\overrightarrow{\rho_x}^{\gamma\gamma'}(\vec{r}_1,s)$ satisfy the normalization condition:

$$4\pi\int \vec{\rho}_x{}^{\gamma\gamma`}(\vec{r}_1,s)_1 s^2 ds = 1 \qquad \text{when } \gamma = \gamma` \qquad (3.21b)$$

Further, the Fermi contributions:

$$\vec{\rho}_x{}^{\gamma\gamma`}(\vec{r}_1,0) = \vec{\rho}_1{}^{\gamma}(\vec{r}_1) \qquad (3.21c)$$

The two Coulomb functions $\vec{\rho}_x{}^{\alpha\beta}(\vec{r}_1,0)$ and $\vec{\rho}_x{}^{\beta\alpha}(\vec{r}_1,0)$ are in general considered to be smaller than $\vec{\rho}_x{}^{\gamma\gamma`}(\vec{r}_1,0)$ although different from zero. They cannot be related to $\vec{\rho}_1{}^{\gamma}(\vec{r}_1)$ in a simpler way.

The model hole function are in general constructed in such a way that the constraints given in equations 3.21a-c are satisfied. Thus, the Fermi function with $\gamma = \gamma`$, is seen to satisfy the constraints of equations 3.21b & 3.21c, whereas the Coulomb Function with $\gamma \neq \gamma`$ satisfies equation 3.21a.

Additional information for different methods used in density functional theory was given in Appendix B.

3.2 Keywords for Computational Chemistry

3.2.1 Molecular Orbitals

There is a second major theory of chemical bonding whose basic ideas are distinct from those employed in valence bond theory. This alternative approach to the study of the electronic structure of molecules is called molecular orbital theory. The theory applies the orbital concept, which was found to provide the key to the understanding of the electronic structure of atoms, to molecular systems.

The concept of an orbital, whether it is applied to the study of electrons in atoms or molecules, reduces a many-body problem to the same number of one-body problems. In essence an orbital is the quantum mechanical description (wave function) of the motion of a single electron moving in the average potential field of the nuclei and of the other electrons which are present in the system. An orbital theory is an approximation because it replaces the instantaneous repulsions between the electrons by some average value. The difficulty in obtaining an accurate description of an orbital is the difficulty in determining the average potential field of the other electrons. For example, the 2*s* orbital in the lithium atom is a function which determines the motion of an electron in the potential field of the nucleus and in the average field of the two electrons in the 1*s* orbital. However, the 1*s* orbital is itself determined by the nuclear potential field and by the average potential field exerted by the electron in the 2*s* orbital. Each orbital is dependent upon and determined by all the other orbitals of the system. To know the form of one orbital we must know the forms of all of them. This problem has a mathematical solution; the exploitation of this solution has

proved to be one of the most powerful and widely used methods to obtain information on the electronic structure of matter.

A molecular orbital differs from the atomic case only in that the orbital must describe the motion of an electron in the field of more than one nucleus, as well as in the average field of the other electrons. A molecular orbital will in general, therefore, encompass all the nuclei in the molecule, rather than being centered on a single nucleus as in the atomic case. Once the forms and properties of the molecular orbitals are known, the electronic configuration and properties of the molecule are again determined by assigning electrons to the molecular orbitals in the order of increasing energy and in accordance with the Pauli Exclusion Principle.

In valence bond theory, a single electron pair bond between two atoms is described in terms of the overlap of atomic orbitals (or in the mathematical formulation of the theory, the product of atomic orbitals) which is centered on the nuclei joined by the bond. In molecular orbital theory the bond is described in terms of a single orbital which is determined by the field of both nuclei. The two theories provide only a first approximation to the chemical bond. (Bader, 2004)

3.2.2 Models Used for Description of Catalytic Surfaces

The calculations cannot describe all the atoms in a solid or a catalyst particle, and a strategy must be chosen to limit the number of atoms treated explicitly. Two basic types of methods exist: (Hammer and Nørskov, 2000)

Cluster methods: which describe only a limited cluster of the surface atoms in the hope that the surface atoms farther away from adsorbate of interest are not important.

Slab methods, whereby the surface is described as a slab with a periodic structure along the surface. The size of the surface unit cell determines the computational effort, and in principle the unit cell should be chosen to be large enough so that the adsorbate in neighboring unit cells do not interact.

3.2.3 The Basis Set Approximation

For small highly symmetric systems, like atoms and diatomic molecules, the Hartree-Fock equations may be solved by mapping the orbitals on a set of grid points. These are referred to as numerical Hartree-Fock methods. However, essentially all calculations use a basis set expansion to express the unknown MOs (molecular orbitals) in terms of a set of known functions. Any type of basis function may in principle be used: exponential, Gaussian, polynomial, cube, plane wave etc. There are two guidelines for choosing the basis functions. One is that they should have a behavior which agrees with the physics of the problem, this ensures that the convergence as more basis functions are added is reasonably rapid. For bound atomic and molecular systems this means that the functions should go towards zero as the distance between nucleus and the electrons become large. The second guideline is practical: the chosen functions should make it easy to calculate all the required integrals. The first criterion suggests the use of exponential functions located on the nuclei; such functions are known to be exact solutions for the hydrogen atom. (Jensen, 1998)

There are two types of basis functions (also called *Atomic Orbitals,* AO, although in general they are not solutions to an atomic Schrödinger equation) commonly used in electronic structure calculations: *Slater Type Orbitals* (STO) and *Gaussian Type Orbitals* (GTO). Although STO provides more accurate results, GTO is more favored due to the ease of the calculation process. Slater type orbitals have the functional form (Jensen, 1998)

$$X_{\xi,n,l,m}(r,\theta,\varphi) = NY_{l,m}(\theta,\varphi)r^{n-1}e^{-\zeta r} \tag{3.22}$$

N is a normalization constant and $Y_{l,m}$ are the usual spherical harmonic functions. The exponential dependence on the distance between the nucleus and the electron mirrors the exact orbitals for the hydrogen atom. However, STOs do not have any radial nodes. (Jensen, 1998)

Nodes in the radial part are introduced by making linear combinations of STOs. The exponential dependence ensures a fairly rapid convergence with increasing number of functions. However, the calculation of three- and four-centre two-electron integrals cannot be performed analytically. STOs are primarily used for atomic and diatomic systems where high accuracy is required and in semi-empirical methods where all three- and four-centre integrals are neglected. (Jensen, 1998)

Gaussian type orbitals can be written in terms of polar or cartesian coordinates:

$$X_{\xi,n,l,m}(r,\theta,\varphi) = NY_{l,m}(\theta,\varphi)r^{(2n-2-l)}e^{-\zeta r^2 r}$$
$$X_{\xi,l_x,l_y,l_z}(x,y,z) = Nx^{l_x}y^{l_y}z^{l_z}e^{-\zeta r^2} \qquad (3.23)$$

where the sum of l_x, l_y and l_z determines the type of orbital (for example $l_x + l_y + l_z = 1$ is a p-orbital). Although a GTO appears similar in the two sets of coordinates, there is a subtle difference. A d-type GTO written in terms of the spherical functions has five components *($Y_{2.2}$, $Y_{2.1}$, $Y_{2.0}$,* $Y_{2.-1}$, *$Y_{2.-2}$),* but there appear to be six components in the Cartesian coordinates *(x^2, y^2, z^2, xy, xz. yz).* The latter six functions, however, may be transformed to the five spherical d-functions and one additional s-function *($x^2 + y^2 + z^2$).* Similarly, there are 1O cartesian "f-functions" which may be transformed into seven spherical f-functions and one set of spherical p-functions. Modem programs for evaluating two-electron integrals are geared to Cartesian coordinates, and they generate pure spherical d-functions by transforming the six Cartesian components to the five spherical functions. When only one d-function is present per atom the saving by removing the extra s-function is small, but if many d-functions and or

higher angular moment functions (f-, g-, h- etc. functions) are present, the saving can be substantial. Furthermore, the use of only the spherical components reduces the problems of linear dependence for large basis sets. (Jensen, 1998)

Having decided on the type of function (STO/GTO) and the location (nuclei), the most important factor is the number of functions to be used. The smallest number of functions possible is a minimum basis set. Only enough functions are employed to contain all the electrons of the neutral atoms. For hydrogen and helium this means a single s-function. For the first row in the periodic table it means two s-functions (1s and 2s) and one set of p-functions (2px, spy and 2pz). Lithium and beryllium formally only require two s-functions, but a set of p-functions is usually also added. For the second row elements, three s-functions (1s, 2s and 3s) and two sets of p-functions (2p and 3p) are used. (Jensen, 1998)

There are many different basis sets available in the literature or built into programs, and the average user usually only needs to select a suitable quality basis for the calculation. Below is a short description of some basis sets (generally called Pople Style Basis Sets).mentioned by Jensen (1998):

a) STO-nG basis sets: Slater Type Orbital consisting of n PGTOs. This is a minimum type basis where the exponents of the PGTO are determined by fitting to the STO, rather than optimizing them by a variational procedure. Although basis sets with n = 2-6 have been derived, It has been found that using more than three PGTOs to represent the STOs gives little Improvement, and the STO-3G basis is a widely used minimum basis. This type of basis set has been determined for many elements of the periodic table. The designation of the carbon/hydrogen STO-3G basis is (6s3p/3s) → [2s1p/1s].

b) k-nlmG basis sets These basis sets have been designed by Pople and co-workers. And are of the split valence type, with the *k* in front of the dash indicating how many PGTOs are used for representing the core orbitals. The *n/m*

after the dash indicates both how many functions the valence orbitals are split into, and how many PGTOs are used for their representation. Two value s (e.g. *nI)* indicate a split valence, while three values (e.g. *nlm)* indicate a triple split valence. The values before the G (for Gaussian) indicate the s- and p-functions in the basis; the polarization functions are placed after the G. This type of basis sets has the further restriction that the same exponent is used for both the sand p-functions in the valence. This increases the computational efficiency, but of course decreases the flexibility of the basis set. The exponents in the PGTO have been optimized by variational procedures.

c) 3-21G This is a split va1ence basis, where the core orbitals are a contraction of three PGTOs, the inner part of the valence orbitals is a contraction of two PGTOs and the outer part of the valence is represented by one PGTO. The designation of the carbon/hydrogen 3-21G basis is (6s3p/3s) → [3s2p/2s]. Note that the 3-21G basis contains the same number of primitive GTOs as the STO-3G, however, it is much more flexible as there are twice as many valence functions which can combine freely to make MOs.

d) 6-31G This is also a split valence basis, where the core orbitals are a contraction of six PGTOs, the inner part of the valence orbitals is a contraction of three PGTOs and the outer part of the valence represented by one PGTO. The designation of the carbon/hydrogen 6-31G basis is (10s4p/4s) → [3s2p/2s]. In terms of contracted basis functions it contains the same number as 3-2IG, but the representation of each functions is better since more PGTOs are used.

e) 6-311G This is a triple split valence basis, where the core orbitals are a contraction of six PGTOs and the valence split into three functions, represented by three, one and one PGTOs, respectively.

To each of these basis sets can be added diffuse and/or polarization functions. Diffuse functions are normally s- and p-functions and consequently go before

the G. They are denoted by + or ++, with the first + indicating one set of diffuse s- and p-functions on heavy atoms, and the second + indicating that a diffuse s-function is also added to hydrogens. The arguments for adding only diffuse functions on non-hydrogen atoms is the same as that for adding only polarization functions on non-hydrogens. Polarization functions are indicated after the G, with a separate designation for heavy atoms and hydrogens. The 6- 31+G(d) is a split valence basis with one set of diffuse sp-functions on heavy atoms only and a single d-type polarization function on heavy atoms. A 6-311++G(2df,2pd) is similarly a triple split valence with additional diffuse sp-functions, and two d- and one f-functions on heavy atoms and diffuse s- and two p- and one d-functions on hydrogens. The largest standard Pople style basis set is 6-311++G(3df, 3pd). These types of basis sets have been derived for hydrogen and the first row elements, and some of the basis sets have also been derived for second and higher row elements. (Jensen, 1998)

If only one set of polarization functions is used, an alternative notation in terms of * is also widely used. The 6-31G* basis is identical to 6-31G(d), and 6-31G** is identical to 6-31G(d,p). A special note should be made for the 3-21G* basis. The 3-21G basis is basically too small to support polarization functions (it becomes unbalanced). However, the 3-21G basis by itself performs poorly for hypervalent molecules, such as sulfoxides and sulfones. This can be substantially improved by adding a set of d-functions. The 3-21G* basis has only d-functions on second row elements (it is sometimes denoted 3-21G(*) to indicate this), and should not be considered a polarized basis. Rather, the addition of a set of d-functions should be considered an *ad hoc* repair of a known flaw. (Jensen, 1998)

3.2.4 Self Consistent Field Theory

Electronic Schröndinger equation can only be solved exactly for the H_2+ molecule, and similar one-electron systems. In general, an approximate that is numerical methods should be relied. By neglecting relativistic effects, each electron has a spin quantum number of ½. In the presence of an external magnetic field, there are two possible states, corresponding to alignment along or opposite to the field. (Jensen, 1998)

To generate approximate solutions the vibrational principle which states that any approximate wave function has an energy above or equal to the exact energy, is employed. This equality holds only if the wave function is the exact function. By making a trial wave function containing a number of parameters, the best trial function of the given form by minimizing the energy as function of these parameters can be generated. (Jensen, 1998)

Another approximation is made at this stage that the electron-electron repulsion is only included as an average effect, that is, electron correlations are neglected. Having selected a single determinant trial wave function, the vibrational principle can be used to derive Hartree-Fock equations. The Hartree-Fock model is a kind of branching point, either additional approximation may be invoked, leading to semi-empirical methods, or it can be improved by adding additional determinants, generating solutions which can be made to converge towards the exact solution of the electronic Schrödinger equation. (Jensen, 1998)

$$F_i\phi'_i = \varepsilon_i\phi'_I \qquad (3.24)$$

F_i : Fock operator

ϕ'_i : canonical Molecular orbitals

ε_i : orbital energy

The Fock operator is an effective one-electron energy operator, describing the kinetic energy of an electron, the attraction to all the nuclei and the repulsion to all the other electrons. This operator is associated with the variation of the total energy, not the energy itself. (The Hamilton operator is not a sum of Fock operators)

The canonical MOs may be considered as a convenient set of orbitals for carrying out the variational calculation. A specific Fock orbital can only be determined if all the other occupied orbitals are known, and iterative methods must therefore be employed for determining the orbitals. A set of functions which is a solution for Hartree-Fock equation are called Self-Consistent Field (SCF) orbitals. (Jensen, 1998)

Each MO is expanded in terms of the basis functions, conventionally called atomic orbitals. To determine the unknown MO coefficients, the Fock matrix must be diagonalized. However, the Fock matrix is only known if all the MO coefficients are known. The procedure (Figure 3.1) therefore starts off by some guess of the coefficients, forms the F matrix, and diagonalizes it. The new set of coefficients then used to calculate a new Fock matrix. This is continued until the set of coefficients used for constructing the Fock matrix is equal to those resulting from the diagonalization (to within a certain threshold). This set of coefficients determines an SCF solution. The potential (or field) generated by the SCF electron density is identical to that produced by solving for the electron distribution. The Fock matrix and therefore the total energy, depends only on the occupied MO. (Jensen, 1998)

To construct the Fock matrix, integrals over all pairs of basis functions and the one electron operator are needed. For M basis functions there are of the order of M2 of such one-electron integrals. These one-integrals are also known as core integrals, they describe the interaction of an electron with the whole frame of bare nuclei. The second part of the Fock matrix involves integrals over four

basis functions and the two-electron operator. In conventional HF methods the two-electron integrals are calculated and saved before the SCF procedure is begun, and then used in each SCF iterations (Figure 3.1). (Jensen, 1998)

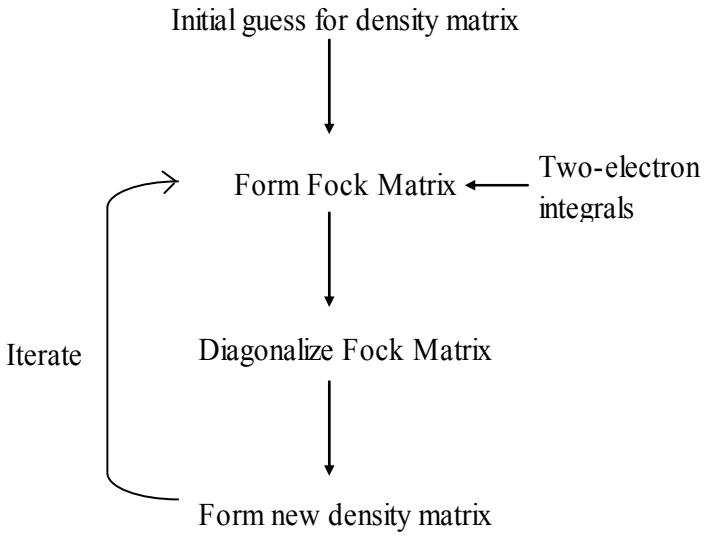

Figure 3.1 Illustration of SCF procedure

3.2.5 SCF Techniques

The procedure for SCF (Jensen, 1998) involves the following steps

1. Calculate all one- and two-electron integrals
2. Generate a suitable start guess for the MO coefficients
3. Form the initial density matrix

4. Form the Fock matrix as the core (one-electron) integrals + the density matrix times the two-electron integrals.

5. Diagonalize the Fock matrix. The eigenvectors contain the new MO coefficients.

6. Form the new density matrix. If it is sufficiently close to the previous density matrix, the final result is obtained, otherwise go to step 4.

There is no guarantee that the above iterative scheme will converge. For geometries near equilibrium and using small size basis sets, the straightforward SCF procedure often converges. Distorted geometries (such as transition structures) and large basis sets containing diffuse functions, however, rarely converge, and metal complexes, where several states with similar energies are possible, are even more troublesome. There are different tricks that can be tried to help converge.

1. ***Extrapolation:*** This is a method for trying to make the convergence faster by extrapolating previous Fock matrices to generate better Fock matrix than the one calculated directly from the current density matrix. Typically the last three matrices are used in the extrapolation.

2. ***Dampling:*** It is the often the reason for divergence, or very slow convergence, is due to oscillations. A given density matrix D_n gives a Fock matrix F_n which upon diagonalization gives a density matrix D_{n+1}. The Fock matrix F_{n+1} from D_{n+1} gives a density matrix of D_{n+2} which is close to D_n, but D_n and D_{n+1} are very different. The dampling procedure tries to solve this by replacing the current density matrix with a weighted average, $D_{n+1}=\alpha D_n+(1-\alpha)D_{n+1}$. The weighting factor a may be chosen as a constant or changed dynamically during the SCF procedure.

3. ***Level Shifting:*** This technique is perhaps best understood in the formulation of a rotation of the MOs which form the basis for the Fock operator. At convergence the Fock matrix elements in the MO basis between occupied and virtual orbitals are zero. The iterative procedure involves mixing (making linear combinations of) occupied and virtual MOs. During the iterative procedure these mixings may be large, causing oscillations or making the total energy increase. The degree of mixing may be reduced by artificially increasing the energy of the virtual orbitals. If a sufficiently large constant is added to the virtual orbital energies, it can be shown, that the total energy is guaranteed to decrease, thereby forcing convergence. The more the virtual orbitals are raised in energy, the more stable is the convergence, but the rate of convergence also decreases with level shifting. For large enough shifts, convergence is guaranteed, but it is likely to occur very slowly.

4. ***Direct Inversion in the Iterative Subspace (DIIS):*** This procedure was developed by Pulay and is an extrapolation procedure. It has proved to be very efficient in forcing convergence, and in reducing the number of iterations at the same time. It is now one of the most commonly used methods for helping SCF convergence.

5. ***Use of Symmetry:*** From group theory it may be shown that an integral can only be non-zero if the integrand belongs to the totally symmetric representation. Furthermore, the product of two functions can only be totally symmetric if they belong to the same irreducible representation. By forming suitable linear combinations of basis functions {symmetry adapted functions), many one- and two-electron integrals need not be calculated as they are known to be exactly zero due to symmetry. Furthermore, the Fock (in an HF calculation) or Hamilton matrix (in a CI calculation) will become block diagonal, as only matrix elements between functions having the same

symmetry can be non-zero. The savings depend on the specific system, but as a guideline the computational time is reduced roughly by a factor corresponding to the order of the point group (number of symmetry operations). Although the large majority of molecules do not have any symmetry, a sizable portion of the small molecules for which *ab initio* electronic structure calculations are possible, are symmetric. Almost all *ab initio* programs employ symmetry as a tool for reducing the computational effort.

3.3 Computational Procedure

3.3.1 Calculation Methods

DFT (Kohn and Sham, 1965) calculations were conducted using Becke's (1988 and 1989) three-parameter hybrid method involving the Lee, Yang, and Parr (1988) correlation functional (B3LYP) formalism. The basis set employed in the DFT calculations was 6-31G** provided in SPARTAN'02 (Wavefunction Inc.) [Hehre, 1993; SPARTAN tutuorial] and modified 6-31G** provided in PQS PQS *Ab Initio* Program Package version 3.1.

Necessary semi-empirical calculations with PM3 formalism were also performed by using SPARTAN'02.

3.3.2 Types of Calculations

There are four types of quantum chemical calculations that were performed during the study. The first type is the "Single Point Energy" calculations; these types of calculations are convenient for property calculations such as vibration frequency and charge calculations, since the total energy of a given geometry is calculated without any geometry changes. The second type is the "Equilibrium

Geometry" calculations. At the end of these calculations, an optimized geometry with the minimum energy is obtained for a given geometry. At the equilibrium geometry, the gradient (first derivative) of the energy with respect to the coordinates is zero, and the force constant (second derivative) is positive where the force constants are represented as the eigenvalues of the Hessian Matrix. The third type is "Transition State Geometry" calculations. In this type of calculation, the molecular structure at the maximum of the potential energy connecting two minima of reactants and products can be obtained. This geometry is also described mathematically as a first order saddle point, being maximum in one direction and minimum in the others. The gradient for a saddle point is zero. However, the second derivative of the energy with respect to the coordinates has a negative value. Therefore, at a transition state geometry, there is only one negative eigenvalue in the Hessian Matrix. For the activated adsorption reactions (reactions that need activation energy to proceed), transition state geometry has always the maximum energy and so gives the activation energy. The last type of the calculations used in the study is "Coordinate Driving" calculations. Coordinate Driving calculations are the series of constrained equilibrium geometry calculations. One can obtain an energy profile for a specific reaction by selecting a reaction coordinate by means of these calculations. All of the calculations except for the single point energy calculations the following parameters were used: SCF density convergence, optimization energy convergence, gradient tolerance and distance tolerance equal to 0.0001, 0.0000001, 0.001 and 0.01 respectively. For the single point energy calculations default values were used in order to obtain more accurate results especially for the vibration frequency data. (Uzun, 2003)

3.3.3 Procedure for Ethylene Hydrogenation on Ni(111)

During the study, the following procedure was followed:

1. 3-D Atomic structures of reactant and catalyst cluster are prepared.

2. Structure of both the reactants and the catalyst cluster are optimized geometrically.

3. Reactant and target cluster atoms are placed with respect to the reaction coordinate identifications.

4. Energy minimization computation is carried out at each reaction coordinate distance specified.

5. Relative energy is calculated by taking the difference between the reactant and cluster alone and the final structure.

6. Activation energies and heats of reaction for each reaction step are calculated and compared.

7. Most probable elementary reaction step is estimated.

Point 1 is the first step in computational chemistry which states building a model. A molecular model consists of a series of atoms, their co-ordinates in three-dimensional space, and their connectivity. Constructing and working with such models requires specialist model building and visualization tools.

In this work, SPARTAN quantum mechanical calculation program is used for both drawing the molecular model and computing the system properties. Ethylene and hydrogen are both drawn directly by the help of building menu of this program. nickel fcc structure was obtained by WYCKOFF parameters (Wkckoff, 1963), as shown in Figure 3.2 which are (4a) 000; ½ 0 ½; ½ ½ 0; 0 ½ ½ with lattice parameter; a = 3.52387 Å.

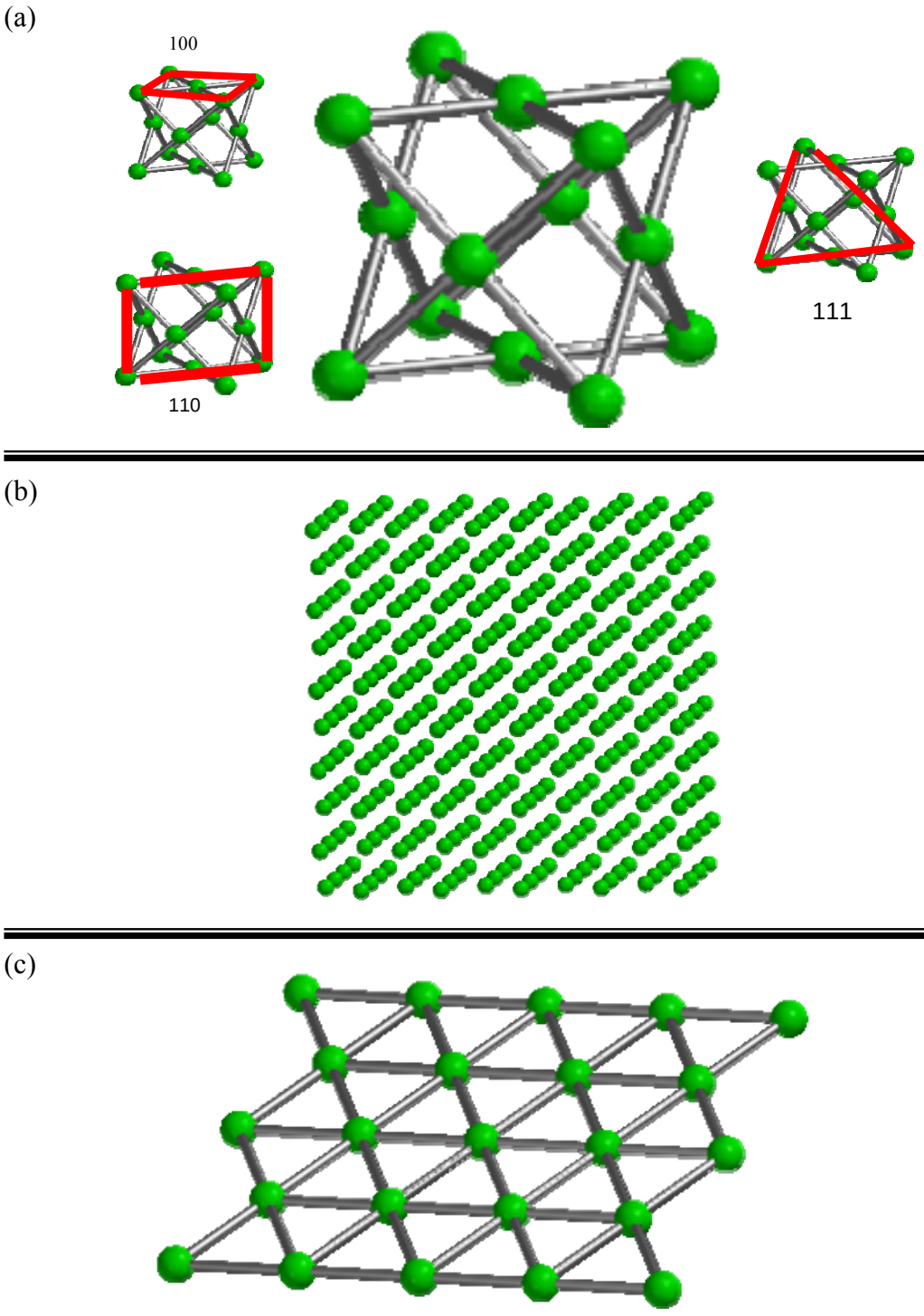

Figure 3.2 a) Unit cell of FCC structured nickel **b)** Enlarged structure of crystalline nickel **c)** Monolayer 111 single crystal surface of nickel (Ni-Ni bond distance is 2.492 Å)

After the formation of one unit cell (Figure 3.2 (a)), it was enlarged in all directions several times to obtain the necessary single crystal surfaces as shown in Figure 3.2(b). Cutting unit cells in the 111 direction resulted in monolayer 111 single crystal surface of nickel, illustrated in Figure 3.2(c).

Then, the finite cluster approximation which represented an infinite surface was used. This cluster approach is a well known and successful approach applied in quantum mechanical calculations (Zhanpeisov et al., 2001 and Izumi et al., 2002). Moreover, this cluster approach could be safely used since chemisorption is a localized phenomenon (Crispin, 1999). Therefore we prepared virtually a finite 4-atom nickel cluster representing this fcc(111) surface in order to investigate the energetics of its interaction with ethylene and hydrogen atoms.

In a continuous Ni(111) surfaces, one nickel atom's dangling orbital was filled with electrons of the adjacent nickel atom. Accordingly, in our cluster, nickel electrons were not kept frozen but their dangling orbital electrons were saturated with hydrogen atoms which were referred neighborhood atoms. Therefore, we have obtained small model for (111) single crystal surface, that is Ni_4H_{26} cluster illustrated in Figure 3.3. During the calculations for ethylene hydrogenation, Ni_4H_{26} cluster was utilized but its hydrogen atoms were not shown in graphical demonstrations in Chapter 4 for clear vision.

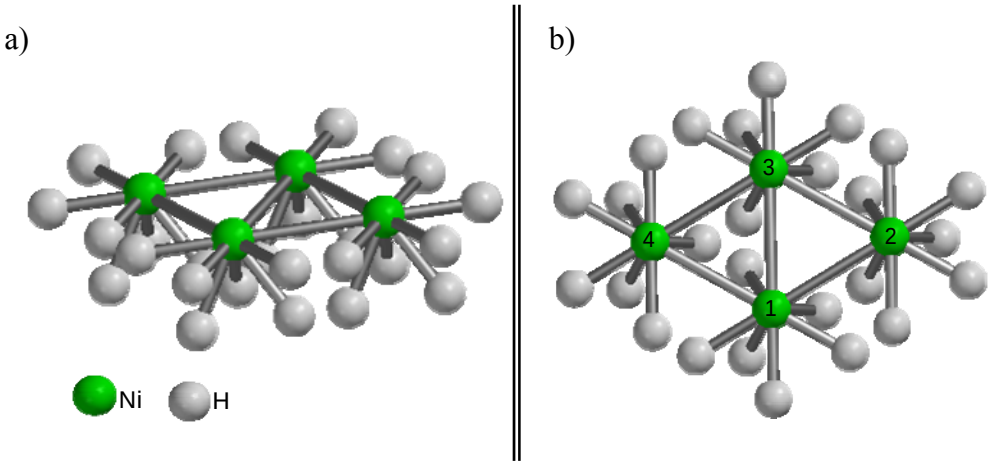

Figure 3.3 a) The structure of Ni_4H_{26} cluster **b)** Top view

Secondly, (Point 2), all of the molecules, both the cluster and the adsorbing molecules are fully optimized geometrically by means of the equilibrium geometry calculations.

Then (Point 3 &4), the adsorbing molecule is located over the active site of the cluster at a selected distance and a coordinate driving calculation is performed by selecting a reaction coordinate in order to obtain the variation of the relative energy with a decreasing reaction coordinate to get an energy profile as a function of the selected reaction coordinate distance. It should be noted that all nickel atoms (Ni-Ni=2.492 Å) and computational hydrogen atoms of the Ni_4H_{26} cluster are kept fixed at their positions during calculations.

Point 5: The relative energy is defined as the following formula:

$$\Delta E = E_{System} - (E_{Cluster} + E_{Reactantse}) \quad (3.25)$$

where E_{System} is the calculated energy of the given geometry containing cluster and the adsorbing molecule at any distance, $E_{Cluster}$ is the energy of the cluster

and $E_{Reactant}$ is that of the reacting molecule. In other words, the relative energy is defined to be the difference between the total enthalpy of formation of the reactant molecule plus nickel cluster at any interatomic distance and the sum of the enthalpies of formation of the free catalyst cluster and the approaching reactant molecule at infinite separation.

After having obtained the energy profile for the desired reaction, the geometry with the minimum energy on the energy profile is reoptimized by means of the equilibrium geometry calculations to obtain the final geometry for the reaction. For the calculated final geometry, vibration frequency and atomic charges are computed by Single Point Energy calculations. Furthermore, from the energy profile, the geometry with the highest energy was taken as the input geometry for the transition state geometry calculations. Starting from these geometries, the transition state structures with only one negative eigenvalue in Hessian Matrix were obtained.

3.3.4 Ni_2 Dimer and Nickel Nanoclusters

Similar to ethylene molecule and hydrogen atoms, nickel dimer was drawn directly by the help of building menu of SPARTAN quantum mechanical calculation program. Equilibrium geometry calculations with neutral charge and different spin multiplicities then single point calculations in order to obtain vibration frequencies were performed by using DFT method with B3LYP formalism and modified 6-31G** provided in PQS *Ab Initio* Program Package.

For Ni_{13} and Ni_{55} nanoclusters, the preparations of the input geometries were much more complex than the other nickel molecules. Those clusters were built by obeying the magic number cluster structure meaning the clusters which have completed and arranged outside geometry. Those structures are constructed by surrounding one single metal atom with metal atom layers by obeying the formula suggested by Schmid et al., (1990);

$y = 10\ n^2 + 2$; where y was the total number of atoms at the n^{th} layer.

For Ni_{13} nanocluster, there is one layer wearing on one Ni atom. Therefore, for the 1^{st} layer, $y = 10x1^2 + 2 = 12$, and the total number of atoms is 1 + 12 = 13.

Ni_{55} nanocluster is built up from Ni_{13} nanocluster by wearing a second layer to that nanocluster. For the 2^{nd} layer $y = 10\ 2^2 + 2 = 42$ and whole number of atoms is 13 + 42 = 55.

In all calculations, nickel nanoclusters were neutral, their electrons were not kept frozen and nickel atoms were free in all directions. Input guesses for Ni_{13} nanocluster were determined by semi-empirical quantum chemical methods using the PM3 formalism provided in SPARTAN'02. Different spin multiplicities were utilized by use of PM3 calculations followed by DFT/B3LYP/modified 6-31G** calculations to determine global minima.

During the calculations of Ni_{55} nanocluster, only semi-empirical quantum chemical methods using the PM3 formalism provided in SPARTAN'02 were employed in order to determine the equilibrium geometry structure with different spin multiplicities.

3.3.5 Comparison of Nickel Single Crystal Surfaces with Nanoclusters

Similar to Ni(111), a double layer finite cluster of Ni_5H_{30} (Figure 3.4) was prepared by cutting crystalline nickel shown in Figure 3.2(b) in the direction of 100. During the calculations, hydrogen atoms were utilized for saturating the dangling orbitals of nickel. All atoms forming finite cluster to represent Ni(100) surface were all fixed in their positions. Therefore, this surface was also a fragment of the unreconstructed 100 surface with fixed Ni-Ni bond length of 2.492 Å.

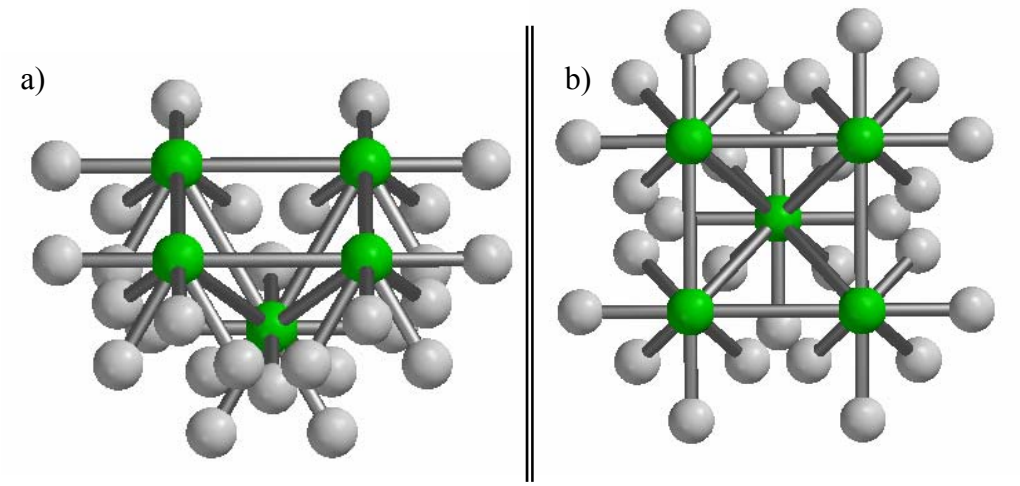

Figure 3.4 a) Ni_5H_{30} cluster representing Ni(100) **b)** Top view

During the ethylene adsorption calculation on spherical surface of Ni_{13} nanocluster, all nickel atoms were free in all directions; system had neutral charge; and different spin multiplicities were tried in order to find optimum geometry.

CHAPTER 4

RESULTS AND DISCUSSION

The aim of this study, as mentioned in Chapter 1, was to theoretically investigate possible elementary steps of reaction mechanism for ethylene hydrogenation on Ni(111) single crystal surface, equilibrium geometrical optimization of small nickel clusters and observation of ethylene adsorption on different nickel surfaces in terms of catalytic activity. The computational procedure in Chapter 3 included the description of essential strategy that we used in our quantum chemical calculations. Base on the methodology, section 4.1 includes ethylene adsorption on nickel single crystal surfaces, such as Ni(100) and Ni(111), and hydrogenation of ethylene on Ni(111) surface. Density functional theory calculations for ethylene adsorption on optimized geometries of nickel dimer and Ni_{13} nanocluster; and equilibrium geometry calculations by use of semi-empirical PM3 method for Ni_{55} nanocluster were discussed in section 4.2. Comparison of adsorption activities of casual single crystal surface with of nanocluster surface was made in section 4.3. This chapter, also, compared our computational results with both experimental and theoretical data.

4.1 Ethylene Interaction with Nickel Single Crystal Surfaces

4.1.1 Investigation of Ethylene Adsorption on Ni(111)

The adsorption of ethylene on Ni(111) surface was achieved by first, geometry optimization of ethylene and of the 4-atom nickel cluster. Single point calculations for bare Ni_4H_{26} cluster were performed by only changing spin multiplicities of the cluster. Comparison of final energies calculated for bare

cluster illustrated that minimum energy was obtained when the spin multiplicity was three. Hence, bare Ni_4H_{26} cluster had a spin multiplicity of three with Ni-Ni bond length of 2.492 Å. All nickel atoms, from 1 to 4, had mulliken charges of 0.042, -0.022, 0.036 and -0.053, respectively, confirming that bare cluster was neutral. The probable reason of this asymmetric charge distribution might be due to the effect of nickel atom placements on (111) single crystal layers. That is, however you constructed the cluster; even with 4 atoms or more, the (111) cluster could not have exact symmetry, contrary to (100) surface. Therefore, it was expected that there should be active nickel surface atoms, which attracted ethylene towards themselves more than the other surface atoms.

C1 of ethylene was targeted to Ni1 of the cluster when their distance between each other was 3.08 Å, as shown in Figure 4.1. Then, ethylene adsorption, Figure 4.2, was obtained by energy profile calculation type with DFT/B3LYP/ 6-31G** formalism. It should be noted that the energy profile graph had relative energy values at C1-Ni1 distances of 4.00 Å and 5.00 Å. Therefore, reaction coordinate calculations were performed also with increasing stepwise manner from 3.08 Å to 5.00 Å. During the calculations, it was observed that when ethylene was far from the surface (4.00 and 5.00 Å), cluster behaved like being bare and total system (cluster + ethylene) spin multiplicity was found as three, noting that no computational results could be obtained with multiplicity of one. But ethylene presence on that cluster at its bond distance with nickel surface resulted that those two unpaired electrons were shared with ethylene. Therefore, total system spin multiplicity became one. As a result, changing spin multiplicity parameter was necessary in order to have accurate computational results.

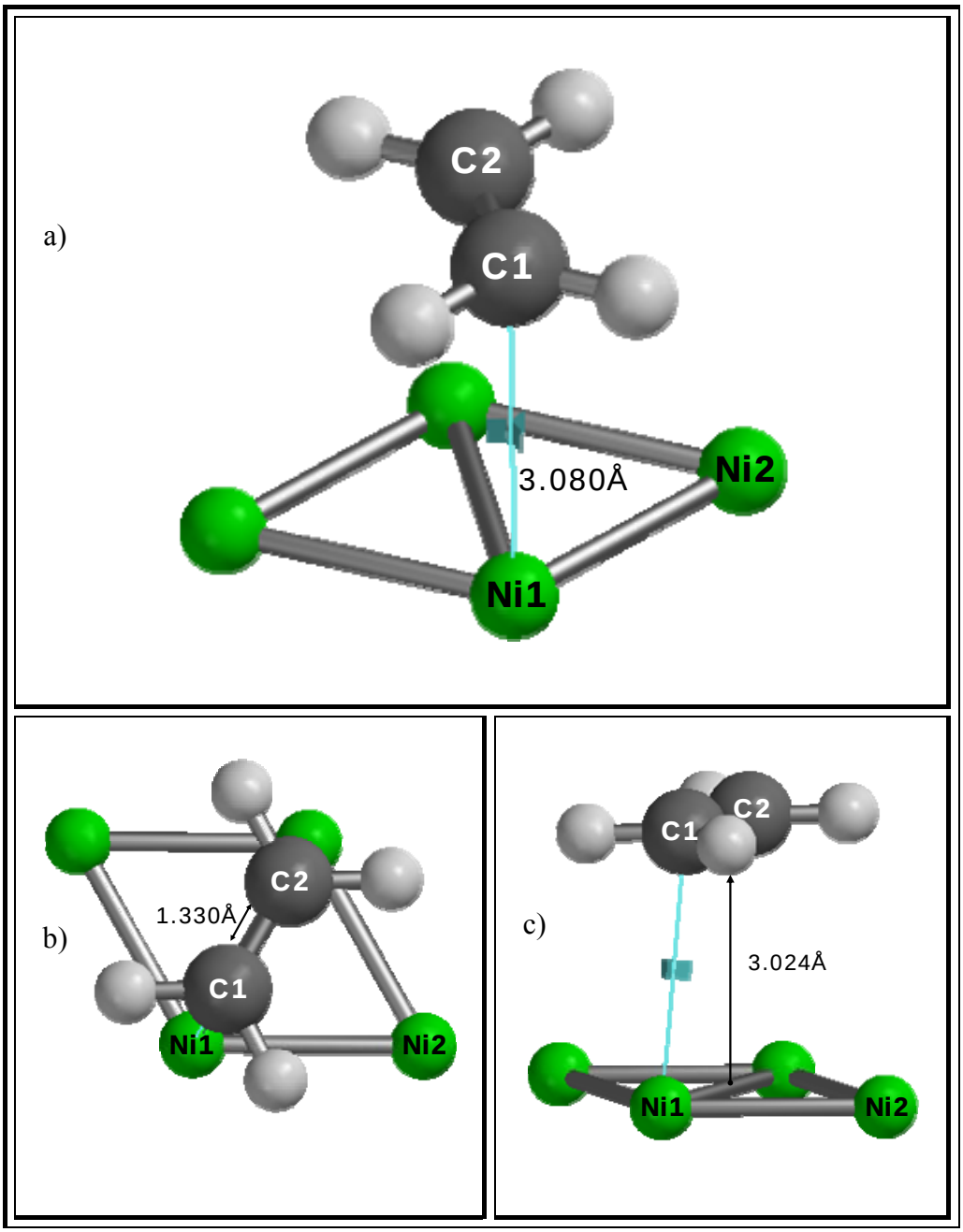

Figure 4.1 a) Input geometry for ethylene adsorption on Ni(111) **b)** Top view **c)** Side view. Pink line shows selected reaction coordinate for energy profile calculations.

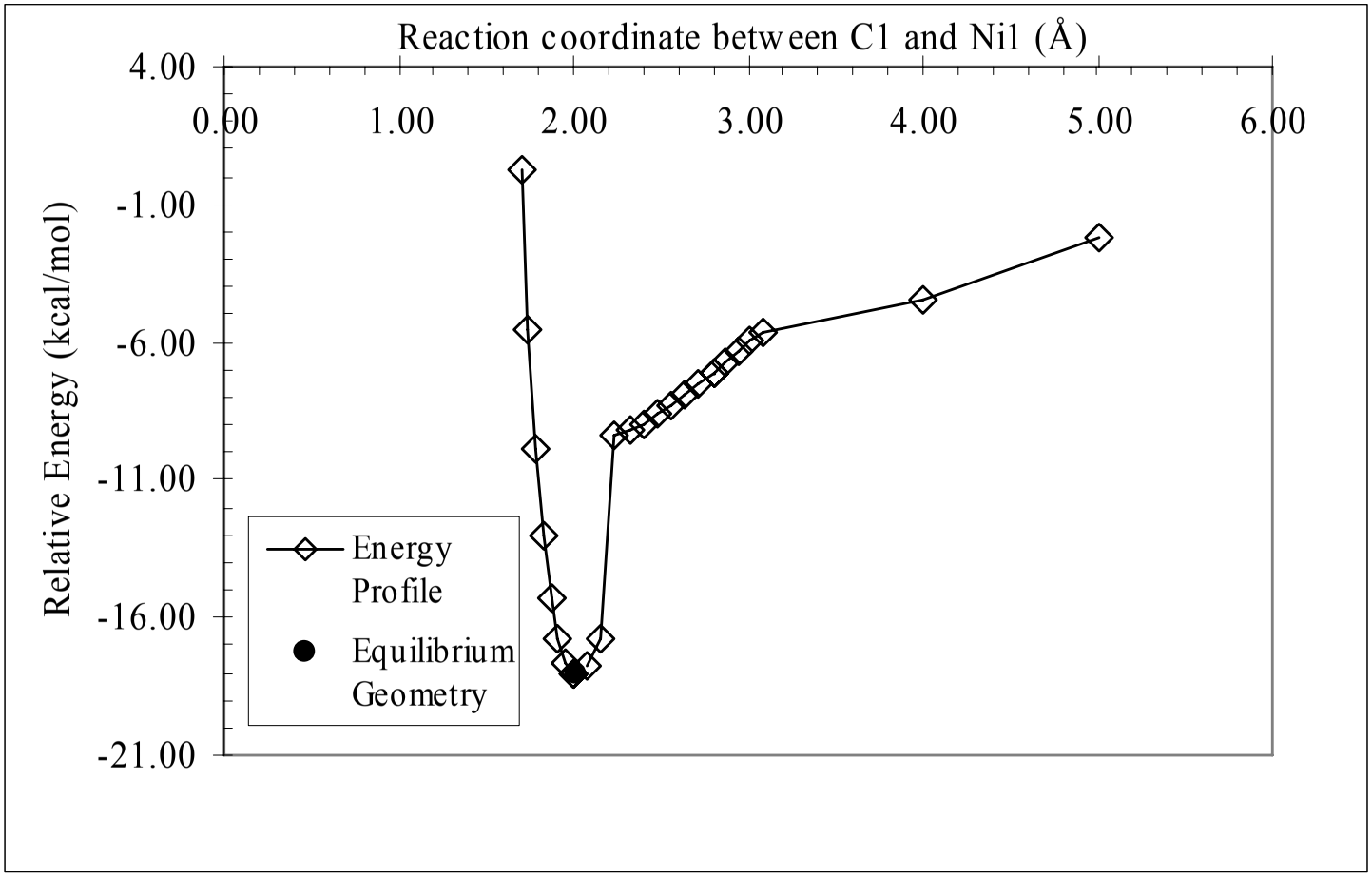

Figure 4.2 Energy profile of ethylene adsorption on Ni(111)

Relative energy of the system was calculated as:

At 5.0 and 4.0 Å: Relative Energy = System (2) – cluster (2) – ethylene (0)

At 4.0 Å to 1.7 Å: Relative Energy = System (1) – cluster (1) – ethylene (0)

where numbers in parenthesis illustrated number of unpaired electrons.

Equilibrium geometry calculation (The input and output files are shown in Appendix C) at minimum point of that profile (Figure 4.2) resulted in -18.0 kcal/mol adsorption energy, supported by -13.0 kcal/mol and -15.0 kcal/mol adsorption energy reported by Fahmi and van Santen (1997), and Sellers and Gislason (1999), respectively. To the best our knowledge, experimental value for heat of adsorption of ethylene on Ni(111) have not reported yet.

As shown in Figure 4.3, computational Ni1-C1 and Ni2-C2 bond distances were 2.015 Å and 2.022 Å, respectively. Hence di-σ bonded ethylene was observed at the minimum energy level. Similarly, C1-C2 bond distance was calculated, as 1.49 Å which showed agreement with experimental value of 1.47 Å (Ibach and Lehwald, 1981) and of 1.60±0.18 Å (Bao et al, 1994) and theoretical value of 1.49 Å (Fahmi and van Santen, 1997). Our computational result for ethylene distance from surface was 1.94 Å, being close to both experimental value of 1.90 Å (Bao et al., 1994) and theoretical value of 1.89 Å (Fahmi and van Santen, 1997).

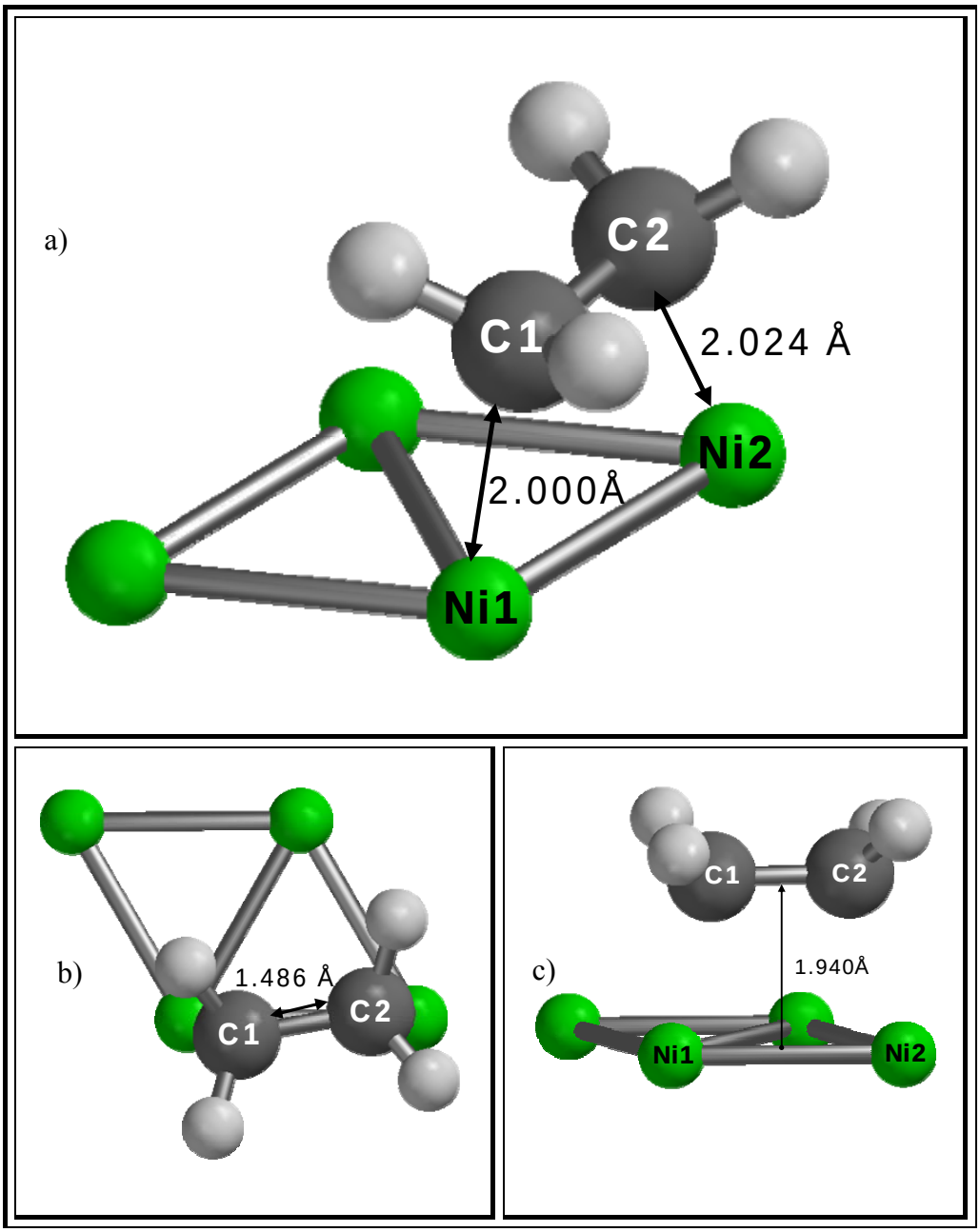

Figure 4.3 a) Equilibrium geometry result of surface ethylene on Ni(111) **b)** Top view **c)** Side view

A density functional study by Fahmi and van Santen (1997) is given in Table 4.1. They used cluster of Ni_4 and Ni_{14} and performed quasi-relativistic spin-unrestricted frozen-core calculations with Vosko-Wilk-Nusair local spin density approximation. 1s electrons of carbon and electrons up to 3p shell of nickel atoms were kept fixed in their geometry optimization calculations. Owing to their methodology, they first performed the optimization of ethylene molecule on Ni_4 cluster and then, directly transferred this result to the 14-atom Ni cluster. They also calculated relative adsorption energy with the formula of Eads=Ecluster+Eadsorbate-E(adsorbate/cluster) which brought sign convention. But they explained that a positive E_{ads} value corresponds to a stable adsorbate/surface system. According to this expression, their calculated adsorption energy for the di-σ orientation was +13.0 kcal/mol, compared with Zuhr and Hudson (1977)'s experimental value of 12.0 kcal/mol which was stated by them as the adsorption of ethylene on Ni(111), although, this number defined energy of desorption of ethylene molecule from Ni(110) surface. As a result, they found the exothermic adsorption value of 13.0 kcal/mol with the geometrical results of di-σ bonded ethylene being consistent with our theoretical results and also with experimental results (Table 4.1).

By using quantum mechanical calculations, vibration frequencies of adsorbed ethylene on Ni(111) were, also, calculated. In Table 4.2, the comparison of our computational results with experimental literature is given. The verification of our final geometry is again proved by closeness of theoretical vibrational frequencies; 734, 877, 1083, 1438, 1213 and 2965 cm^{-1} to experimental data of 720-740, 880, 1088-1100; 1418-1440; 1200 and 2943-2970 cm^{-1} (Cooper and Raval, 1995; Lehwald and Ibach, 1979), respectively.

Table 4.1 Theoretical and experimental results of ethylene adsorption on Ni(111)

References	Method	Heat of ads. (kcal/mol)	Structure	Bond distance (Å)		Distance from surface (Å)
				C-C	C-Ni	
Present study	**DFT**	**-18.00**	**di-σ**	**1.49**	**2.015 2.022**	**1.94**
Ibach and Lehwald (1981)	exp.			1.47		
Bao et al. (1994)			di-σ	1.60±0.18		1.90
Fahmi and van Santen (1997)	DFT	4 and -13	di-σ	1.49	1.95	1.89
Sellers and Gislason (1999)	theo.*	-15.00				

*statistical mechanical approach

Table 4.2 Vibrational frequencies of ethylene on Ni(111)

	Experimental (cm^{-1})		Present Work (cm^{-1})
	Cooper and Raval (1995)	Lehwald and Ibach (1979)	
ρCH2 (rock)	-	720-740	734
τCH2 (twist)	-	880	877
χCH2 (wag)	1088	1100	1082
αCH2 (scissor)	1418	1440	1438
νC=C (stretch)	-	1200	1213
νCH2 (stretch)	2943	2950-2970	2965

4.1.2 Investigation of Ethylene Hydrogenation on Ni(111)

4.1.2.1 Adsorbed Ethylene Convergence to Surface Ethyl

As mentioned previously, two possible elementary steps were considered to form surface bound ethyl: "Bulk" or "Surface" hydrogen atom reaction with adsorbed ethylene. It is important to notice that the term of bulk hydrogen was used to represent hydrogen atoms emerging from bulk of Ni metal to the surface. Those two probable elementary steps were named as Alternative 2 and 2'. It is worth noting that bulk hydrogen atom is 24.0 kcal/mol more energetic then surface hydrogen.

4.1.2.1.1 Bulk Hydrogen Atom Reaction with Adsorbed Ethylene

Starting point for the reaction is to form bulk hydrogen atom at 180 K as in the actual case. Noting that at 180 K, those subsurface hydrogen atoms sort from the nickel matrix and become gas phase hydrogen atom (Daley et al., 1994). Therefore, unbounded hydrogen atom (H1 written with red color) was simulated by directly placing it at a distance of 3.00 Å from one carbon of adsorbed ethylene, as illustrated in Figure 4.4. Then, reaction coordinate between them was formed in order to perform energy profile calculation decreasing in a stepwise manner with step size of 0.1 Å. This gradual graph was shown in Figure 4.5. The reaction expression could be given as;

$MCH_2\text{-}CH_2M + H_{(b)} \rightarrow M + MCH_2\text{-}CH_3$

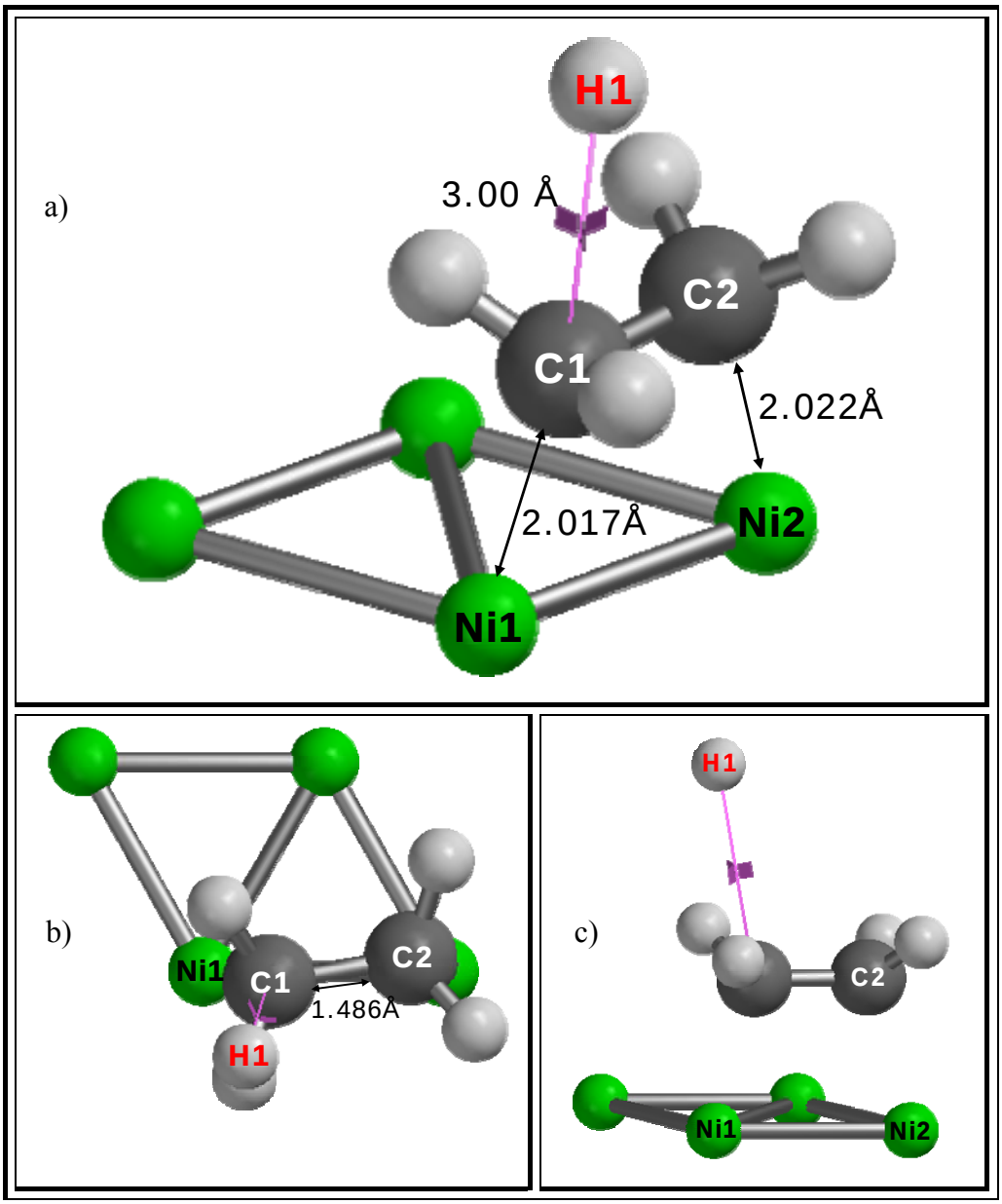

Figure 4.4 Alternative 2 **a)** Starting geometry for adsorbed ethylene reaction with historically called bulk H atom **b)** Top view **c)** Side view

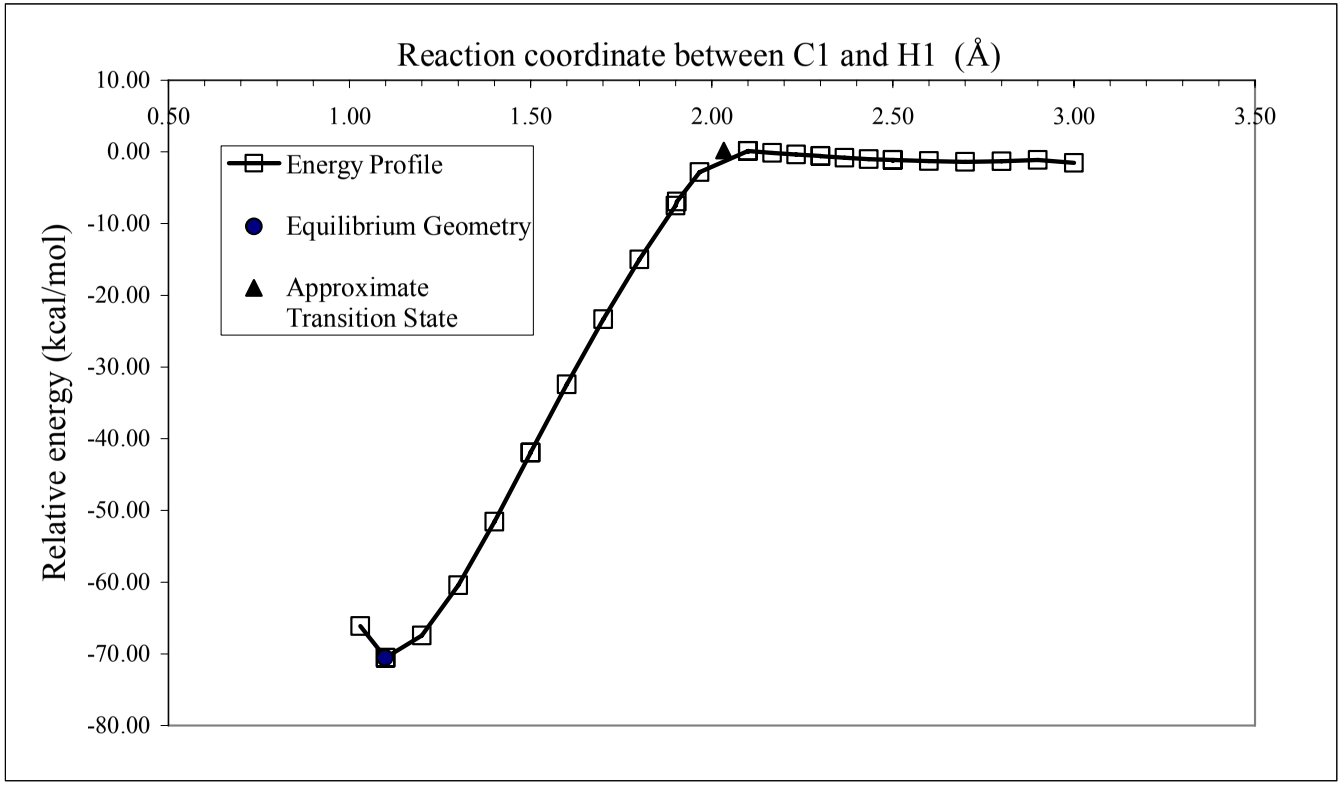

Figure 4.5 Energy profile of Alternative 2 (Bulk hydrogen atom reaction with adsorbed ethylene)

During the calculation, because of the presence of one unpaired electron of hydrogen atom, spin multiplicity of the total system (Ni cluster + ethylene + 1H atom) was selected as two. Relative energy in the y axis of Figure 4.5 was calculated by following the formula where numbers in parenthesis illustrated number of unpaired electrons.

Relative energy = Alternative 2 EP (1) – [Step 1 EG (0) + 1H atom EG (1)]

Approximate transition state geometry and the equilibrium geometry for this step are shown in Figure 4.6 and 4.7, respectively. By expressing transition state as approximate, it was described that this geometry is the one obtained by energy profile calculation whereas; equilibrium geometry is obtained by giving the minimum point of this energy profile as input to the program without holding hydrogen atom and ethylene at constrained distance.

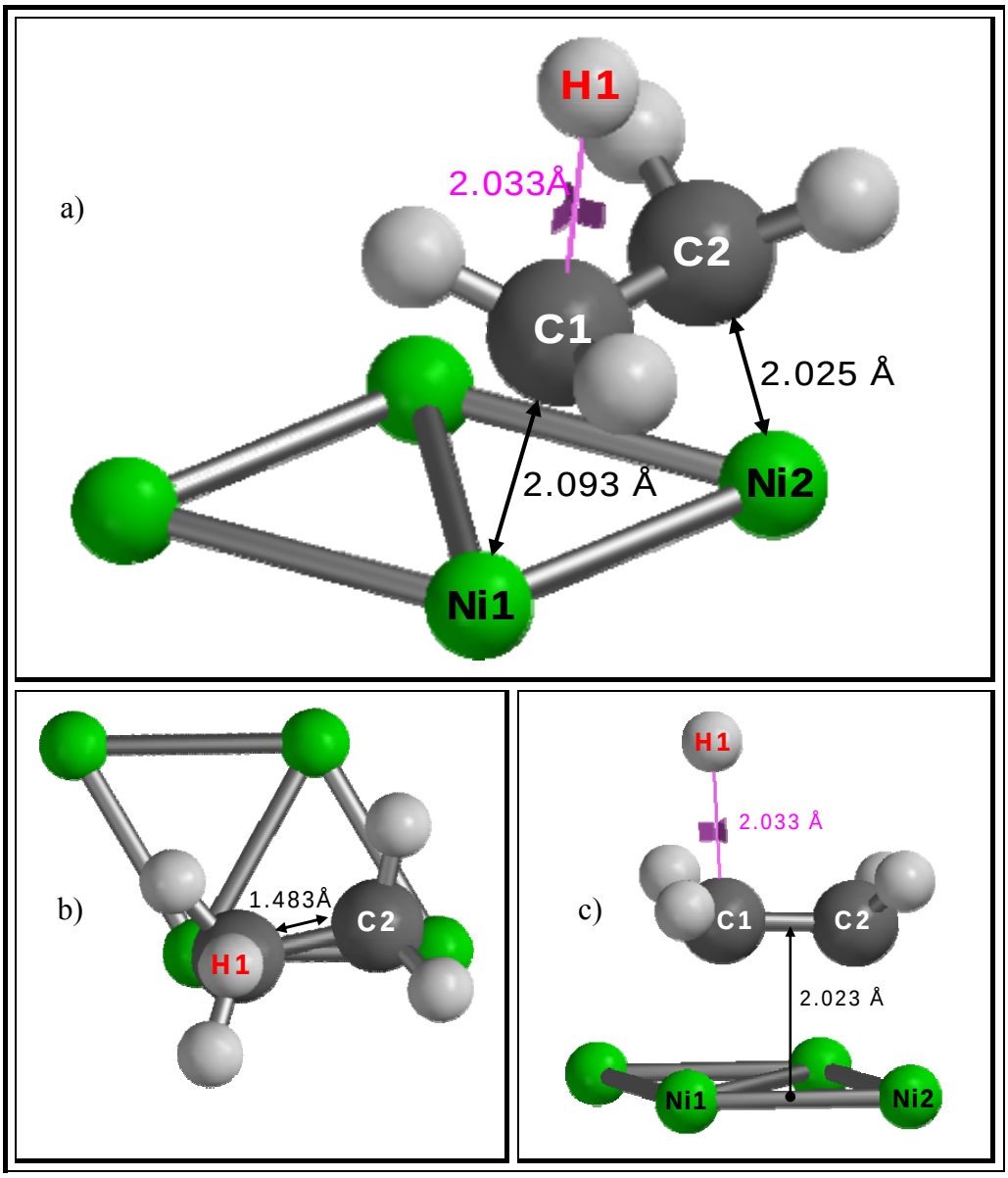

Figure 4.6 Alternative 2 **a)** Approximate transition state geometry **b)** Top view **c)** Side view

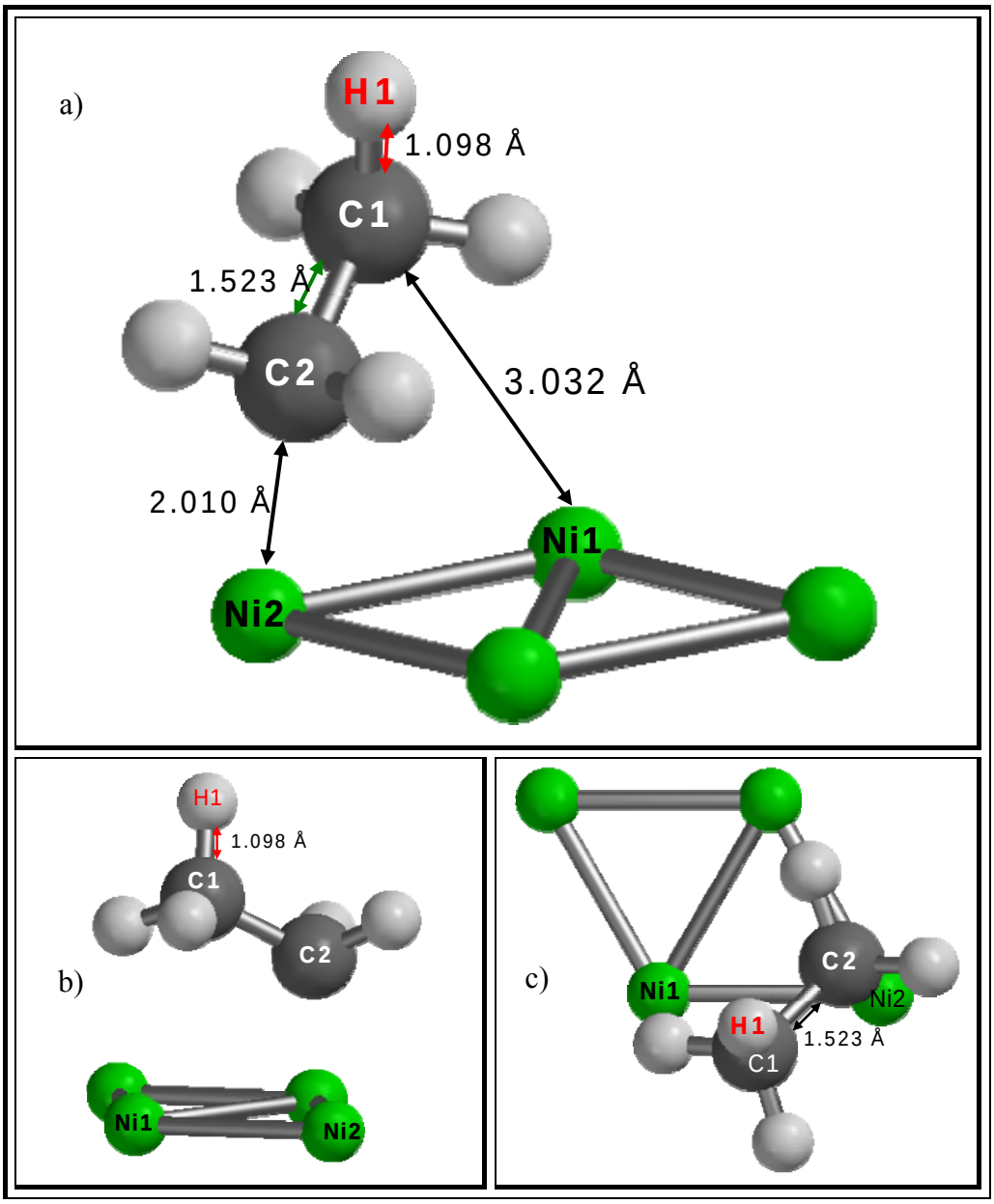

Figure 4.7 Alternative 2 **a)** Equilibrium geometry result of surface ethyl on Ni(111) **b)** Top view **c)** Side view

4.1.2.1.2 Surface Hydrogen Atom Reaction with Adsorbed Ethylene

In this elementary step consideration, first surface hydrogen atom was formed by simple equilibrium geometry calculation. The adsorption site of the hydrogen atom was found as hcp type (Figure 4.8), as mentioned in the literature. This geometry became our input structure for reaction coordinate calculation between surface H atom and adsorbed ethylene. For each point, geometry optimization was done by decreasing this distance gradually with a range of 0.1 Å as in the previous alternative step. Figure 4.9 illustrates the energy profile.

It should be noted that formation of surface hydrogen resulted in exothermic energy of 41.08 kcal/mol. This was why Figure 4.9 did not initiate from the zero relative energy.

The reaction expression can be given as;

$MCH_2\text{-}CH_2M + H_{(s)} \rightarrow M + MCH_2\text{-}CH_3$

Similar to previous possibility for half-hydrogenation of ethylene, spin multiplicity of the total system (Ni cluster + ethylene + 1H atom) was selected as two. Relative energy was given as follows:

Relative energy = Alternative 2' EP (1) – [Step 1 EG (0) + 1H atom EG (1)]

where numbers in parenthesis illustrated number of unpaired electrons.

Transition state geometry and the equilibrium geometry for this step were shown in Figure 4.10 and Figure 4.11, respectively. In this particular step, the most difficult calculation type, that is computation for transition state investigation could be performed.

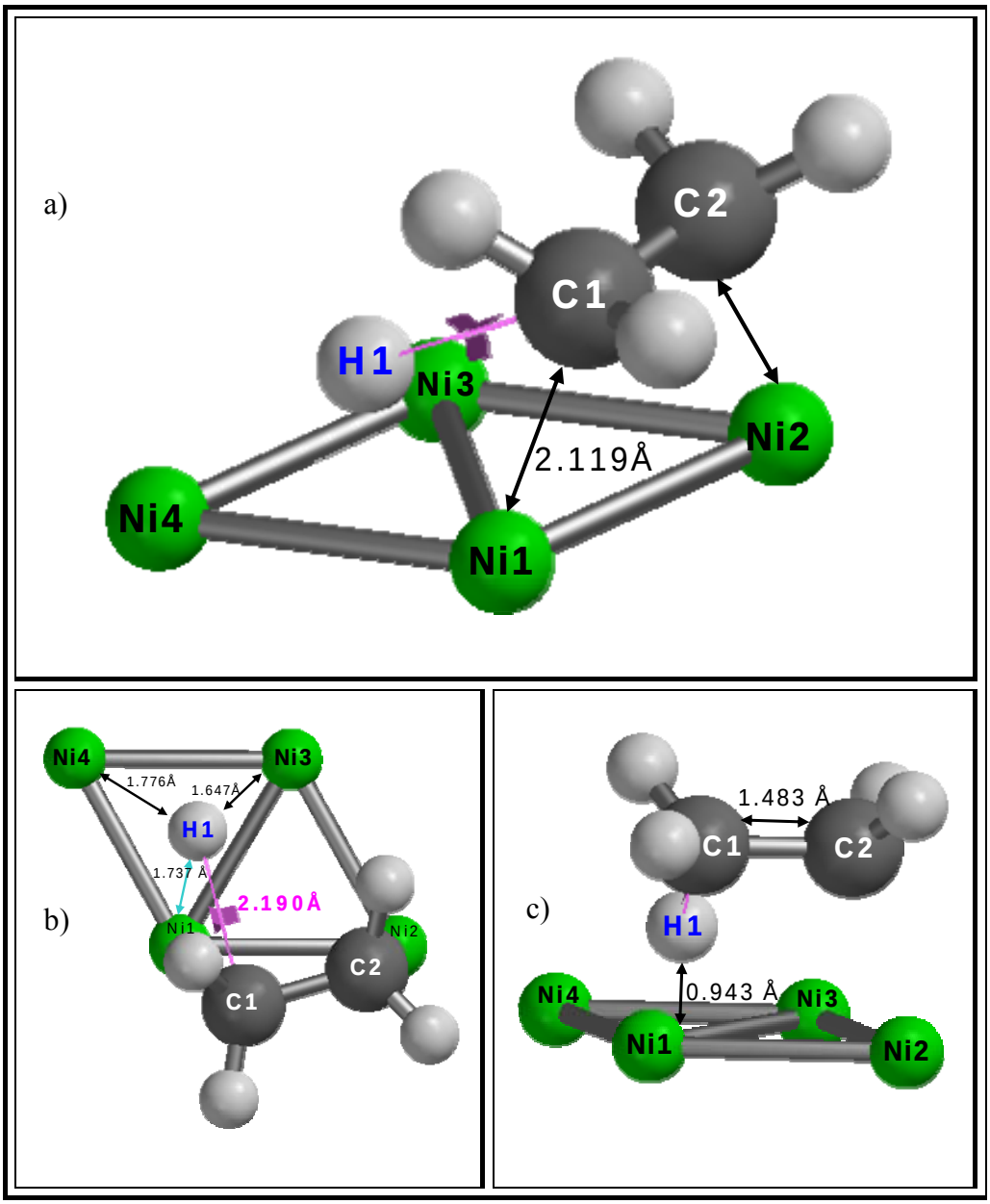

Figure 4.8 a) Equilibrium geometry calculation result for the adsorption of hydrogen on Ni(111) surface containing pre-adsorbed ethylene **b)** Top view **c)** Side view. This geometry was starting point for Alternative 2'- surface hydrogen atom reaction with adsorbed ethylene.

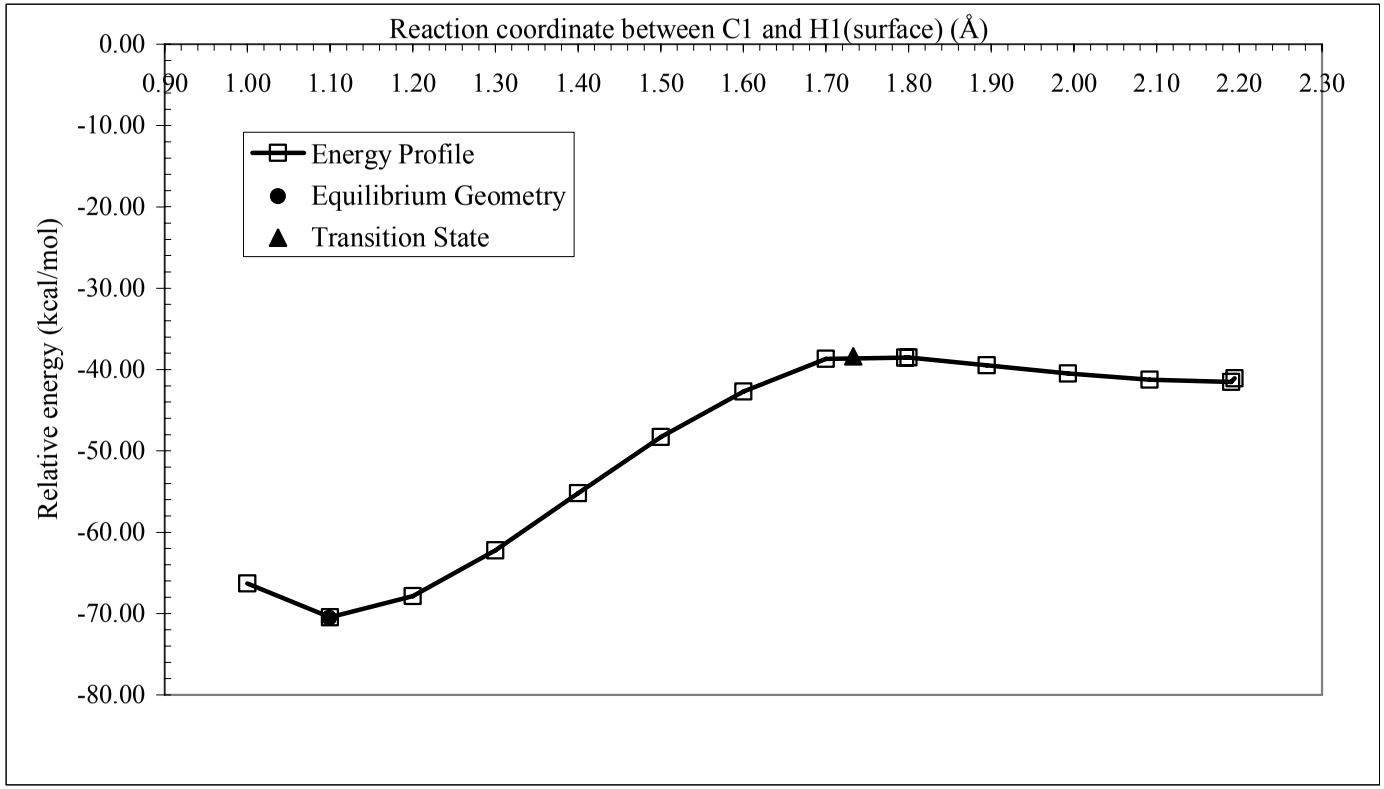

Figure 4.9 Energy Profile of Alternative 2' (Surface hydrogen atom reaction with adsorbed ethylene)

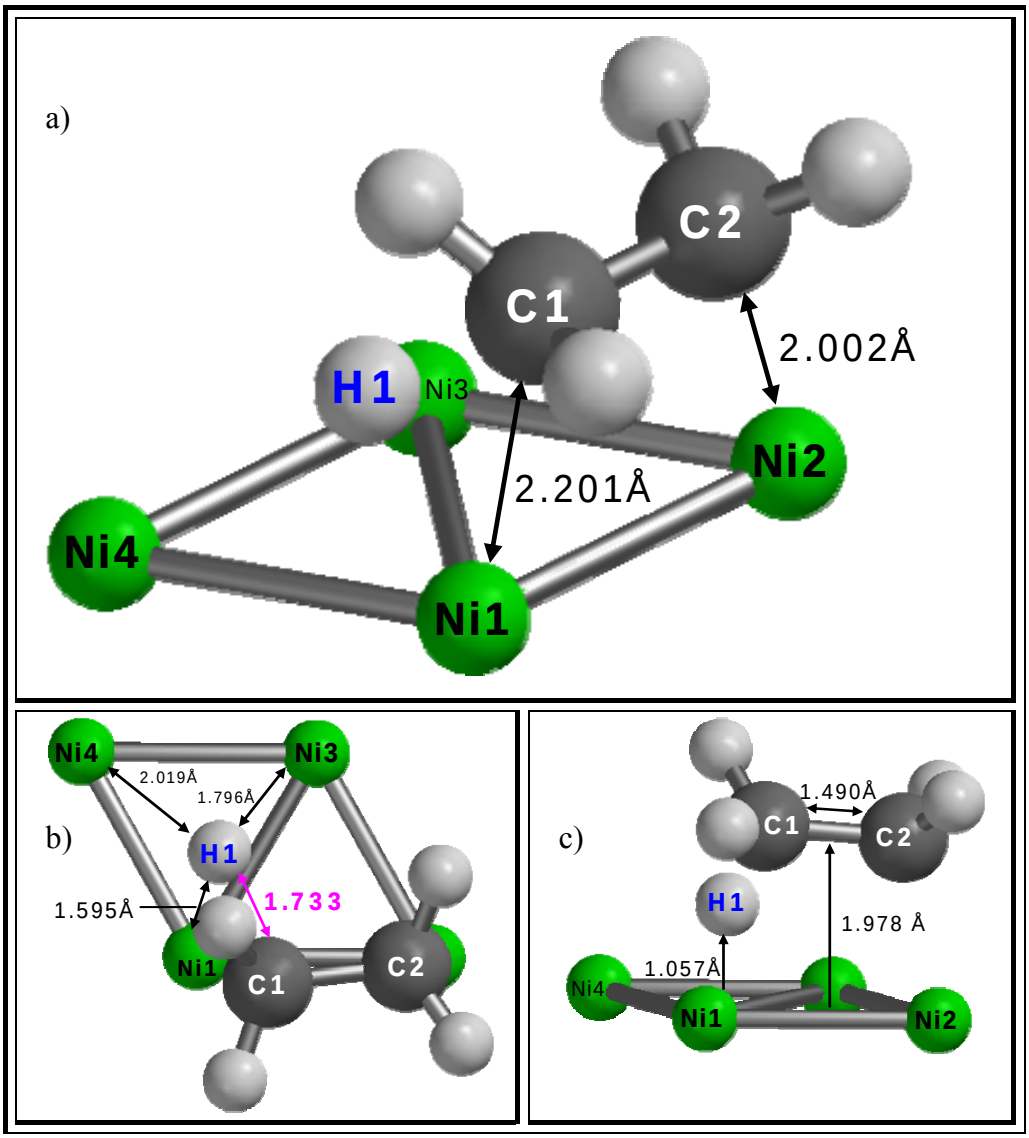

Figure 4.10 Alternative 2' **a)** Transition state geometry **b)** Top view **c)** Side view

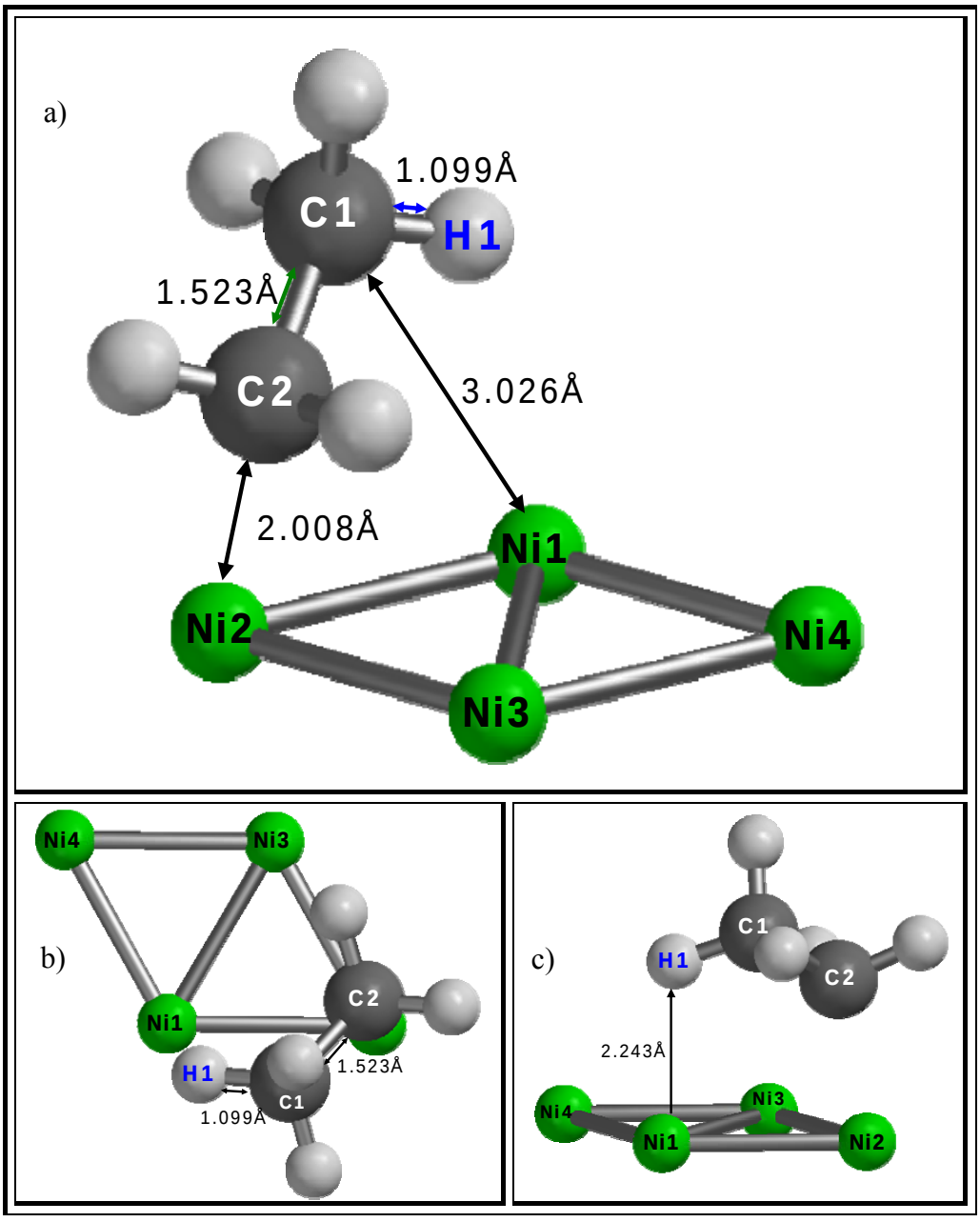

Figure 4.11 Alternative 2' **a)** Equilibrium geometry result of surface ethyl on Ni(111) **b)** Top view **c)** Side view

4.1.2.1.3 Comparison of Bulk Hydrogen and Surface Hydrogen Reactivity towards Adsorbed Ethylene on Ni(111)

As illustrated in Figure 4.5 and Figure 4.9, pre-adsorbed ethylene interaction with bulk hydrogen (Alternative 2) and surface hydrogen (Alternative 2') have occurred with activation barrier of 0.19 kcal/mol and 2.72 kcal/mol, respectively. Therefore, ethylene reaction with bulk hydrogen is much more favorable than with the other one as determined by Ceyer and co-workers (1994, 2001).

Almost non-activated process for Alternative 2 had relative energy of -70.55kcal/mol like heat of 2' reaction of -70.53 kcal/mol. Similarities between theoretically computed heats of reactions of 2 and of 2' conformed that adsorbed ethylene reaction with hydrogen atom was not dependent on path followed, as expected thermodynamically.

Approximate transition state geometry of ethylene reaction with bulk hydrogen (Figure 4.6) and transition state geometry of ethylene reaction with surface hydrogen (Figure 4.10) on Ni(111) resulted C-C and C1-Ni bond distances of 1.483 Å and 2.093 Å; 1.490 Å, and 2.201 Å, respectively. The height of the hydrocarbon complex from surface was a bit closer in Alternative 2 (1.978 Å) then in Alternative 2' (2.023 Å).

Optimization of the minimum point in the energy profiles, shown in Figure 4.7 and Figure 4.11, resulted in C-C bond length of surface ethyl as 1.523 Å for both possibilities. As expected, the increase in this length (C-C bond length of adsorbed ethylene was 1.486 Å) illustrated that bond characteristic had turned from double to single. Moreover, C1, which was reacted with hydrogen atom, departed from the nickel surface since this carbon had shared its unpaired electron with hydrogen atom instead of nickel atom. Final C2-Ni2 bond lengths were very similar: 2.010 Å for Alternative 2 and 2.008 Å for Alternative 2'.

4.1.2.2 Adsorbed Ethyl Convergence to Gas Phase Ethane

As mentioned in literature survey, type of second hydrogen atom which was used for convergence of surface ethyl to ethane has not been known yet whereas the identity of first hydrogen, forming ethylene to surface ethyl was stated as bulk hydrogen atom. Therefore, similar to the second elementary step investigation, two types of hydrogen atoms - bulk and surface hydrogen atoms - were quantum mechanically simulated to react with preformed surface ethyl on Ni(111) surface.

Before initiation of energy profile calculations, formation of surface hydrogen atom was performed by using equilibrium geometry calculations. The adsorption site of the hydrogen atom was found as hcp, as mentioned in the literature.

4.1.2.2.1 Bulk Hydrogen Atom Reaction with Surface Ethyl

The reaction expression can be given as;

$MCH_2\text{-}CH_3 + H_{(b)} \rightarrow M + CH_3\text{-}CH_{3(g)}$

Energy profile calculation was conceived to perform between surface ethyl and unbounded hydrogen atom. Therefore, unbounded hydrogen atom was simulated by directly placing it at certain distance. But, during the calculation, it was observed that this hydrogen atom was required by nickel atoms more than by surface ethyl, that is, this hydrogen atom was adsorbed by surface instead of reacting with surface ethyl. Hence we decided to form a surface hydrogen atom before launching the reaction coordinate calculation. The probable reason could be the formation of vacancy in nickel octets which was previously filled by electrons of ethylene. Input geometry, Figure 4.12, contained a system of surface ethyl and surface hydrogen on Ni-4 cluster and bulk hydrogen atom with a reaction coordinate between H2 and C2. As shown in Figure 4.13, relative energy versus reaction coordinate graph was obtained with respect to results of

both energy profile calculation with step size of 0.1 Å and the equilibrium geometry (EG) calculation. Structure of approximate transition state geometry (Figure 4.14) was calculated by performing closer step sized energy profile computation. Moreover, energy profile graph was ended at C2-H2 distance of 1.900 Å. Because at that distance, surface ethyl with hydrogen complex was departed from Ni(111). Figure 4.15 illustrated the departure with distances of Ni1-C1 as 4.739 Å and Ni2-C2 as 4.153 Å. Therefore, the formation of gas phase hydrocarbon complex was occurred. Hence, reaction coordinate calculation was continued by using this gas phase complex as input file without including nickel cluster. Energy profile of non-catalytic reaction between C2 and H2 was added to catalytic energy profile (Figure 4.13) at the C2-H2 distance of 1.90 Å and final structure for gas ethane molecule was shown in Figure 4.15.

Relative energy was calculated by following the formula where numbers in parenthesis illustrated number of unpaired electrons:

Relative energy =Alternative 3 EP (3) – [Step 3-Input EG (2) + 1H atom EG (1)]

According to this expression, spin multiplicity of the total system was selected as four since there were three unpaired electrons in the total system including equilibrium geometry calculation results of the formation of surface hydrogen atom on ethyl bounded nickel cluster and of one single H atom.

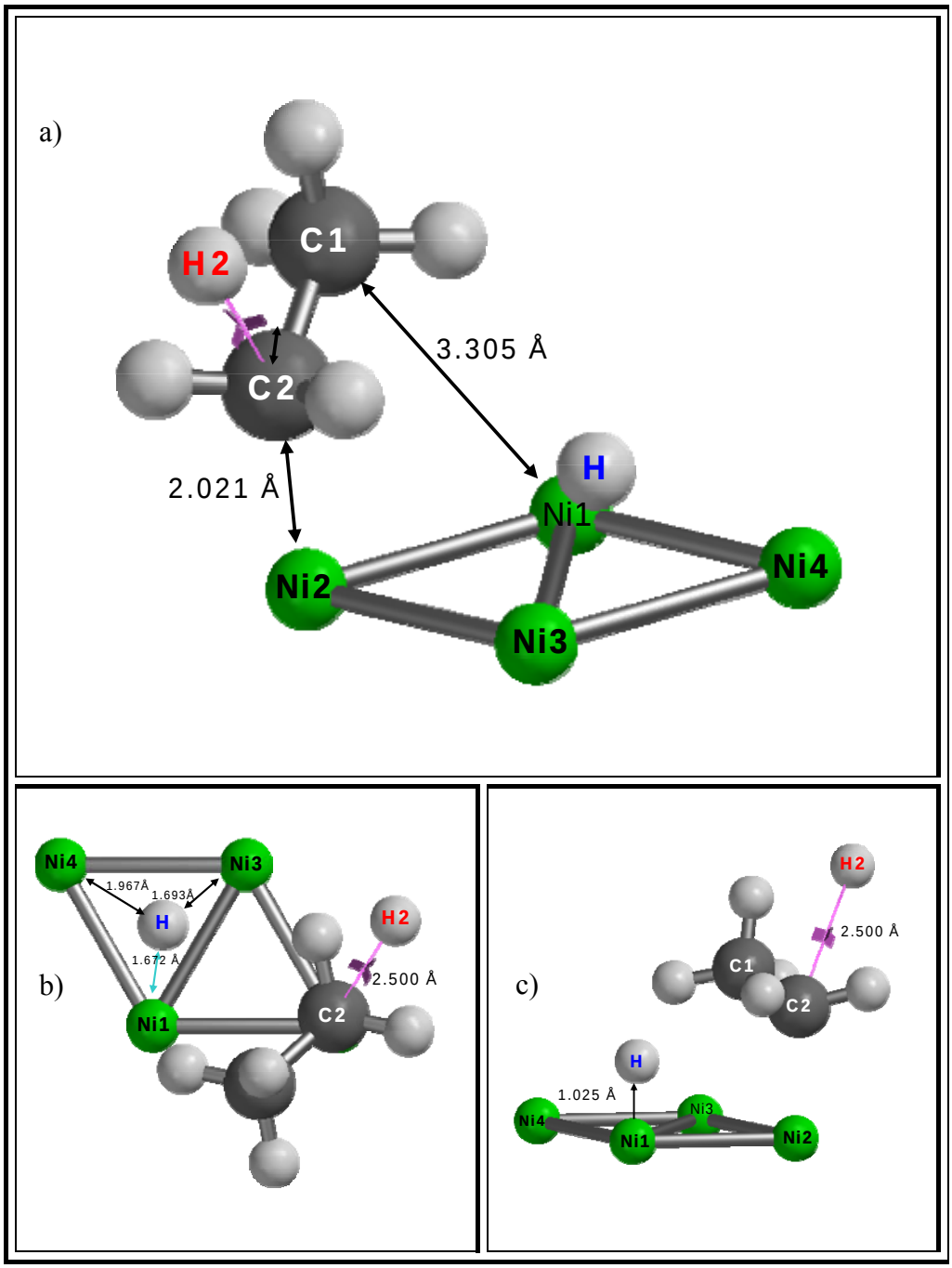

Figure 4.12 Alternative 3 **a)** Starting geometry for preformed ethyl reaction with historically called bulk H atom **b)** Top view **c)** Side view

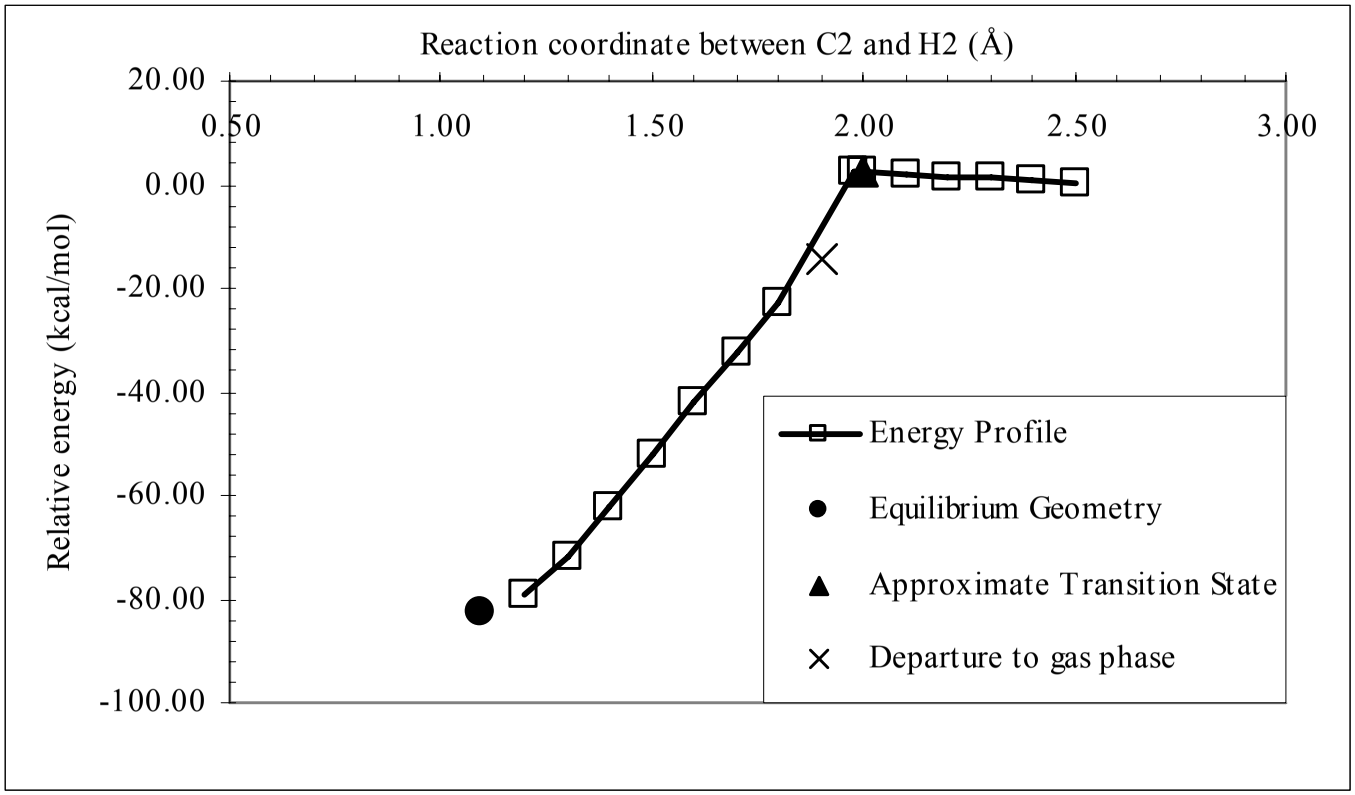

Figure 4.13 Energy Profile of Alternative 3 (Bulk hydrogen atom reaction with surface ethyl)

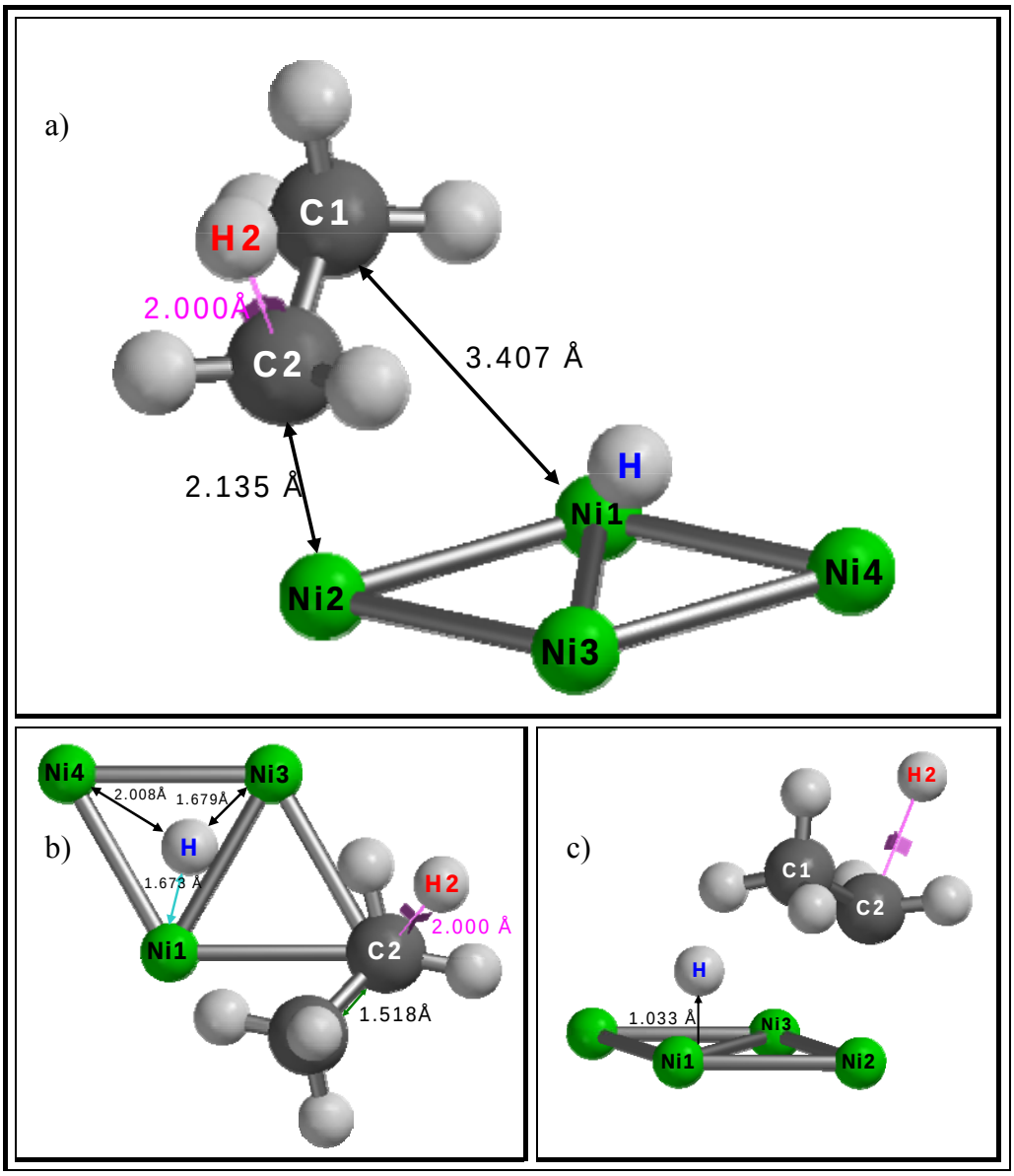

Figure 4.14 Alternative 3 **a)** Approximate transition state geometry **b)** Top view **c)** Side view

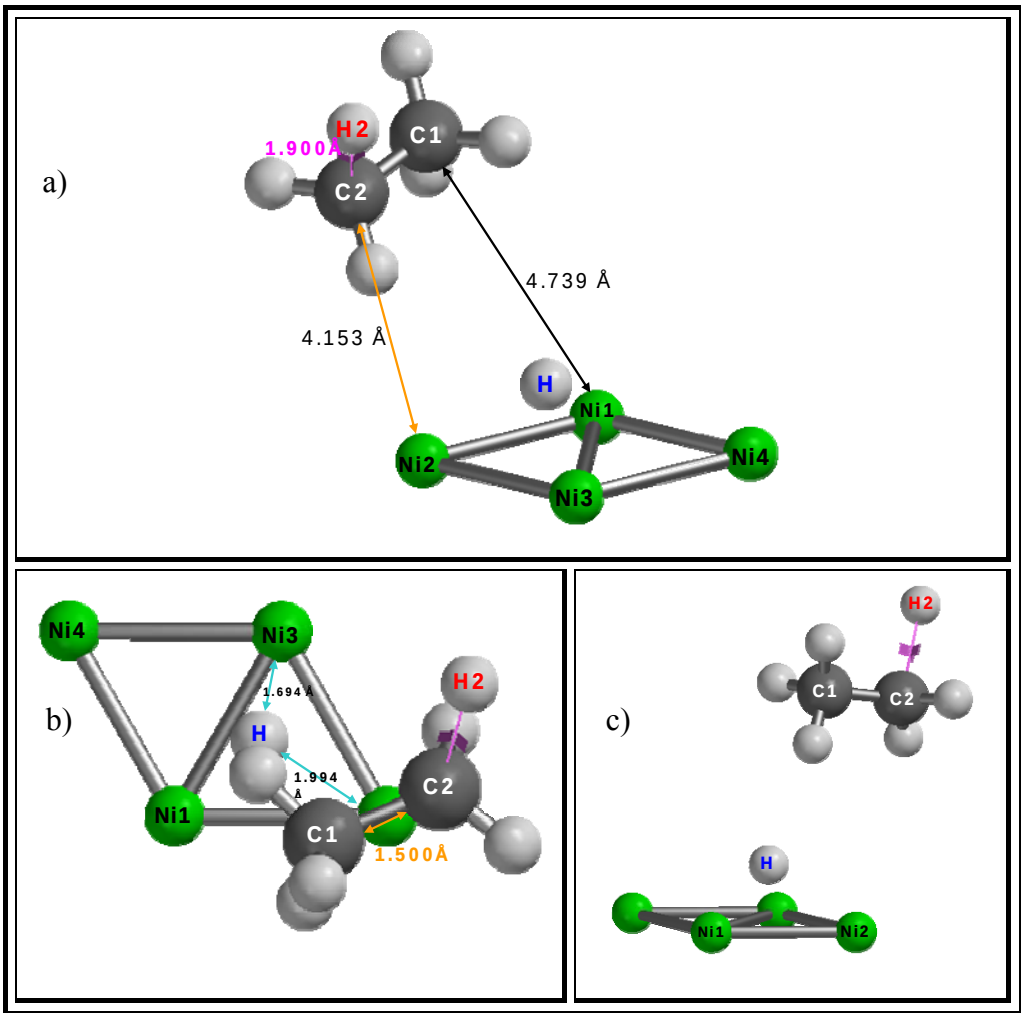

Figure 4.15 Alternative 3 **a)** Departure of hydrocarbon complex to gas phase **b)** Top view **c)** Side view

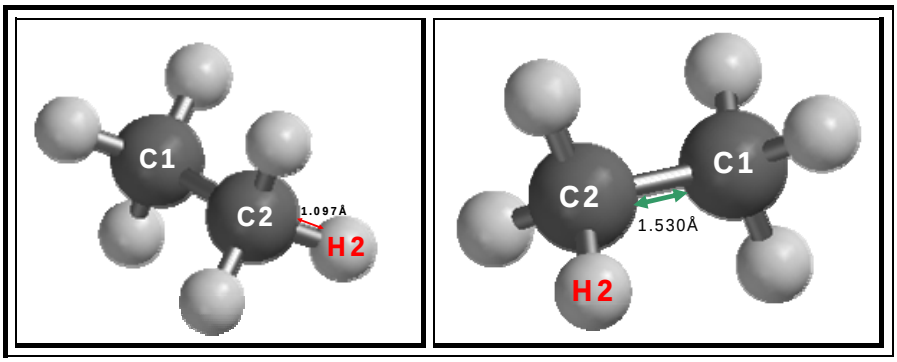

Figure 4.16 Alternative 3: Equilibrium geometry result of gas phase ethane

4.1.2.2.2 Surface Hydrogen Atom Reaction with Surface-bound Ethyl

The reaction expression can be given as;

$CH_3\text{-}CH_2M + H_{(s)} \rightarrow M + CH_3\text{-}CH_3$

In this elementary step consideration, second surface hydrogen atom, shown in Figure 4.17, was reacted with surface-bounded ethyl by virtual calculation of reaction coordinate between H2 and C2. For each point, geometry optimization was performed by decreasing this distance gradually with a step size of 0.1 Å as in the previous alternative step. Figure 4.18 summarized the energy profile graph, showing relative energy changes against reaction coordinate. Relative energy was calculated by the help of the following equation:

Relative energy = [Alternative 3' EP (2)] – [Alternative 3-Input EG (2)]

where numbers in parenthesis illustrated number of unpaired electrons, EP means Energy Profile DFT calculation result and EG means Energy Profile DFT calculation result. As expected, spin multiplicity of the total system was kept as three during computations. Because, subtractions of total number of unpaired electrons of input geometry from of converged geometries should be equal to zero. Transition state geometry and the equilibrium geometry for this step quantitatively expressed on Figure 4.19 and Figure 4.20, respectively.

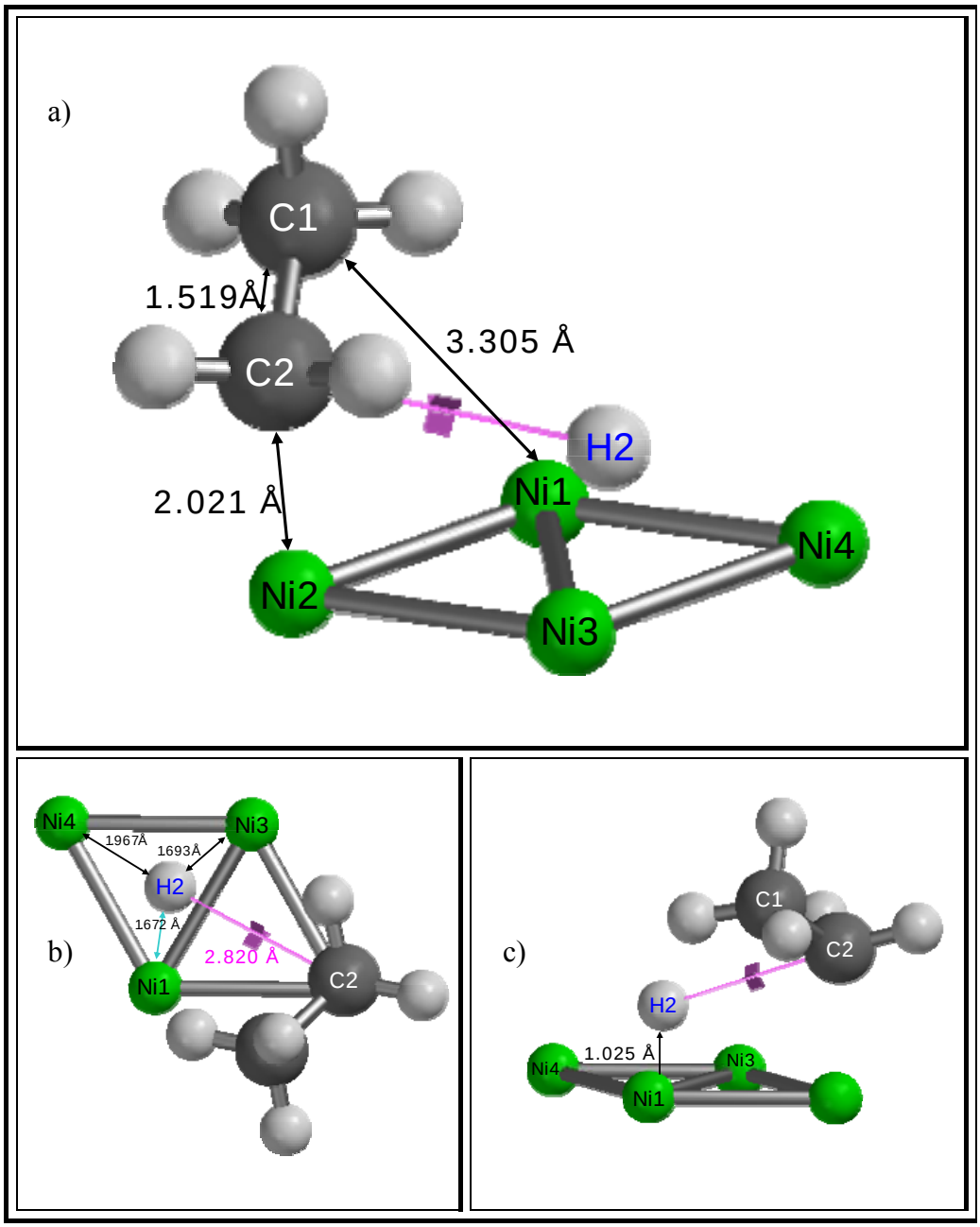

Figure 4.17 a) Equilibrium geometry calculation result for the adsorption of hydrogen on Ni(111) surface containing preformed ethyl **b)** Top view **c)** Side view. This geometry was starting point for Alternative 3'- surface hydrogen atom (H2) reaction with adsorbed ethylene.

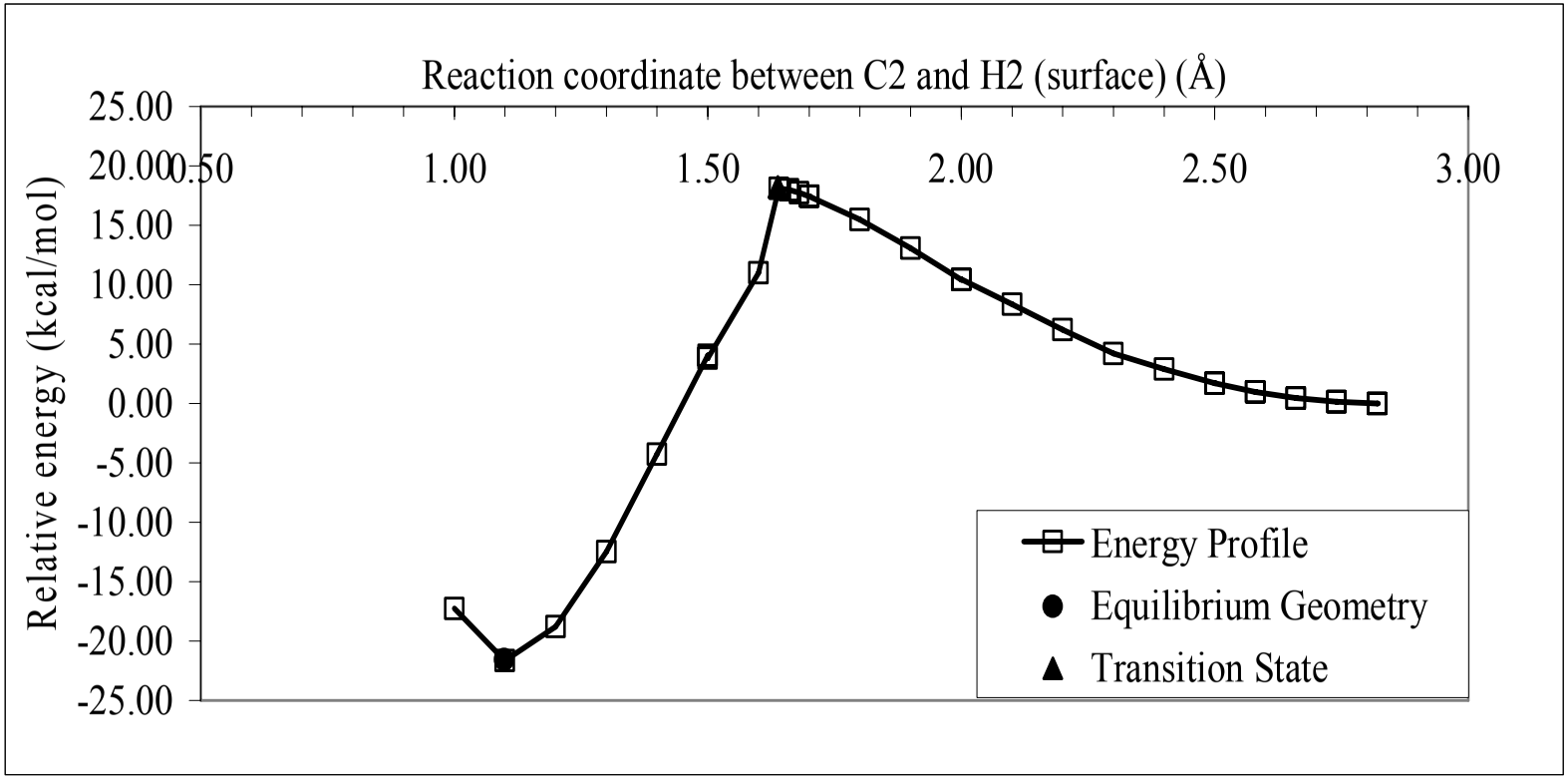

Figure 4.18 Energy profile of Alternative 3' (Surface hydrogen atom reaction with surface ethyl)

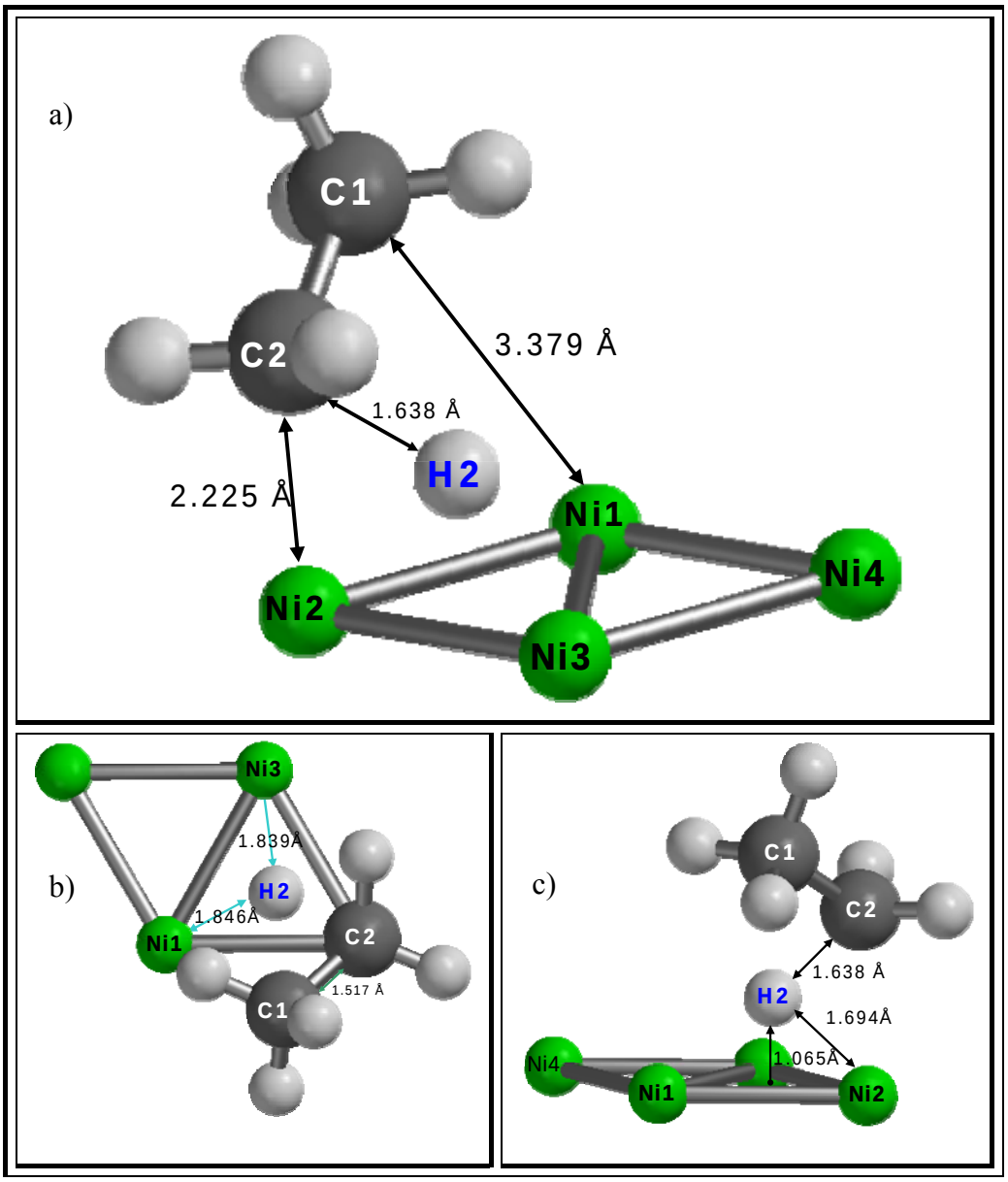

Figure 4.19 Alternative 3' **a)** Transition state geometry **b)** Top view **c)** Side view

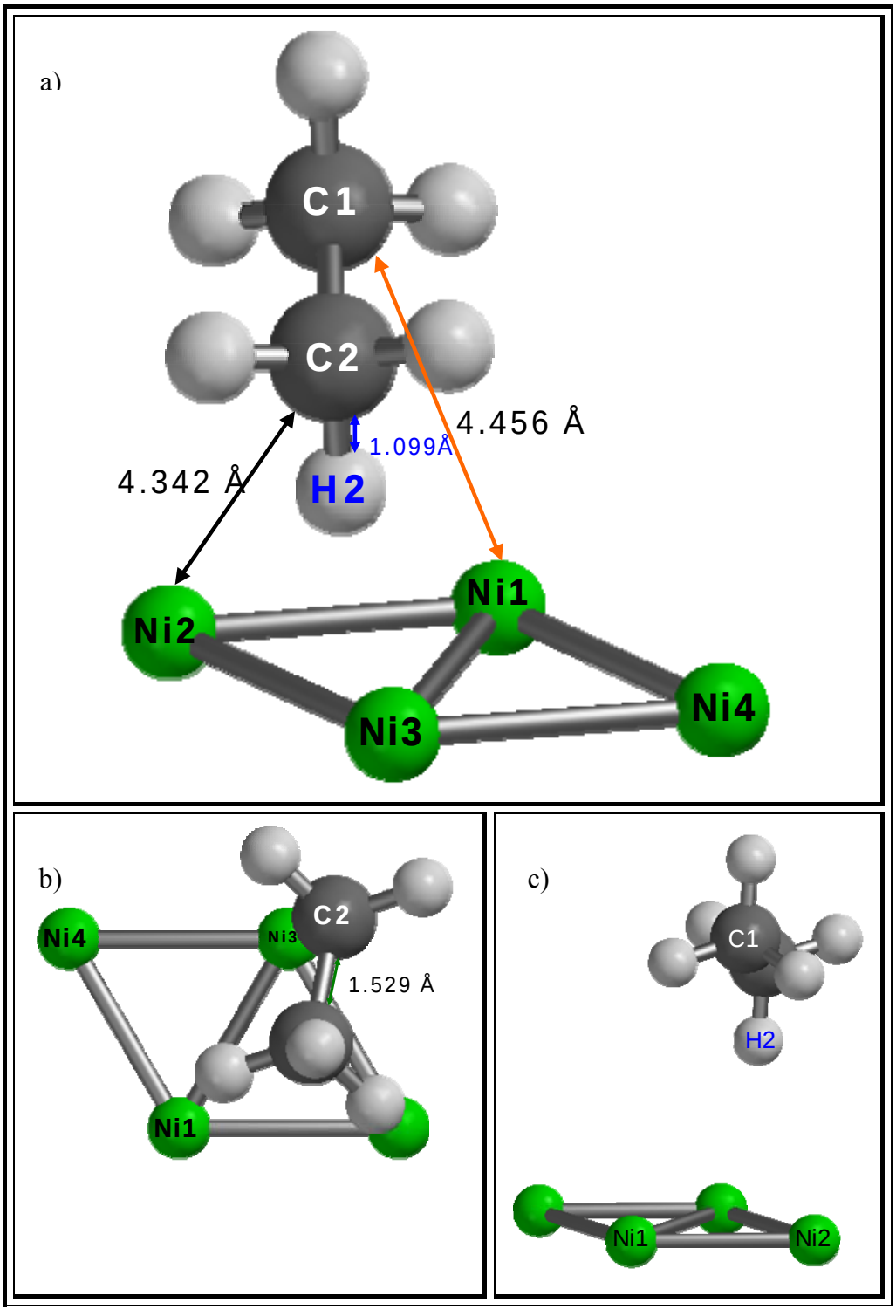

Figure 4.20 Alternative 3' **a)** Equilibrium geometry result of ethane formation on Ni(111) **b)** Top view **c)** Side view

4.1.2.2.3 Comparison of Bulk Hydrogen with Surface Hydrogen Reactivity towards Surface Ethyl on Ni(111)

Coordinate driving calculations indicated that activation for the formation of volatile ethane molecule from bulk hydrogen (2.40 kcal/mol) atom has required rather lower energy than from surface hydrogen atom (18.24 kcal/mol). The resulting heat of reaction for Alternative 3 became -82.58 kcal/mol which was slightly lower than heat of reaction of -77.43 kcal/mol for Alternative 3'. It was concluded that the experimentally unknown form of the second hydrogen atom should be explicitly bulk hydrogen by use of quantum mechanical method of density functional theory.

C-C bond length at transition state geometries of Alternative 3 and of Alternative 3', shown in Figure 4.14 and Figure 4.19, were very close to each other as 1.518 Å and 1.517 Å, respectively. Interaction with surface hydrogen atom marginally elongated the bond distance of C2-Ni2 as compare to with bulk hydrogen atom.

At the end of the global reaction, gas phase ethane C1-C2 and C2-H2 bond lengths were computed as 1.530 Å and 1.097 Å; 1.529 Å and 1.099 Å, respectively, for both alternatives. Hence, the results of both tested elementary steps were almost geometrically identical, as can be expected.

4.1.2.3 Resultant Mechanism for Ethylene Hydrogenation on Ni(111)

Most probable elementary steps for reaction mechanism of ethylene convergence to ethane on Ni(111) surface found by DFT quantum mechanical methods. Firstly, ethylene adsorption on bare Ni (111) surface was performed. In agreement with literature, di-σ bonded ethylene was observed with non-activated adsorption energy of -18.00 kcal/mol. Second step and third step were the formation of ethane from adsorbed ethylene by use of two types of hydrogen atom, separately. The first type was bulk hydrogen atom, representing for hydrogen atoms emerging from the bulk of Ni metal to the surface and the other one was the surface hydrogen atom. It was found that the interaction of first surface ethylene and then surface ethyl radical with surface hydrogen atom have required considerably higher total activation barrier (20.96 kcal/mol) than with bulk hydrogen atom (2.56 kcal/mol). As a conclusion, bulk hydrogen atom was determined to be rather reactive than surface hydrogen atom during the hydrogenation reaction of ethylene on Ni (111). This situation was briefly summarized in Figure 4.21.

By using density functional formalism, global reaction, that is, convergence of ethylene to ethane, result in exothermic energy in the range of 165.98 kcal/mol to 171.0 kcal/mol. By using heat of formation of ethylene and H atom and ethane which were found experimentally by Chase, 1998; Cox et al., 1984 and; Prosen and Rossini, 1945, respectively, heat of global reaction can be calculated as follows:

$CH2=CH2 + 2H \rightarrow CH3\text{-}CH3$

$\Delta H_{rxn} = \Delta H_{f.ethane} - \Delta H_{f.ethylene} - 2\Delta H_{f.hatom}$

$= -20.24 - (+12.54) - 2x(+52.1) = -137.0$ kcal/mol

$\Delta H_{rxn} = \Delta H_{Step\ 1} + \Delta H_{Step\ 2/2'} + \Delta H_{Step\ 3/3'} \approx -169$ kcal/mol

As shown, gas phase reaction of ethylene with two hydrogen atoms brought about energy of -137.0 kcal/mol. Hence our quantum mechanical results were thermodynamically consistent.

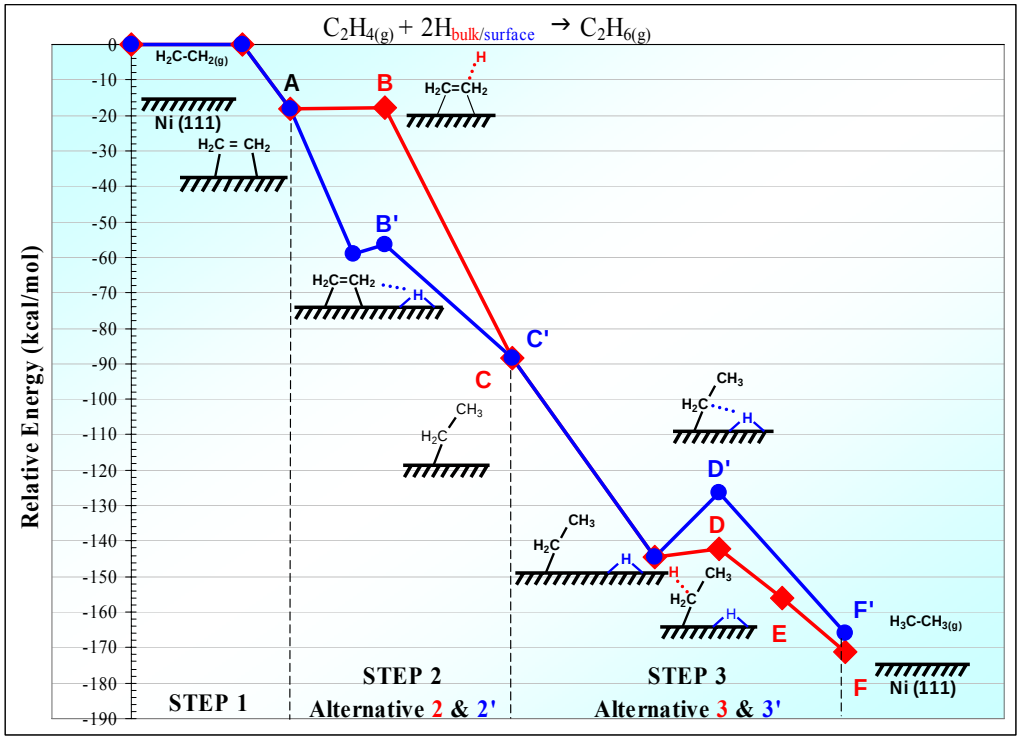

Figure 4.21 Global reaction for ethylene hydrogenation on Ni(111)

4.1.3 Investigation of Ethylene Adsorption on Ni(100)

Ethylene adsorption on Ni(100) was also simulated by utilizing SPARTAN'02 density functional theory B3LYP formalism with 6-31G** basis set. Ethylene was placed at a relevant side of the Ni(100) surface and only equilibrium geometry calculations were performed. The resultant geometry was illustrated in Figure 4.22.

Vattuone et al. (2000) have investigated the adsorption of ethylene and acetylene on Ni(100) and Pd(100) at room temperature by single crystal adsorption calorimetry (SCAC). They reported that ethylene adsorption on Ni(100) initially occured with exothermic energy of 48.75 kcal/mol which decreased rapidly to energy level of 33.94 kcal/mol and remained constant thereafter. Our computational results indicated that ethylene adsorbed molecularly on Ni(100) with adsorption energy of -31.8 kcal/mol agreeing well with experimental value by Vattuone et al. (2000). Moreover, Crispin et al. (1999) performed investigations for this particular adsorption by means of density functional theory utilizing basis set of DNP and they reported adsorption energies of -15 to -27 kcal/mol on different sides of Ni(100). Our result was comparable with that of Crispin et al. (1999), as well.

Ethylene had a side of π-bond with respect to the Ni at the second layer on Ni(100). This result has fitted very well with experimental studies by Zaera and co-workers (1987, 1988 and 1990); by Nishijima et al. (1989) and with theoretical study by Crispin et al. (1999).

Equilibrium geometry calculations exhibited that height of ethylene from surface, average bond lengths of C-Ni and C-H and C-C bond length were found as 1.596 Å, 2.085 Å, 1.102 Å and 1.501 Å, respectively.

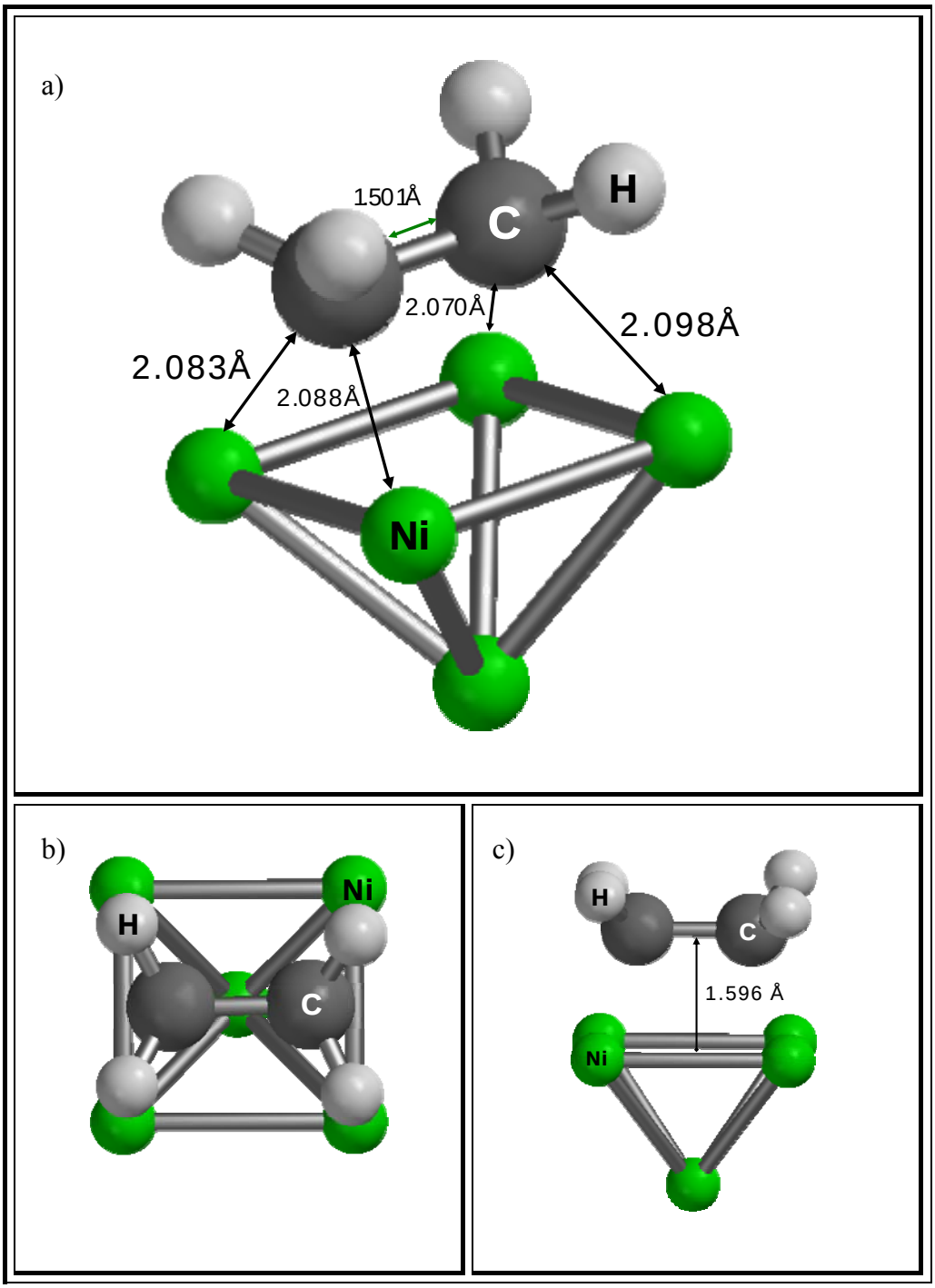

Figure 4.22 a) Equilibrium geometry result of adsorbed ethylene on Ni(100) **b)** Top view **c)** Side view

4.2 Ethylene Interaction with Small Nickel Clusters

4.2.1 Quantum Chemical Investigation of Nickel Dimer

4.2.1.1 Equilibrium Geometry Calculation of Ni_2

Ground state calculations were performed to determine binding energy and bond length of Ni_2 by use of DFT/B3LYP/(modified)6-31G** provided by PQS program. All parameters were kept constant in the input file except the spin multiplicity of the dimer which was changed as one and three.

The calculation for binding energies (eV/atom) for nickel dimer was performed by the following formula:

$$\text{eV/atom} = \frac{\{\text{Binding energy of } Ni_n\} \quad - n \{\text{single Ni atom energy}\}}{n} \qquad (4.1)$$

In the equation 4.1, above, n was the number of atoms involved in the clusters. Therefore, this formula could be, also, used for binding energy calculations of Ni_{13} and Ni_{55} clusters. It should be noted that energy of single nickel atom was also needed for the binding energy calculations. Hence, single Ni atom was also simulated and the same theoretical method was utilized. Its spin multiplicity was found as three.

A comparison of the calculated values of bond length, binding energies and vibration frequencies for Ni_2 dimer with those reported in both experimental and theoretical literature was given in Table 4.3. Ni_2 experimental binding energy and bond length were in the range of 0.933 eV/atom to 1.19 eV/atom and 2.10 Å to 2.30 Å, respectively. The most recent theoretical calculations of nickel dimers were achieved by Chen et al. (1999 and 2002) and by Calleja et al. (1999) using DFT/BLYP, DFT/NRLMOL-3 and ab initio DFT methods respectively. They

have found binding energies of 1.43 eV/atom, 1.22 eV/atom, and 1.199 eV/atom, and bond lengths of 2.12 Å, 2.14 Å and 2.17 Å, respectively. It can be concluded that the binding energy of 1.078 eV/atom and bond length of 2.278 Å obtained in this study can be favorably compared with experimental and theoretical data. Ni_2 dimer was calculated having neutral charge with triplet spin multiplicity as suggested theoretically by Chen et al (2002), Calleja et al. (1999), Castro et al. (1997) and Reuse and Khanna (1995). The vibration frequency has been found as 275 cm^{-1} which was comparable with Moskovits and Hulse (1977) experimental value of 330 cm^{-1}.

Table 4.3 Semi-empirical and density functional theory computation results for Ni_2 dimer together with available theoretical and experimental studies.

	The authors	Method	B.E.(eV)/atom	Distance, Å	Vibration (cm^{-1})
Theoretical	Grigoryan and Springborg (2003)	EAM	1.81	2.12	
	Chen et al.(2002)	DFT/NRLMOL-3	1.43	2.12	
	Michelini et al.(2001)	DFT		2.13	
	Chen et al.(1999)	DFT/BLYP	1.22	2.14	
	Calleja et al.(1999)	ab initio	1.199	2.17	
	Castro et al. (1997)	VWN	1.82	2.05	354
		GGA (P86)	1.74	2.1	337
		GGA-NS	1.18		
	Lathiotakis et al. (1996)	TB-MD	0.93	2.2	254
	Reuse and Khanna (1995)	DFT/LSD	1.61	2	
	Mlynarsky ans Salahub (1991)	LDA	1.82	2.03	
		NL	1.44	2.11	
	Tomonari et al. (1986)	SCF	0.238	2.3	
		CI	1.39	2.3	
	Basch and Newton (1980)	SCF	0.457	2.33	
		CI	0.713	2.33	
		DFT/B3LYP (SM3)	1.078	2.278	275
Experimental	The authors		B.E.(eV)/atom	Distance, Å	Vibration (cm^{-1})
	Chen et al. (1999)		1.045	2.16	
	Nour et al. (1987)		1.04	2.2	
	Morse et al. (1984)		1.034 ± 0.005	2.155 ± 0.005	
	Handbook of Chem&Phys.(1980)		1.18	2.1	
	Basch and Newton (1980)		0.933	2.24 ± 0.04	
	Ahmed and Nixon (1979)				380.9
	Moskovits and Hulse (1977)				330
	Kant (1964)		1.19	2.3	

4.2.1.2 Ethylene Adsorption on Single Ni atom and on Ni_2 Dimer

Energy adsorption on single Ni atom has been performed on singlet potential surfaces for $Ni(C_2H_4)$. It was theoretically observed that π-bonded ethylene was formed on single Ni atom with adsorption energy of -14.35 kcal/mol, fitting very well with a CASSCF calculation of -14.20 kcal/mol by Widmark et al. (1985). As it was evident from Figure 4.23, an excellently symmetrical equilibrium geometry structure in terms of bond lengths was obtained. The computed C-C, C-H and Ni-C bond distances were 1.462 Å, 1.094 Å and 1.818 Å, respectively, showing very good agreement with respective bond lengths of 1.094 Å, 1.461 Å, 1.816 Å from recent DFT study at the level of B3LYP with basis set of 6-31G** by Alexander and Trevor (2004).

$Ni_2(C_2H_4)$ complex was also investigated by means of density functional theory. The system spin multiplicity was found as three providing relative energy of -42.94 kcal/mol which was comparable with CASSCF binding energy of -27.2 kcal/mol by Ozin et al. (1978). As in the previous case, π-bonded form of ethylene had perfectly symmetrical equilibrium geometry with respect to Ni atoms, as illustrated in Figure 4.24. C-C, C-H, Ni-C and Ni-Ni bond lengths were calculated as 1.407 Å, 1.089 Å, 1.968 Å and 2.138 Å, respectively.

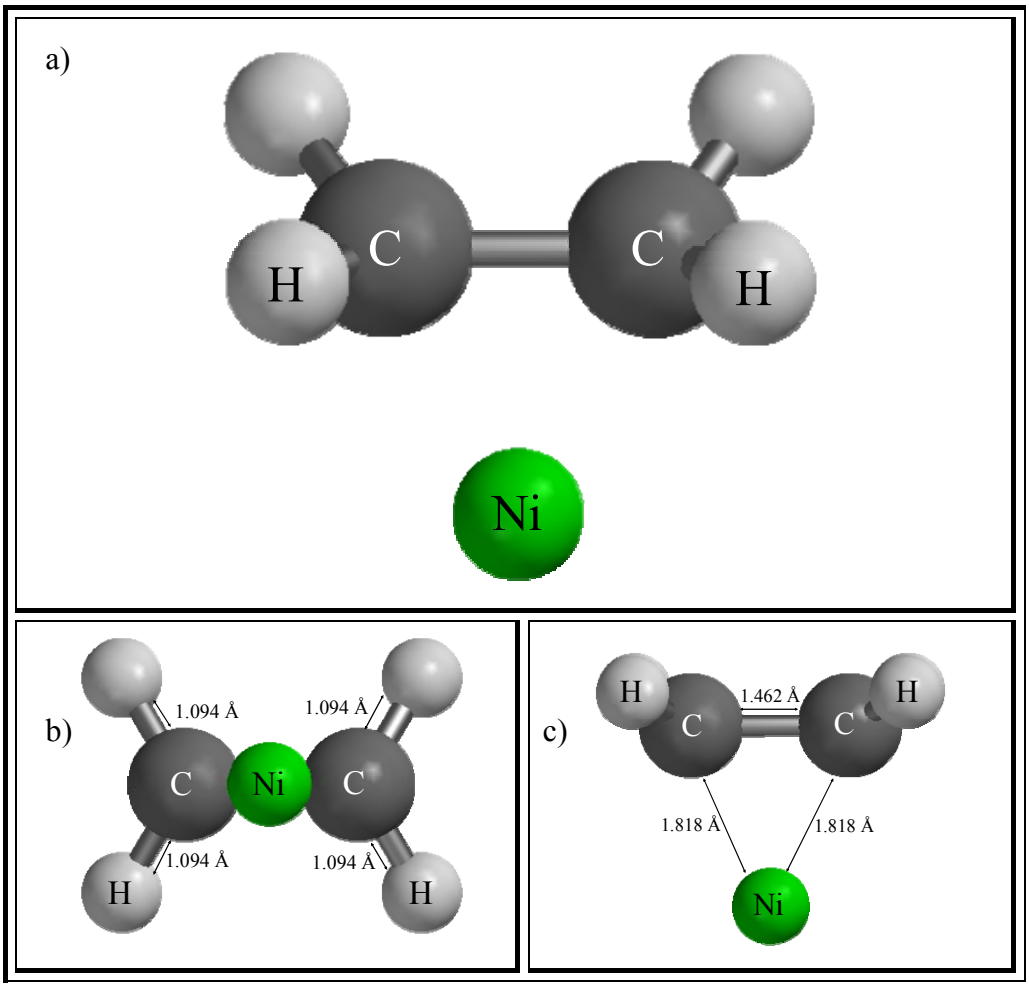

Figure 4.23 a) Equilibrium geometry structure for $Ni(C_2H_4)$ **b)** Top view **c)** Side view

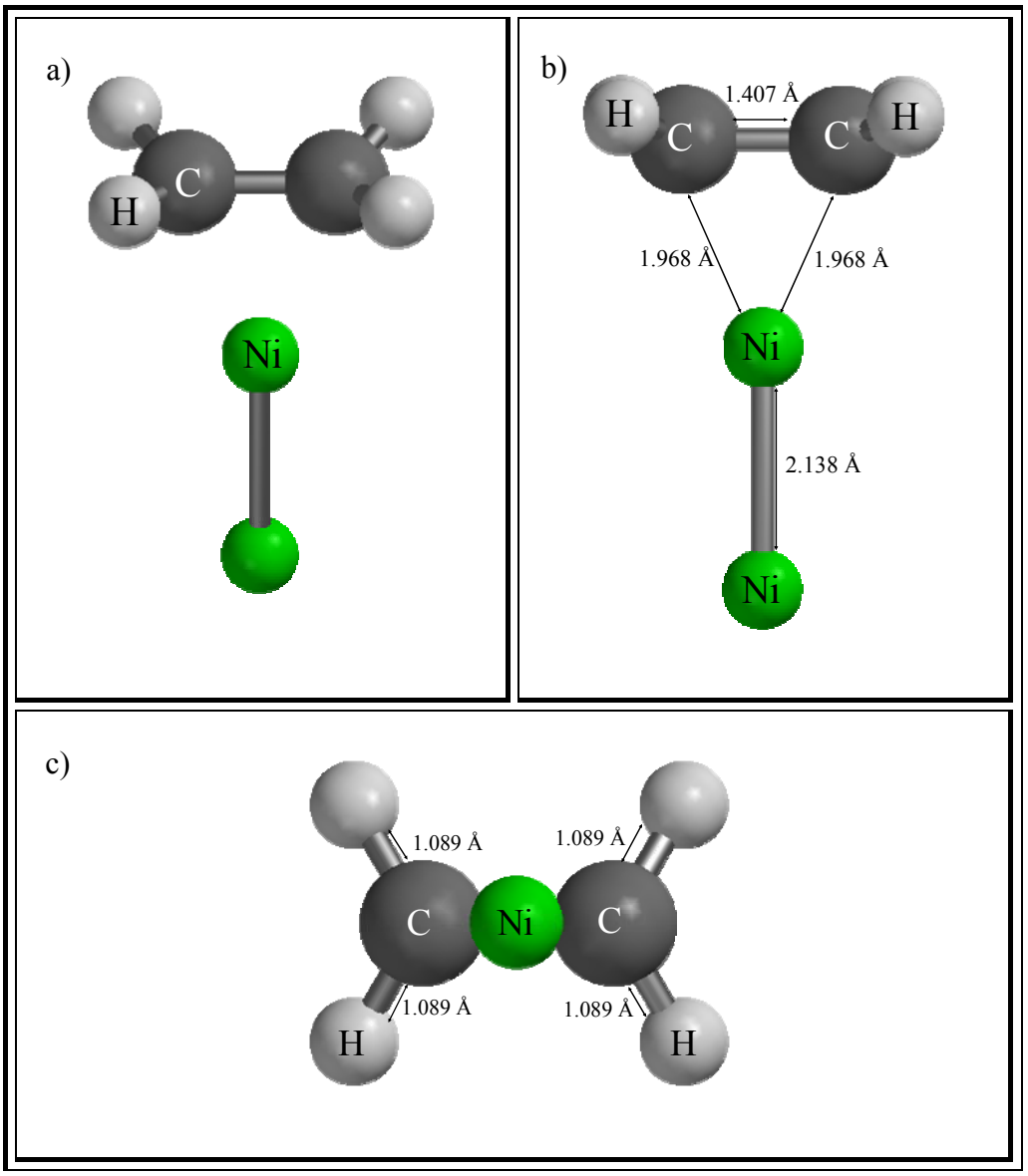

Figure 4.24 Equilibrium geometry structure for $Ni_2(C_2H_4)$ **b)** Top view **c)** Side view

4.2.2 Quantum Chemical Investigation on Ni_{13} Nanocluster

4.2.2.1 Optimization of Ni_{13} Cluster

The first magic number cluster following nickel dimer is Ni_{13}. Magic number clusters are in general constructed by surrounding one single metal atom with metal atom layers by obeying the formula suggested by Schmid et al., (1990); the total number of atoms, y, for the nth layer, $y = 10\ n^2 + 2$. Hence, Ni_{13} cluster was developed by surrounding one single nickel atom with 12 nickel atoms conforming with Mackay icosahedral structure as suggested theoretically by Northby (1987), Raghavan et al. (1989), Stave and DePristo (1992), Pellarin et al. (1994), Lathiotakis et al. (1996) and experimentally by Nayak et al. (1997). Semi-empirical PM3 method calculations were then performed in order to have a more precise structure to be used as a first guess in DFT calculations.

Similar to nickel dimer optimization calculations, different spin multiplicities were utilized in order to find the most stable nanocluster by using density functional theory with B3LYP formalism and m6-31G** basis set. A spin multiplicity was determined of 9, matching Calleja et al. (1999) theoretical suggestion. Equilibrium geometry calculation was given in details in Appendix C. Table 4.4 compares the available theoretical literature data in terms of binding energy and bond lengths with the values obtained in our calculations. Similar to Ni_2, Ni_{13} binding energy was found by use of the equation 4.1. All of the methods indicated an IC structure for Ni_{13} as obtained in our calculations given in Figure 4.25. It can be also observed that the results reported by Calleja et al. (1999) using DFT method match our results much better when compared with other theoretical methods that did not use an advanced quantum chemical method such as DFT. Our calculations showed that optimum geometry of Ni_{13} cluster had the binding energy of 2.70 eV/atom, the bond length of 2.37 Å (center-to-vertex) and of 2.49 Å (vertex-to-vertex) which were consistent with Calleja et al. (1999) theoretical results of 2.76 eV/atom, 2.41 Å and 2.53 Å.

Table 4.4 Theoretical studies for IC Ni_{13} cluster

The authors	Method	B.E (eV)/atom	Distance (Å)
Grigoryan and Springborg (2003)	EAM	3.38	2.36 (c-v)/2.48 (v-v)
Luo (2002)	TB-MD	2.99	2.383 (mean)
Calleja et al. (1999)	ab initio DFT	2.757	2.41 ± 0.03 (c-v)
			2.53 ± 0.03(v-v)
Lathiotakis et al. (1996)	TB-MD	3.16	2.57
		fcc 2.73	fcc 2.48
Reuse and Khanna (1995)	DFT/LSD	4.26	2.23 (c-v)/2.34(v-v)
Raghavan et al.(1989)	CEM	2.72	2.25
This study	DFT / B3LYP / m6-31 G** with SM9	2.70	2.371±0.004 (c-v)
			2.493±0.002 (v-v)

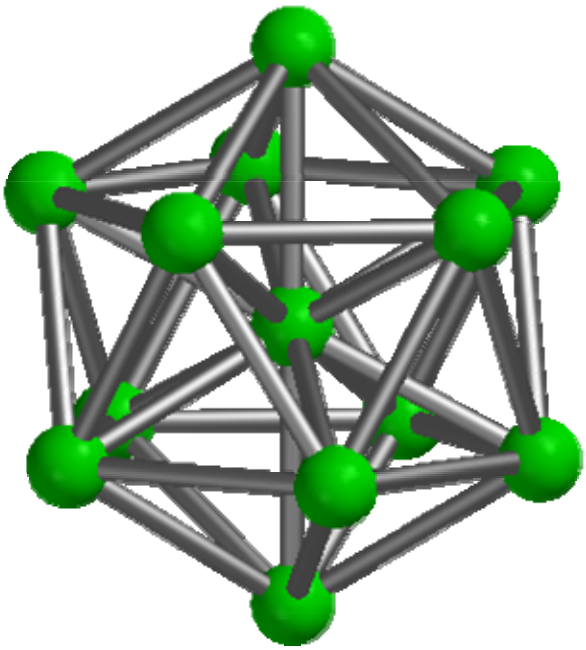

Figure 4.25 Icosahedral structure of Ni_{13} Nanocluster (Center atom has a coordination number of 12 whereas the surface atoms are 6 coordinated)

The parameter of $n^{-1/3}$, where n is the number of atoms in the cluster, has a linear relationship with binding energy of clusters. This parameter is an effective surface volume ratio. It allows mapping all particle sizes from the single atom to the bulk into the one picture. The intercept of the resulting line with the binding energy axis gives estimation for theoretically probable binding energy of bulk nickel at an infinite number of atoms. In this study, the computed binding energies of Ni_2 dimer and Ni_{13} nanocluster were used for investigating the above correlation. These findings are compared with experimental and theoretical literature values as shown in Figure 4.26.

Theoretical binding energies of 2-atom, 13-atom and 55-atom nickel clusters and their resultant intercepts were summarized in Table 4.5. Figure 4.26 and Table 4.5 included also bulk nickel experimental binding energy of 4.45 eV/atom determined by Voter and Chen (1987). Based on the intercepts, the best correlation result was performed by Luo (2002) who studied nickel clusters with atom numbers 3 to 55. Most probable reason could be that utilization of results for two magic numbered clusters, i.e. Ni_{13} and Ni_{55} nanoclusters provided more precise correlations than the utilization a nickel dimer and Ni_{13} nanocluster. It should be noted that, Lathiotakis et al. (1996) also used TB-MD method but their theoretical data resulted in over-estimated bulk value of 5.69 eV/atom. Here, the techniques used during the calculations really affected the accuracy of the results. That is, Lathiotakis et al. (1996) used minimal parameter tight binding molecular dynamics whereas Luo (2002) preferred tight binding molecular dynamics with the simulated annealing technique, achieving a value of 4.45 eV/atom.

A comparison of both our DFT/B3LYP/m6-31G** and Calleja's (1999) DFT result 4.56 eV/atom and 4.57 eV/atom, indicates good agreement with the experimental bulk binding energy value of 4.45 eV/atom by Voter and Chen (1987).

Table 4.5 Recent theoretical binding energies for Ni_2 dimer, Ni_{13} and Ni_{55} nanoclusters and their probable binding energies for bulk nickel (intercept)

The authors	Method	Ni_2 B.E (eV)/atom	Ni_{13} B.E (eV)/atom	Ni_{55} B.E (eV)/atom	Intercept (eV)/atom
Grigoryan and Springborg (2003)	EAM	1.81	3.38	3.83	4.93
Luo (2002)	TB-MD with the simulated annealing technique		2.99	3.55	4.45
Calleja et al. (1999)	ab initio DFT	1.199	2.757		4.56
Lathiotakis et al. (1996)	TB-MD with minimal parameter	0.93	3.16	4.10	5.69
Reuse and Khanna (1995)	DFT/LSD	1.61	4.26		7.32
Present study	DFT / B3LYP / m6-31 G** with SM9	1.078	2.70		4.57
Voter and Chen (1987)	EXPERIMENTAL				4.45

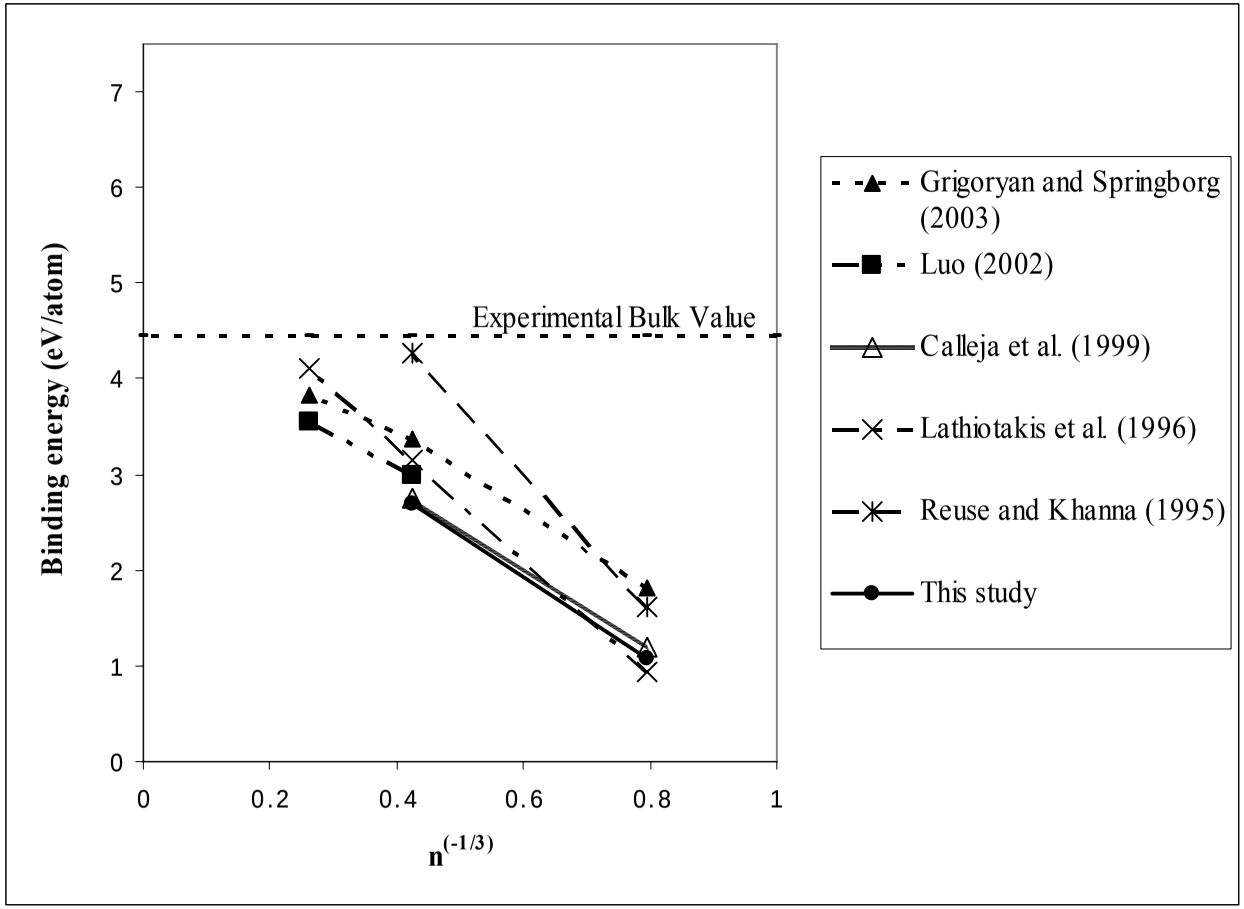

Figure 4.26 Binding energy variations (n is the number of atoms)

4.2.2.2 Ethylene Adsorption on Ni_{13} Cluster

Ethylene adsorption on Ni_{13} cluster was also studied quantum mechanically. Only equilibrium geometry calculations were performed to make energetic comparison with single crystal surfaces by utilizing SPARTAN'02 density functional theory B3LYP formalism with 6-31G** basis set.

It was found that ethylene adsorbed molecularly on Ni_{13} nanocluster with adsorption mode of di-σ, as shown Figure 4.27. The system spin multiplicity of 9 was determined to be correct value. Average C-Ni and C-H bond lengths, C-C bond distance and the height of ethylene from the surface were calculated as 1.946 Å, 1.098 Å, 1.489 Å and 1.88 Å, respectively. The resultant energy of ethylene adsorption on Ni_{13} cluster was -43.42 kcal/mol.

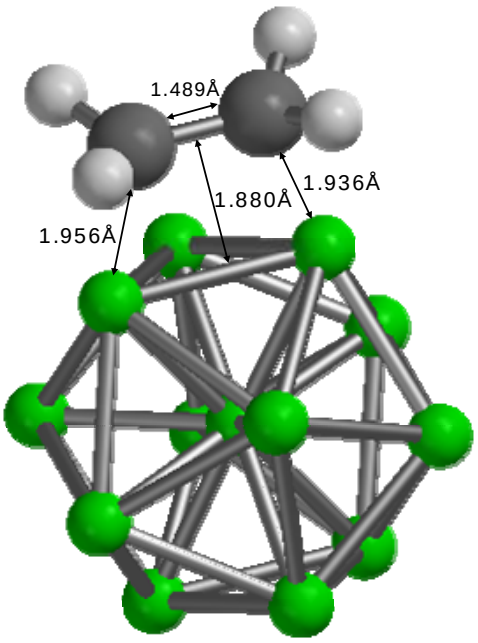

Figure 4.27 Equilibrium geometry structure of adsorbed ethylene on Ni_{13} nanocluster

4.2.3 Quantum Chemical Investigation of Ni_{55} nanocluster

The ground state equilibrium geometry calculation of Ni_{55} nanocluster was performed by semi-empirical PM3 formalism. The most significant result of our study was icosahedral structure of Ni_{55} (Figure 4.28) which was suggested experimentally by Parks et al. (1991), and Pellarin et al. (1994), and theoretically by Lathiotakis et al. (1996), Luo (2002) and Grigoryan et al. (2003).

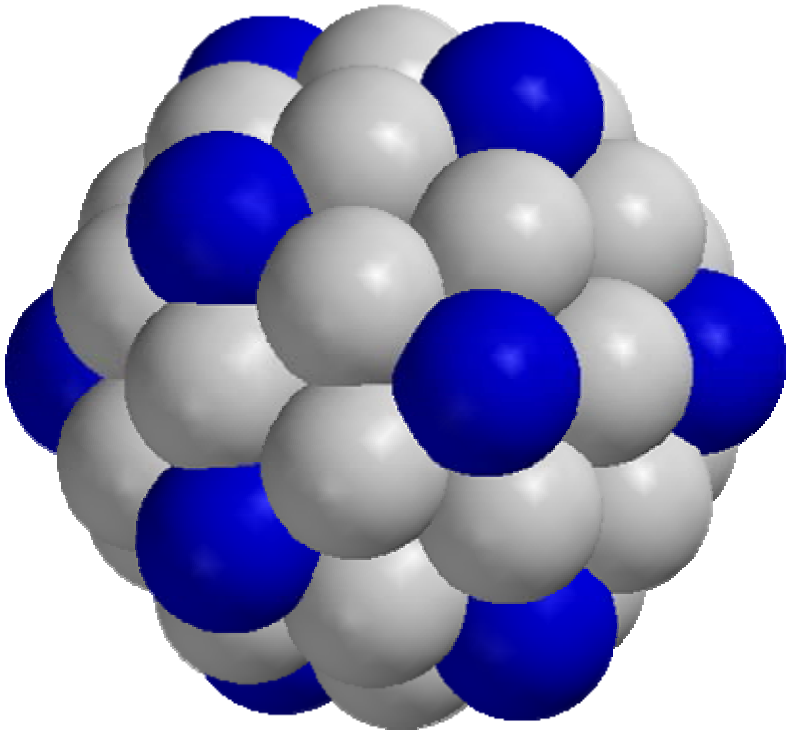

Figure 4.28 Icosahedral structure of Ni_{55} Cluster (shaded atoms are apex atoms which have coordinate number of 6 whereas the others are 8 coordinated)

The results found from equilibrium geometry calculations are compared with each other as shown in Table 4.6. EAM method by Grigoryan and Springborg (2003) and Luo (2002) resulted in bond length of 2.59 Å and 2.45 Å; binding energy of 4.27 eV/atom and 3.55 eV/atom, respectively. They also reported IC Ni_{13} binding energies and bond lengths as 3.38 eV/atom; 2.99 eV/atom and 2.42 Å; 2.38 Å, respectively. It was mentioned before that by using Ni_{13} and Ni_{55} theoretical results, a correlation line can be drawn in terms of (number of atoms in the cluster)$^{-1/3}$ versus binding energy. The intercept of binding energy axis gives bulk nickel (infinite numbers of atoms) probable binding energy estimated theoretically. The intercepts of theoretical studies by Lathiotakis et al. (1996), Grigoryan and Springborg (2003) and Luo (2002) were calculated as 5.69 eV/atom, 4.93 eV/atom and 4.45 eV/atom, respectively. Since bulk nickel binding energy was experimentally reported as 4.45 eV/atom by Voter and Chen (1987), Luo (2002) results have become very reliable for the comparison.

Table 4.6 Theoretical values of binding energy and bond length of IC Ni_{55} nanocluster

References	Method	B.E (eV)/atom	Mean Distance (Å)
Grigoryan and Springborg (2003)	EAM	3.83	2.59
Luo (2002)	TB-MD	3.55	2.45
Lathiotakis et al. (1996)	TB-MD	4.27	2.59

Table 4.7 summarizes semi-empirical guesses by showing the effect of change in spin multiplicity of the neutral system. The optimum geometry for Ni_{55} nanocluster, which had a spin multiplicity of 11, resulted in the bond length of 2.26 Å (center-to-vertex), of 2.39 Å (vertex-to-vertex of first layer), and of 2.43 Å (vertex-to-vertex of second layer) and average bond length of 2.44 Å which were conformed by average TB-MD bond length of 2.45 Å (Luo, 2002). As expected, semi-empirical calculations have overestimated binding energy of Ni_{55} nanocluster with a value of 6.495 eV/atom but the final structure might be a well-estimated input geometry for more precise calculations such as DFT.

Table 4.7 Comparison of semi-empirical PM3 method spin multiplicity trials for Ni_{55} cluster

Ni_{55}		Binding energy (ev/atom)	Bond Length (Å)
Semi-empiricalPM3	SM1	6.3591	2.262 ± 0.006 (c-v1) 2.379 ± 0.006 (v1-v1) 2.435 ± 0.06 (v2-v2)
	SM3	-	
	SM5	6.4358	
	SM7	6.4456	
	SM9	6.4663	
	SM11	6.4953	
	SM13	6.4915	

4.3 Ethylene Adsorption on Different Nickel Surfaces

Pool (1990) mentioned that nanoclusters have potentials of being catalysts which show high activity and selectivity because the high percentage of nanocluster metal atoms are on the surface and the nanocluster structure is different from mass. Lopez et al. (2004) have proven quantum mechanically this statement by making comparative investigation of carbon monoxide adsorption on nanosized gold particles and its single crystal surfaces. They have simulated Au (111) and Au (210) surfaces; and Au_{10} nanocluster where CO adsorption energies were +3.45 kcal/mol, -5.77 kcal/mol and -11.5 kcal/mol, respectively. Therefore, CO adsorption energies had diminished sequentially from plane surfaces of Au (111), then Au (210) to the nanosized Au_{10} cluster depending on their coordination numbers of 9, 7 and 5, respectively. As a result, Lopez et al. (2004) stated that the chemical activity of gold was strongly dependent on the coordination number of the gold atoms.

By the light of just mentioned observations, ethylene adsorption was selected as a model for comparing activities of different nickel surfaces in present study. Chosen structures were single crystal surfaces of Ni(111) and Ni(100) and nanometer-size Ni_{13} cluster where a Ni atom was 9, 8 and 6 coordinated, respectively. Ethylene adsorption on mentioned surfaces had been given previously as -18.0 kcal/mol, -31.80 kcal/mol and -43.42 kcal/mol, respectively. Their final geometries and coordination number versus adsorption energy graph were in given in Figure 4.29. This figure also shows that the strength of Ni-C bond varied strongly with Ni coordination number. It was concluded that ethylene adsorption energies decreased by approximately 25.0 kcal/mol going from Ni(111) to nanosized Ni_{13} cluster where the Ni atoms have a coordination number of 9 and 6, respectively. Quantum mechanical calculations resulted that catalytic activity of nickel was highly dependent on the coordination number of Ni atom.

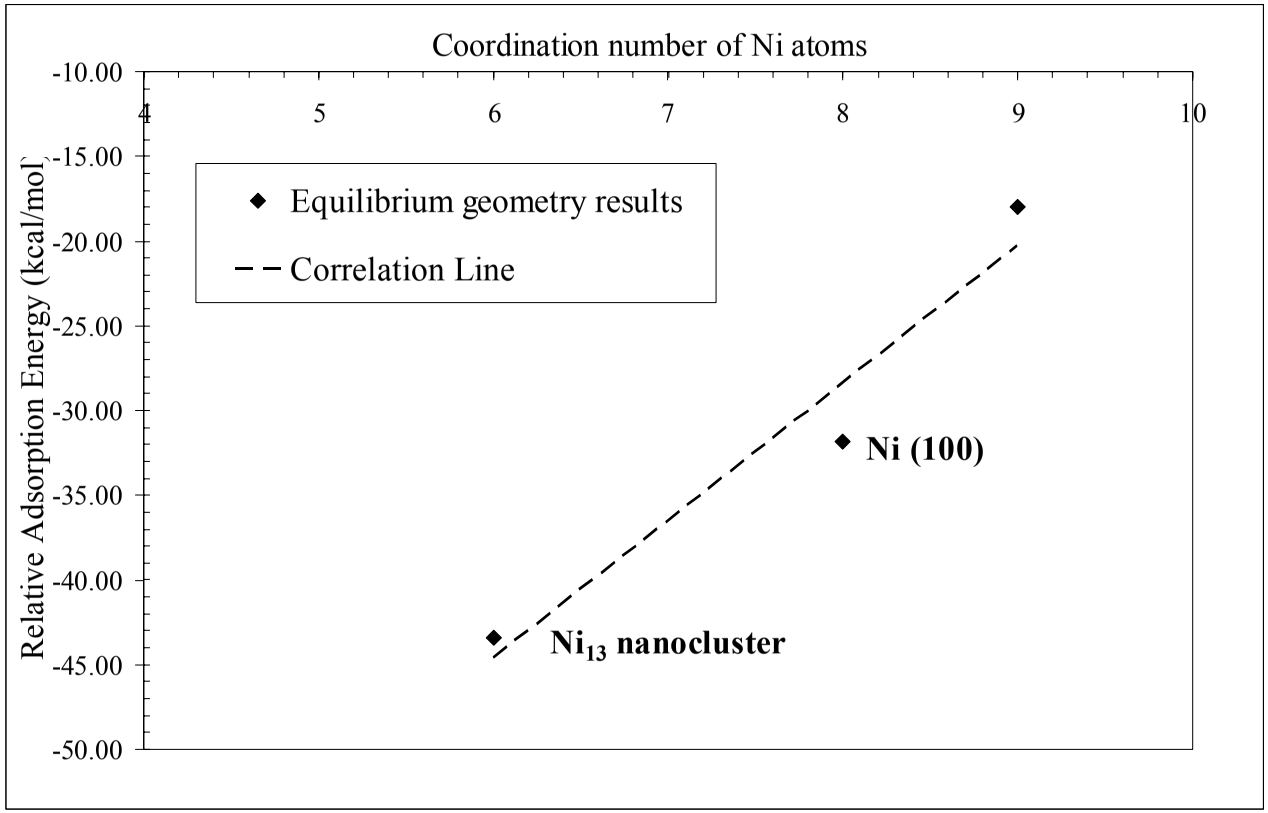

Figure 4.29 The correlation between relative ethylene adsorption energies with respect to the coordination number of Ni atoms in a series of different nickel cluster surfaces

CHAPTER 5

CONCLUSIONS

In this research, ethylene adsorption on nickel single crystal surface and nickel nanoclusters and ethylene hydrogenation on Ni(111) surface were performed by means of quantum mechanical calculations.

Density functional theory with B3LYP/6-31G** was utilized for the simulation of ethylene hydrogenation on Ni(111). Ethylene adsorption on bare Ni(111) surface was the first step of ethylene hydrogenation mechanism. Coordinate driving calculations have shown agreement with both experimental and theoretical literature that ethylene adsorbed molecularly with an adsorption mode of di-σ by non-activated process whose energy was calculated as -18.00 kcal/mol. Second step was the half-hydrogenation of adsorbed ethylene to form surface surface ethyl. Two kinds of hydrogen atom were considered. One form is bulk hydrogen representing for hydrogen atoms emerging from the bulk of Ni metal to the surface. Surface bound hydrogen atom was the other type representing the hydrogen which could be produced by the dissociative chemisorption of gaseous H_2. It was found that the interaction of surface hydrogen (2.72 kcal/mol) with pre-adsorbed ethylene have required slightly higher activation barrier than of bulk hydrogen (0.19 kcal/mol). The resultant heats of reactions for both possible elementary steps were -70.53 kcal/mol and -70.55 kcal/mol, respectively. Third and final elementary step was the hydrogenation of surface ethyl by use of bulk hydrogen atom and surface hydrogen, separately. Bulk hydrogen atom was considerably reactive than surface hydrogen atom since the computations indicated that the interaction with surface ethyl bounded on Ni(111) necessitated activation barriers of

2.37 kcal/mol and 18.24 kcal/mol to form ethane, respectively. Surface ethyl reaction with bulk hydrogen theoretically produced energy of -77.40 kcal/mol whereas volatile ethane formation from surface hydrogen atom resulted in slightly higher energy of -82.58 kcal/mol. Calculated global reaction energy of -170 kcal/mol was thermodynamically consistent with gas phase global reaction energy experimentally reported as -140 kcal/mol. As a result, quantum mechanical calculations provided good agreement with experimental studies (Ceyer and co-workers) exhibiting that the surface-bound hydrogen on Ni(111) was not able to activate the hydrogenation whereas bulk H atom is very active and readily hydrogenate ethylene to produce gas phase ethane. Moreover, the type of hydrogen reacting with surface ethyl on Ni(111), reported as unknown by Haug et al., was theoretically determined as bulk hydrogen.

Ni clusters ranging from 2 to 55 atoms have also been studied quantum mechanically in terms of their structures, binding energies and bond lengths by use of semi-empirical (PM3) and density functional theory (DFT) methods. The results compare quite favorably with the available extensive experimental and some theoretical work in the literature. Ni_2 dimer had binding energy of 1.078 eV/atom fitting very well to experimental data. 13- and 55-atom Ni clusters have been optimized energetically and the resulting icosohedral (IC) geometry was in very good agreement with the literature values as well. Correlation line obtained with respect to binding energies of Ni_2 dimer and Ni_{13} nanocluster via number of atoms in the cluster indicated that our DFT results provided estimation for bulk nickel binding energy of 4.57 eV/atom showing good agreement with experimental value of 4.45 eV/atom.

Based on the fact that Ni nanocluster catalysts have a potential of having high activity in hydrocarbon reactions than traditional supported Ni catalysts, ethylene adsorption was carried out by use of density functional theory formulated by B3LYP with basis set of 6-31G**. Single crystal surfaces of

Ni(111) and Ni(100) and surface of Ni_{13} nanocluster were selected according to the coordination number of the nickel atoms which were 9, 8 and 6, respectively. The computations indicated that chemical activity of nickel surfaces gradually augmented while coordination number of one nickel atom in the surface declined. It was found that ethylene has adsorbed molecularly with relative energies of -18.00 kcal/mol, -31.4 kcal/mol and -43.42 kcal/mol on Ni(111), Ni(100) and Ni_{13} nanocluster, respectively. As a result, the fall in ethylene adsorption energies was considered to be strongly dependent on coordination number of the nickel atoms in the surfaces.

As future work, geometry optimization of 55-atom nanocluster will be performed by means of density functional theory performed at B3LYP/modified-6-31G** level. Binding energy of this geometry will then be inserted in the mentioned correlation line. By this way, probable binding energy of bulk nickel can be theoretically estimated more precisely. Then, ethylene hydrogenation reaction mechanism on Ni_{13} and Ni_{55} nanocluster will be investigated quantum mechanically in order to compare catalytic activities of Ni(111) single crystal surface with of those nanoclusters.

REFERENCES

Accelrys Software Inc. I, "Quantum Mechanical Simulation", http://www.accelrys.com/technologies/modeling/materials/qm/, last visited day: January, 2005.

Accelrys Software Inc. II, "Atomistic Simulation", http://www.accelrys.com/technologies/modeling/materials/atomistic/, last visited day: January, 2005.

Ahmed, F., Nixon, E.R., J. Chem. Phys. 71, 3547 (1979).

Alexander, B.D., Trevor, J. D., J. Phys. Chem. A, 108, 146 (2004).

AZoM, A to Z of Materials**,** The Premier On-Line Materials Information Site, Supplier and Expert Directory, "Nickel", http://www.azom.com/details.asp?ArticleID=617, last visited day: March, 2005.

Bader, R.F.W., "An Introduction to the Electronic Structure of Atoms and Molecules", http://www.chemistry.mcmaster.ca/esam/Chapter_8/intro.html; last visited day: December, 2004.

Bao, S., Hofmann, Ph., Schindler, K.-M., Fritzsche, V., Bradshaw, A.M., Woodruff, D.P., Casado, C., Asensio, M.C., J. Phys. Condens. Matter 6, L93 (1994).

Bao, S., Hofmann, Ph., Schindler, K.-M., Fritzsche, V., Bradshaw, A.M., Woodruff, D.P., Casado, C., Asensio, M.C., Surf.Sci. 323 19 (1995).

Basch, J.W., Newton, M.D., J. Chem. Phys. 73, 4492 (1980).

Becke, A. D., *Phys. Rev., B*., 38, 3098 (1988).

Becke, A. D., Roussel, M. R. *Phys. Rev., A.*, 39, 3761, (1989).

Beeck, O., Disc. Faraday Soc. 8, 118 (1950).

Benninghoven, A., Beckmann, P., Grefendorf, D., Schemmer, M., Appl. Surf. Sci. 6, 288 (1980).

Bertolini, J.C., Rousseau, J., Surf. Sci. 83, 531 (1979).

Brouwer, F., "Chapter 5. Quantum chemistry in Molecular Modeling/Semi-empirical quantum chemistry", http://www.cmbi.kun.nl/~borkent/compcourse/fred/ch57.html, last visited day: March, 2004.

Bürgi, T., Trautman, T.R., Gostein, M., Lahr, D.L., Haug, K.L., Ceyer, S.T., Surf.Sci. 501, 49 (2002).

Calleja, M., Rey, C., Alemany, M.M.G., Gallego, L.J., Ordejon, P., Sanchez-Portal, D., Artacho, E., Soler, J.M., Phys.Rev.B 60, 2020 (1999).

Cattania, M.G., Simonetta, M., Tescari, M., Surf. Sci. 82, 615 (1979).

Carr, R. G., Sham, T. K., Eberhardt, W. E., Chem. Phys. Lett. 113, 63 (1985).

Castro, M., Jamorski, C., Salahub, D.R., Chem. Phys. Lett. 271, 133 (1997).

Ceyer, S.T., Acc. Chem. Res. 34, 737 (2001).

Chase, M.W., Jr., NIST-JANAF Thermochemical Tables, Fourth Edition, J. Phys. Chem. Ref. Data, Monograph 9, 1-1951 (1998).

Chen, B., Castleman, A.W., Ashman, C., Khanna, S.N., Int. J. Mass Spec., 220, 171 (2002).

Chen, B., Castleman Jr, A.W., Khanna, S.N., Chem. Phys. Lett., 304, 423 (1999).

Christmann, K., Behm, R.J., Ertl, G., Van Hove, M.A., and Weinberg, W.H., J.Chem.Phys. 70, 4168 (1979).

Christmann, K., Schober, O., Ertl, G., Neumann, M., J.Chem.Phys. 60, 4528 (1974).

Clark, T., "A Handbook of Computational Chemistry", *John Wiley & Sons*, New York (1985).

CMM (Center for Molecular Modeling) "Molecular Mechanics", http://cmm.info.nih.gov/modeling/guide_documents/molecular_mechanics_document.html, last visited day: September, 2004.

CMM (Center for Molecular Modeling) "Quantum Chemistry", http://cmm.info.nih.gov/modeling/guide_documents/quantum_mechanics_document.html, last visited day: April, 2005.

Cooper, E., Raval, R., Surf. Sci. 331-333, 94 (1995).

Cox, J.D., Wagman, D.D., Medvedev, V.A., "CODATA Key Values for Thermodynamics", Hemisphere Publishing Corp., New York (1984).

Crispin, X., Lazzaroni, R., Geskin, V., Baute, N., Dubois, P., Jerome, R., Bredas, J.L., J.Am.Chem.Soc. 121, 176 (1999).

Daley, S.P., Utz, A.L., Trautman, T.R., Ceyer, S.T., J.Am.Chem.Soc. 116, 6001, (1994).

Dalmai-Imelik, G., Massardier, J., In Proceedings of the Sixth International Congress on Catalysis; Bond, G.C., Wells, P.B., Tompkins, F.C., Eds.; Chemical Society, London, pp 90-100 (1977).

Demuth, J.E., Eastman, D.E., Phys.Rev. Letters 32, 1123 (1974).

Demuth, J.E., (a) IBM J. Res. Dev. 22, 265 (1978).

Demuth, J.E., (b) Surf.Sci. 76, L603 (1978).

Demuth, J.E., Surf.Sci. 84, 315 (1979).

Eley, D.D,. Faraday Soc. Disc. 8, 34 (1950).

Fahmi, A., van Santen, R.A., Surf.Sci. 371, 53 (1997).

Godby, R., "Fundamental Problems in Density-Functional Theory" http://www-users.york.ac.uk/~rwg3/resint_dft.html, last visited day: October, 2004.

Gorwara Chemical Industries, "Activated Nickel Catalyst", http://www.gorwara.com/products.html, last visited day: April, 2005.

Greeley, J., Mavrikakis, M., Surf. Sci. 540, 215 (2003).

Grigoryan, V. G., Springborg, M., Chem. Phys. Lett. 375, 219 (2003).

Grunes, J., Zhu, J., Somorjai, G.A., Chemical Communication 18, 2257 (2003).

GSU (Georgia State University) Department of Physics and Astronomy, "The Wavefunction", http://hyperphysics.phy-astr.gsu.edu/hbase/quantum/wvfun.html, last visited day: November, 2003.

Gwathmey, A.T., Cunningham, R.E., Advan. Catalysis 10, 57 (1958).

Hammer and Nørskov, Advances in Catalysis, 45, 71 (2000).

Hammer, L., Hertlein, T., Müller, K., Surf. Sci. 178, 693 (1986).

Handbook of Chemistry and Physics, 61st ed., CRS Press, Boca Raton, FL. (1980).

Hasse, W., Günter, H.L., Henzler, M., Surf. Sci. 126, 479 (1983).

Haug, K. L., Bürgi, T., Gostein, M., Trautman, T. R., Ceyer, S. T., J. Phys. Chem. B, 105, 11480 (2001).

Hehre, W., Burke, L.D., Shusterman, A.J., A Spartan Tutorial, Wavefunction, Inc., Irvine CA (1993).

Ho, J., Zhu, L., Parks, E. K., Riley, S. J., J. Chem. Phys. 99, 1409 (1993).

Horiuti, J., Polanyi, M., Trans. Faraday Soc. 30, 1164 (1934).

Ibach, H., Mills, D.L., Electron Energy Loss Spectroscopy and Surface Vibrations; Academic Press, New York, p.307 (1982).

Izumi, Y., Kiyotaki, F., Yoshitake, H., Aika, K., Sugihara, T., Tatsumi, T., Tanizawa, Y., Shido, T., Iwasawa, Y., Chem. Commun., 2402 (2002).

Jensen, F., "Introduction to Computational Chemistry", John Wiley & Sons, New York (1998).

Johnson, A.D., Maynard, K.J., Daley, S.P., Yang, Q.Y., Ceyer, S.T., Phys. Rev. Lett. 67, 927 (1991).

Johnson, A.D., Daley, S.P., Yang, Q.Y., Utz, T., Ceyer, S.T., Science 257, 223 (1992).

Kant, A., J. Chem. Phys. 41, 1872 (1964).

Klauda, J.B., Garrison, S.L., Jiang, J., Arora, G., Sandler, S.I., J.Phys. Chem. A 108, 107 (2004).

Klimesch, P., Henzler, M., Surf. Sci. 90, 57 (1979).

Klinke II, D.J., Broadbelt, L.J., Surf. Sci. 429, 169 (1999).

Koh, H.P., Hughes, R., J. Cat., 33, 7 (1974).

Kohn, W., Sham, L. J., Phys. Rev., 140, A1133 (1965).

Kresse, G., Hafner, J., Surf. Sci. 459, 287 (2000)

Lapujoulade, J., Neil, K.S., J. Chem. Phys. 57, 3535 (1972).

Lathiotakis, N.N., Andriotis, A. N., Menon, M., Connolly, J., J. Chem. Phys. 104, 992 (1996).

Lee, C., Yang, W., Parr, R. G. *Phys. Rev., B.*, 37, 785, (1988).

Lehwald, S., Ibach, H., Surf.Sci 89, 425 (1979).

Lopez, N., Janssens, T.V.W., Clausen, B.S., Xu, Y., Mavrikakis, M., Bligaard, T., Nørskov, J.K., Journal of Catalysis 223, 232 (2004).

Luo, C., Modelling Simul. Mater. Sci. Eng. 10, 13 (2002).

Maynard, K.J., Johnson, A.D., Daley, S.P., Ceyer, S.T., Faraday Discuss. Chem. Soc. 91, 437 (1991).

Merkle, R.C., Nanotechnology 2, 134 (1991).

Michelini, M.C., Diez, R.P., Jubert, A.H., Int. J.Quant.Chem. 85, 22 (2001).

Minot, C., Markovits, A., J.Mol.Struc. (THEOCHEM) 424, 119 (1998).

Mlynarski, P., Salahub, D.R., J.Chem.Phys. 95, 6050 (1991).

Morse, M.D., Hansen, G.P., Langridge-Smith, P.R.R., Zheng, L.S., Geusic, M.E., Michalopoulos, D.L., Smalley, R.E., J. Chem. Phys. 80, 5400 (1984).

Moskovits, M., Hulse, J.E., J. Chem. Phys. 66, 3988 (1977).

Nayak, S.J., Khanna, S.N., Rao, B.K., Jena, P., J. Phys. Chem., 101, 1072 (1997).

Nishijima, M., Yoshinobu, Y., Sekitani, T., Onchi, M., J. Chem. Phys. 90, 5114 (1989).

Northby, J.A., J. Chem. Phys. 87, 6166 (1987).

Nour, E.M., Alfaro-Franco, C., Gingerich, K.A., and Laane, J., J. Chem. Phys. 86, 4779 (1987).

Nutt, W.R., "Semi-Empirical Methods", http://www.chm.davidson.edu/ronutt/che401/SemiEmp/SemiEmp.htm, last visited day: May, 2003.

OMNI (Organization for Minnesota Nanotechnology Initiatives), *Introduction*, http://www.nano.umn.edu/omni/intro.html, last visited day: March, 2004.

Ozin, G. A., Power, W. J., Upton, T. H., Goddard W. A., J. Am.Chem. Soc., 100, 4750 (1978).

Parks, E.K., Winter, B.J., Klots T.D., SJ. Riley, J. Chem. Phys. 94, 1882 (1991).

Parks, E.K.,. Zhu, L, Ho J.,. Riley SJ, J. Chem. Phys. 100, 7206 (1994).

Parks, E.K., Zhu, L., Ho J., SJ. Riley, J. Chem. Phys. 102, 7377 (1995).

Pellarin, M., Baguenard, B., Vialle, J. L., Lerme, J., Broyer, M., Miller, J., Perez, A., Chem. Phys. Lett. 217, 349 (1994).

Perdew, J. P., Phys. Rev., B., 33, 8822, (1986); 34, 7406, (1986).

Perdew, J. P., Wang, Y., Phys. Rew. B., 33, 8800, (1986).

Perdew, J. P., Wang, Y., Phys. Rew. B., 45, 13244, (1991).

Pool, R., Science 248, 1186 (1990).

Pople J. A., Beveridge, D.L., "Approximate Molecular Orbital Theory", McGraw-Hill, New-York (1970).

Pople, J. A., Gill, P. M. W., Handy, N. C., Int. J. Quantum Chem. 56, 303 (1995).

Prosen, E.J. Rossini, F.D., J. Res. NBS, 34, 263 (1945).

Raghavan, K., Stave, M.S.,and DePristo, A.E., J. Chem. Phys. 91, 1904 (1989).

Reuse, F.A., Khanna, S.N., Chem. Phys. Lett. 234, 77 (1995).

Roco, M.C., Alivisatos, P., Williams, S., The Interagency Working Group on Nano Science, Engineering and Technology (IWGN), "Vision for Nanotechnology R&D in the Next Decade; Examples of nanotechnology applications", http://www.wtec.org/loyola/nano/jan99ws/tsld005.htm and http://www.wtec.org/loyola/nano/jan99ws/tsld006.htm, last visited day: April, 2005.

Sandler, S.I., Fluid Phase Equilibria 210, 147 (2003).

Schmid, G., Endeavour, New Series 14, 172 (1990).

Schmid, G., V. Maihack, F. Lantermann, S. Peschel, J. Chem. Soc., Dalton Trans. 589, (1996).

Sellers, H., Gislason, J., Surf.Sci. 429, 147 (1999).

Sham T.K., Carr, R.G., J. Chem. Phys. 84, 4091 (1986).

Spartan'02 Windows, Tutorial and User's Guide, Wavefunction, Inc., Irvine CA (2001).

Stave, M.S., Depristo, A.E., J. Chem. Phys. 97, 3386 (1992).

Tomonari, M., Tatewaki, H., Nakamura, T., J. Chem. Phys. 85, 2875 (1986).

Uzun, A., M.S. thesis "Quantum Chemıcal Sımulatıon of No_x Reductıon by Ammonıa (Scr Reactıon) on V_2o_5 Catalyst Surface", METU, Ankara (2003).

Vattuone, L., Yeo, Y.Y., Kose, R., King, D.A., Surf.Sci. 447, 1 (2000).

Voter, A.F. Chen, S.P. Mater. Res. Soc. Symp. Proc. 82, 175 (1987).

Widmark, P. O.; Roos, B. O.; Siegbahn, P. E. M. J. Phys. Chem. 89, 2180 (1985).

Winkler, A., Rendulic, K.D., Surf.Sci.118, 19 (1982).

Wyckoff, R.W.G., "Crystal Structures", Second addition, Interscience (1963).

Yang, H., Whitten, J.L., J. Chem. Phys. 98, 5039 (1993).

Zaera F., and Hall, R.B., J.Phys.Chem. 91, 4318 (1987); Surf.Sci. 180, 1 (1987).

Zaera, F., Fischer, D.A., Carr, R.G., and Gland, J.L., J. Chem Phys. 89, 5335 (1988).

Zaera, F.J.Catal. 121, 318 (1990).

Zhanpeisov, N.U., Higashimoto, S., Anpo, M., Inter. J. Quan. Chem., 84, 677 (2001).

Zhu, X.-Y. and White, J.M., Surf. Sci. 214, 240 (1989).

Zuhr, R.A., Hudson, J.B., Surf.Sci. 66, 405 (1977).

APPENDICES

A: Background of the Quantum Chemistry

In the Born-Oppenheimer approximation, it is assumed that the motion of the nuclei is so slow that the electrons instantaneously follow them. This is because mass(proton) ~ 2000xmass(electron). Therefore the electronic wavefunction obeys the Schrodinger equation with the nuclei at rest. This equation results in the separation of wave function into

$$\Psi \approx \Psi_N \Psi_{elec} \tag{A.1}$$

where the first term in the product of equation (A.1) accounts for the motion of the nuclei and the second term involves the electron motion. Furthermore, introducing center-of mass and relative coordinates, the nuclear wave function reduces to

$$\Psi_N \approx \Psi_{trans}(C.M.)\Psi_{rot}\Psi_{vib} \tag{A.2}$$

where the center-of mass translation, and rotational and vibrational contributions to the nuclear wave function are now explicitly shown. Thus, the problem of determining the structure of a complex molecule reduces to solving each Schrödinger equation for the electronic motion, the translational motion of the center of mass, and the rotational and vibrational of the nuclei separately. The electronic energy is estimated therefore by the Schrödinger equation for a molecule with n electrons calculation procedure is similar for the other types of motion

$$\hat{H}_{elec}(1,2,\ldots,n)\Psi_{elec}(1,2,\ldots,n) = E_{elec}\Psi_{elec}(1,2,\ldots,n) \tag{A.3}$$

and for a given intermolecular distance the total energy of the system is

$$E_T^0 \approx E_{elec} + \sum_{A<B} e^2 Z_A Z_B r_{AB}^{-1} \qquad \text{(A.4)}$$

where the second term is the electrostatic internuclear repulsion energy and A, B designate different nucleus.

Molecular orbital theory is concerned with electronic wave functions only, and henceforth the electronic subscripts will be dropped from the electronic Hamiltonian and wave function. The molecular energy given by equation (A.4) is the energy at absolute zero with no contributions from the translational, rotational or vibrational motions. The later forms of energy must be considered to determine thermochemistry under conditions of practical interest as

$$E_T \approx E_{trans} + E_{vib} + E_{rot} + E_{elec} \qquad \text{(A.5)}$$

Once the total energy E_T^0 of equation (A.4) is known for a given molecular geometry, a potential energy hypersurface (PES) can be generated as function of geometry, and the minima on the (PES) corresponds to the most stable configuration, or in mathematical terms for molecules or radicals,

$$\partial E_T^0 / \delta g_i = 0$$

$$\partial^2 E_T^0 / \delta (g_i)^2 > 0$$

where g_i is any geometrical variable.

The heat of formation for the molecule can then be obtained from the total energy of equation (A.5) via

$$\Delta H_f = E_T - \sum_{k=1}^{n} E_k^A + \sum_{i=1}^{N} \Delta H_{fi}^A \qquad \text{(A.6)}$$

where E_k^A and ΔH_{fi}^A are the electron energies and the heats of formation of individual atoms, respectively. Clearly, this approach requires the accurate knowledge of the atomic heats of formation, which may or may not be available.

The electronic Hamilton (non-relativistic) of a molecule is given by the following expression in atomic units ($h/2\pi = e = m = 1$)

$$\hat{H} = -\sum_{p} \tfrac{1}{2}\nabla_p^2 - \sum_{A}\sum_{P} Z_A r_{Ap}^{-1} + \sum_{p<q} r_{pq}^{-1} \qquad \text{(A.7)}$$

where A designate the nuclei, p, q electrons, and r is the interparticle distance.

The solutions to the electronic Schrödinger equation (A.3) are infinite but for stationary, bound states only the continuous, single-value eigenfunctions that vanish at infinity need to be considered, and the electronic energies are the eigenvalues E_i or

$$\hat{H}\Psi_i = E_i\Psi_i \qquad \text{(A.8)}$$

The eigenfunctions are normalizable and mutually orthogonal (i.e., orthonormal) or mathematically they satisfy the condition

$$\int \Psi_i \Psi_j d\tau = \left\langle \Psi_i \middle| \Psi_j \right\rangle = \delta_{ij} \qquad \text{all i ,j} \qquad \text{(A.9)}$$

In equation A.9, the interaction is over the volume element for the electron, and it is given with the matrix or Dirac notation for the integral, where δ_{ij} is the Kronecker delta. The electronic energy of the system E_i is the expectation value of the Hamiltonian or the solution for E_i is

$$\int \Psi_i \hat{H} \Psi_j d\tau = \left\langle \Psi_i \middle| \hat{H} \middle| \Psi_j \right\rangle = E_i \tag{A.10}$$

The complete treatment of a quantum-mechanical problem involving electronic structure requires the complete solution of the Schrödinger equation (A.3). This is only possible for one-electron systems, and for many-electron systems, where the electron repulsion term in the Hamilton renders an analytical solution impossible, the variation principle is applied. This method in its full form is completely equivalent to the differential equations, and it has many advantages in the ways it can be adapted to approximate solution wave functions (Pople, 1970). The variation principle states that if ψ is a solution to equation (3.8) then for any small change $\delta\psi$

$$\delta E = \delta \langle \Psi | \hat{H} | \Psi \rangle = 0 \tag{A.11}$$

If this criterion is applied to an electronic wave function ψ, in the appropriate number of dimensions, all the eigenfunctions ψ_i for the Hamilton will be obtained. If only an approximation to the wave function ψ is used, and then the eigenfunctions ψ_i and eigenvalues E_i are only approximations to the correct values, with the accuracy of the estimates improving as better approximations for the total wave function ψ is used.

The orbital approximation suggests that the total electron wave function ψ can be written as the Hartree product of one-electron wave functions, $\psi_i\eta(\zeta)$, called spin orbitals consisting of the product of spatial and spin functions, where $\eta(\zeta)$ is the spin function that can take values α or β, or

$$\Psi(1,2,\ldots,n) = O(s) A\left[\psi_1(1)\alpha(1)\psi_2(2)\beta(2)\psi_3(3)\alpha(3)\ldots\psi_n(n)\beta(n)\right] \tag{A.12}$$

In equation (A.12) A is the antisymmetrizer, ensuring that the wave function changes sign on interchange of any two electrons in accordance with the Pauli exclusion principle, and O(S) is a spin projector operator that ensures that the wave function remains an eigenfunction of the spin-squared operator S^2

$$S^2\Psi = S(S+1)\Psi \tag{A.13}$$

O(S) can become quite complex but for a closed shell molecule, with all electrons paired in the spin orbitals O(S)=1. Thus, for a closed-shell system with 2n electrons, and two electrons paired in each spatial orbital, the many-electron wave function becomes

$$\Psi(1,2,...,n) = A\left[\psi_1(1)\alpha(1)\psi_1(2)\beta(2)\psi_2(3)\alpha(3)..\psi_n(2n-1)\alpha(2n-1)\psi_n(n)\beta(n)\right] \tag{A.14}$$

Equation (A.14) is known as *Slater determinant* which is the proper form for the many electron wave function for closed shells as a single determinant of spin orbitals. The discussion now proceeds to the details of the actual determination of the electron spatial orbitals ψ_i for a closed-shell system. This involves the application of the variational principle or equation (A.11) for the solution of (A.14). The best molecular orbitals, therefore, are obtained by varying all the contributing one-electron functions ψ_1, ψ_2, ψ_3,... ψ_n, in the Slater determinant equation (A.14) until the electronic energy achieves its minimum value. This will give the best approximation to the many-electron wave function, ψ and the electron orbital or molecular orbitals ψ_i so obtained are referred to as *self consistent* or *Hartree-Fock* molecular orbitals.

Mathematically, the problem involves the minimization of the total electron energy with the orthonormality constraint for the electron orbitals as

$$\text{Minimize } G = E - 2\sum_i \sum_j \varepsilon_{ij} S_{ij} \tag{A.15}$$

where, Orthonormality $S_{ij} = \int \psi_i * \psi_j d\tau = \delta_{ij}$ (A.16)

and $E = \langle \Psi(1,2,\ldots,n) | \hat{H} | \Psi(1,2,\ldots,n) \rangle$ (A.17)

where ψ(1,2,3,....,n) is given by equation (A.14)

The minimization consists of setting δG = 0 and leads to the following differential equations (see Pople, 1970 for derivations).

$$\left[\hat{H^{core}} + \sum_j 2 J_j - \hat{K}_j \right] \psi_i = \varepsilon_i \psi_i \qquad \text{i =1,2,…,n} \qquad \text{(A.18)}$$

or, $\hat{F} \psi_i = \varepsilon_i \psi_i$ i = 1,2,…,n (A.19)

In equation (A.19) F is the one-electron Hartree-Fock Hamiltonian operator consisting of the terms defined in equation (A.18) within the square brackets. Equation (A.19) is known as the *Hartree-Fock* equation and states that the best molecular orbitals are eigenfunctions of the Hartree-Fock equation Hamiltonian operator. The first operator of the Hartree-Fock Hamiltonian in equation (A.18) is the one-electron Hamiltonian for an electron moving in the field of the bare nuclei, which is defined as

$$\hat{H}(p)^{core} = -\tfrac{1}{2} \nabla_p^2 - \sum Z_A r_{pA}^{-1} \qquad \text{(A.20)}$$

The second operator accounts for the average effective potential of all other electrons affecting the electron in the molecular orbital ψ_i, can be defined by

$$\hat{J}_j(1) = \int \psi_j^*(2) \frac{1}{r_{12}} \psi_j(2) d\tau_2 \qquad \text{(A.21)}$$

The final operator in the square bracket of equation (A.18) is the exchange potential and it arises from the effect of the antisymmetry of the total wave function on the correlation between electrons of parallel spin and it can be defined by

$$K_j(1)\psi_i(1) = \left[\int \psi_j^*(2)\frac{1}{r_{12}}\psi_i(2)d\tau_2\right]\psi_j(1) \qquad \text{(A.22)}$$

To account for the correlation of electrons of different spin, the term missing in equation (A.18), Configuration Interaction (CI) method can be applied. This method incorporates virtual orbitals or nonbonding orbitals into the total wave function. This is beyond the scope of this discussion. For more information see Pople (1970)

The eigenvalues of equation (A.18) or (A.19) are the energies of electrons occupying the orbitals ψ_i are thus known as orbital energies, defined as

$$\varepsilon_i = H_{ij}^{core} + \sum_i \left(2J_{ij} - K_{ij}\right) \qquad \text{(A.23)}$$

where the one-electron core energy for an electron moving in the field of bare nuclei is

$$H_{ij}^{core} = \int \psi_i^*(1)\hat{H}^{core}\psi_i d\tau_j \qquad \text{(A.24)}$$

the coulomb interaction energy is given by

$$J_{ij} = \iint \psi_i^*(1)\psi_j^*(2)\frac{1}{r_{12}}\psi_i(1)\psi_j(2)d\tau_1 d\tau_2 \qquad \text{(A.25)}$$

and the exchange energy is

$$K_{ij} = \iint \psi_i^*(1)\psi_j^*(2)\frac{1}{r_{12}}\psi_j(1)\psi_i(2)d\tau_1 d\tau_2 \qquad \text{(A.26)}$$

The general procedure for solving the Hartree-Fock equations is iterative. A first solution for the molecular orbitals ψ_i is assumed for generating the Hartree-Fock operator F. The set of molecular orbitals generated by this estimate of the Hartree-Fock operator is then used to repeat the calculations and so on until the orbital no longer changes, within a certain tolerance, on further interaction. These orbitals are said to be *self consistent with the potential field they generate*. In addition to the n occupied orbitals, there will be unoccupied orbitals called virtual orbitals of higher energy.

The method outlined above for solving the Hartree-Fock equation is impractical or molecular systems of any size and other approaches must be found (Pople, 1970). The most rewarding approach consists of approximating the molecular orbitals by a *linear combination of atomic orbitals* or LCAO in the form

$$\psi_i = \sum_{\mu} c_{\mu i} \phi_{\mu} \tag{A.27}$$

where the ϕ_μ are the atomic orbitals constituting the molecular orbital or basis set.

In carrying out numerical calculations of molecular orbitals, it is necessary to have convenient analytical forms for the atomic orbitals of equation (A.27) for each type of atom in the molecule. The solutions of the Schrödinger equation for one-electron systems (H-atom) can be written in the form by separation of variables

$$\Phi(r, \theta, \phi) = R_{n,l}(r) Y_{lm}(\theta, \phi) \tag{A.28}$$

where r, θ, and ϕ are the spherical coordinates centered on the atom. The angular part of the above equation or $Y_{lm}(\theta,\phi)$ are the spherical harmonics defined as

$$Y_{lm}(\theta,\varphi) = \Theta_{lm}(\theta)\phi_m(\varphi) \tag{A.29}$$

where l is the azimutal quantum number, and m is the magnetic quantum number. For the radical part of the atomic function, the so called *Slater Type Orbitals* (STO) are used with the form

$$R_{n,l}(r) = (2\varsigma)^{n+1/2}\left[(2n)!\right]^{-1/2} r^{n-1} \exp(-\varsigma r) \tag{A.30}$$

where n is the principle quantum number, and l is the orbital exponent, a function of the atomic number.

The variational principle is then applied as previously outlined except the total electron wave function consists of the product of molecular orbitals such as given in equation (A.27) above and the orthonormality of the electron wave function leads to

$$\sum_{\mu\nu} c^{*}_{\mu i} c_{\nu j} S_{\mu\nu} = \delta_{ij} \tag{A.31}$$

where $S_{\mu\nu}$ is the overlap integral for the atomic orbitals, defined as

$$S_{\mu\nu} = \int \phi_{\mu}(1)\phi_{\nu}(1) d\tau_1 \tag{A.32}$$

This leads to the so called *Roothan equations* given by

$$\sum_{\nu}\left(F_{\mu\nu} - \varepsilon_i S_{\mu\nu}\right)C_{\nu i} = 0 \qquad\qquad i = 1,2,\ldots,n \tag{A.33}$$

where the elements of the matrix representation of the Hartree-Fock hamiltonian are

$$F_{\mu\nu} = H_{\mu\nu} + \sum_{\lambda\sigma} P_{\lambda\sigma}\left[(\mu\nu|\lambda\sigma) - \tfrac{1}{2}(\mu\lambda|\nu\sigma)\right] \tag{A.34}$$

and

$$H_{\mu\nu} = \int \phi(1)\, \hat{H}^{core}\, \phi_{\nu}(1) d\tau_1 \tag{A.35}$$

$$P_{\mu\nu} = 2\sum_{i}^{occ} c_{\mu i}^{*} c_{\nu i} \tag{A.36}$$

$$(\mu\nu|\lambda\sigma) = \iint \phi_{\mu}^{*}(1)\phi_{\nu}^{*}(1)\frac{1}{r_{12}}\phi_{\lambda}(2)\phi_{\sigma}(2)d\tau_1 d\tau_2 \tag{A.37}$$

The matrix of elements $P_{\mu\nu}$ is the electron density matrix, $H_{\mu\nu}$ are the elements of the core Hamiltonian with respect to atomic orbitals, and equation (A.37) is the general two-electron interaction integral over atomic orbitals. Equations (A.33) are algebraic equations in contrast with the differential equations (A.18) or (A.19) previously derived.

The Roothan equation (A.33) can be written in matrix from as

$$FC = SCE \tag{A.38}$$

where E is the diagonal matrix of the ε_i. The matrix elements of the Hartree-Fock Hamiltonian operator are dependent on the orbitals through the elements $P_{\mu\nu}$, and the Roothan equations are solved by first assuming an initial set of linear expansion coefficients $c_{\mu i}$, generating the corresponding density matrix $P_{\mu\nu}$ and computing a first guess to $F_{\mu\nu.}$ The diagonalization procedure is affected by standard matrix eigenvalue techniques, and new expansion coefficients are calculated. The whole process is repeated until the coefficients no longer change within a given tolerance on repeated iteration (Pople, 1970).

B: DFT Formalisms

Local Density Methods

In the Local Density Approximation (LDA) it is assumed that the density locally can be treated as a uniform electron gas, or equivalently that the density is a slowly varying function. The exchange-correlation energy for the homogeneous electron gas can be written as:

$$E_{xc}^{LDA} = E_x^{LDA} + E_c^{LDA} \tag{B.1}$$

The first term, representing the exchange energy, has the form:

$$E_x^{LDA} = -9/4\alpha_{ex}\left[3/4\pi\right]^{1/3}\sum_{\gamma}\int\left[\rho_1^{\gamma}(\vec{r}_1)\right]^{4/3}d\vec{r}_1 \tag{B.2}$$

where the electron gas value for the exchange scale factor α_{ex} is 2/3. The exact exchange energy in the Kohn-Sham theory is simply E_{xc} corresponding to single determinantal wave function constructed from the exact Kohn-Sham orbitals. The second term, representing the correlation energy, has the form:

$$E_c^{LDA} = \int \rho_1(\vec{r}_1)\varepsilon_c\left[\rho_1^{\alpha}(\vec{r}_1)\rho_1^{\beta}(\vec{r}_1)\right]d\vec{r}_1 \tag{B.3}$$

where $\varepsilon_c\left[\rho_1^{\alpha}, \rho_1^{\beta}\right]$ represents the correlation energy per electron in a gas with the spin densities ρ_1^{α} and ρ_1^{β}. The specific correlation energy, $\varepsilon_c\left[\rho_1^{\alpha}, \rho_1^{\beta}\right]$, is not known analytically. However, approximations of increasing accuracy have been developed.

Simplified versions of LDA were known long before the formal development of DFT. Of particular importance is Hartree-Fock-Slater, or Xα. This method is

retains only the exchange part (see equation B.2) of the total expression for the exchange-correlation energy given in equation B.3 and adopts in many cases values for the exchange scaling factor that differs somewhat from 2/3.

The exchange-correlation hole functions for the homogeneous electron gas satisfy the general constraints given in equation 3.21 and can thus be used as models for calculations on atoms and molecules by substituting the corresponding (in homogeneous) electron densities into the expression for the exchange-correlation energy in equation B.1.

The LSDA approximation in general underestimates the exchange energy by ~10%, thereby creating errors which are larger than the whole correlation energy. Electron correlation is furthermore overestimated. Despite the simplicity of the fundamental assumptions, LSDA methods are often found to provide results with accuracy similar to that obtained by wave mechanics HF methods. (Jensen, 1998)

Gradient Corrected Methods

Improvements over the LSDA approach have to consider a non-uniform electron gas. A step in this direction is to make the exchange and correlation energies dependent not on the electron density, but also on derivatives of the density. Such methods are known as Gradient Corrected or Generalized Approximation (GGA) methods (a straightforward Taylor expansion does not lead to an improvement over LSDA, it actually makes things worse, thus the name generalized gradient approximation). GGA methods are also sometimes referred to as non-local methods, although this somewhat misleading since the functionals since the functionals depend only on the density (and derivatives) at a given point, not on a space volume as for example the Hartree-Fock exchange energy.

Perdew and Wang, 1986 (PW86) proposed modifying the LSDA exchange expression to that shown in equation B.4, where x is a dimensionless gradient variable, and a, b, c being suitable constants (summation over equivalent expressions for the α and β densities is implicitly assumed).

$$\varepsilon_x^{PW86} = \varepsilon_x^{LDA}(1 + ax^2 + bx^4 + cx^6)^{1/15}$$
$$x = \frac{|\nabla\rho|}{\rho^{4/3}} \tag{B.4}$$

Becke (1988) proposed a widely used correction (B or B88) to the LSDA exchange energy, which has the correct $-r^{-1}$ asymptotic behavior for the energy density (but not for the exchange potential).

$$\varepsilon_x^{B88} = \varepsilon_x^{LDA} + \Delta\varepsilon_x^{B88}$$
$$\Delta_x^{B88} = -\beta\rho^{1/3}\frac{x^2}{1 + 6\beta x \sinh^{-1} x} \tag{B.5}$$

The β parameter is determined by fitting to known atomic data and x is defined in equation B.5. Another functional form (not a correction) proposed by Becke and Roussel, 1989 (BR) has the form:

$$\varepsilon_x^{BR} = -\frac{2 - 2e^{-ab} - abe^{-ab}}{4b}$$
$$a^3 e^{-ab} = 8\pi\rho$$
$$a(ab - 2) = b\frac{\nabla^2\rho - 2D^2}{\rho} \tag{B.6}$$
$$D = \sum_i^N |\nabla\phi_i|^2 - \frac{(\nabla\rho)^2}{4\rho}$$

This functional contains derivatives of the orbitals, not just the gradient of the total density, and is computationally slightly more expensive. Despite the

apparent difference in functional form, exchange expressions B.5 & B.6 have been found to provide results of similar quality.

Perdew and Wang (1991) have proposed an exchange functional to be used in connection with the PW91 correlation functional given below.

$$\varepsilon_x^{PW91} = \varepsilon_x^{LDA}\left(\frac{1 + xa_1 \sinh^{-1}(xa_2) + (a_3 + a_4 e - bx^2)x^2}{1 + xa_1 \sinh^{-1}(xa_2) + a_5 x^2}\right) \tag{B.7}$$

where $a_{1\text{-}5}$ and b again are suitable constants and x is defined in equation B.4.

There have been various gradient corrected functional forms proposed for the correlation energy. One popular functional (not a correction) is due to Lee, Yang and Parr, 1988 (LYP) and has the form:

$$\begin{aligned}
\varepsilon_c^{LYP} &= -a\frac{\gamma}{(1 + d\rho^{-1/3})} - ab\frac{\gamma e^{-c\rho^{-1/3}}}{9(1 + d\rho^{-1/3})\rho^{8/3}} \\
&\quad \times \left[\begin{array}{l} 18(2^{2/3})C_F(\rho_\alpha^{8/3} + \rho_\beta^{8/3}) - 18\rho t_w \\ + \rho_\alpha(2t_w^\alpha + \nabla^2\rho_\alpha) + \rho_\beta(2t_w^\beta + \nabla^2\rho_\beta) \end{array}\right] \\
\gamma &= 2\left[1 - \frac{\rho_\alpha^2 + \rho_\beta^2}{\rho^2}\right] \\
t_W^\sigma &= \frac{1}{8}\left(\frac{\left|\nabla\rho_\sigma\right|^2}{\rho_\sigma} - \nabla^2\rho_\sigma\right)
\end{aligned} \tag{B.8}$$

where the a, b, c and d parameters are determined by fitting to data for the helium atom. The t_w functional is known as the local Weizsacker kinetic energy density. Note that the γ-factor becomes zero when all the spins are aligned

($\rho=\rho_\alpha$, $\rho_\beta=0$), i.e., the LYP functional does not predict any parallel spin correlation in such a case (e. g. the LYP correlation energy in triplet He is zero).

Perdew proposed a gradient correction to the LSDA result. It appeared in 1986 and is known as by the acronym P86. Then the formalism proposed by Perdew was modified by Perdew and Wang in 1991, this modified form of the formalism is known as PW91 or P91.

It should be noted that several of the proposed functionals violate fundamental restrictions, such as predicting correlation energies for one-electron systems (for example P86 and PW91) or failing to have the exchange energy cancel the coulomb self-repulsion.

C. Input and Output Files of SPARTAN'02 and PQS

Input file and normal output file for equilibrium calculation of ethylene adsorption on Ni(111) were given in Table C.1 and Table C.2, respectively. It should be noted that input geometry was the point with the minimum energy in the energy profile given in Figure 4.2.

Table C.3 illustrated PQS output file for Equilibrium Geometry Calculation of Ni_{13} nanocluster which included PQS input file, as well.

Table C.1 SPARTAN'02 input file for equilibrium geometry calculation of ethylene adsorption on Ni(111)

```
C OPT B3LYP 6-31G** PARTIAL CONVERGE SCF_CONVERGENCE=4
C SCFCYCLE=10000 GEOMETRYCYCLE=1000
 GRADIENTTOLERANCE=1.E-3
 DISTANCETOLERANCE=1.E-2 PRINTLEV=4
Molecule001
0 1
28   3.275825855   1.142049098   1.457237138
28   1.107472194   2.129069994   0.727327517
28   1.201461886  -0.237757107   1.500652430
28  -0.966891881   0.749263789   0.770742704
 1  -2.298879179  -0.136735169   0.798620353
 1  -1.640717666   0.274452679  -0.600561324
 1  -2.359231736   1.383048032   0.302054458
 1  -1.027244387   2.269047042   0.274176650
 1  -0.308730262   1.160451531  -0.628438920
 1  -0.248377915  -0.359331670  -0.131872918
 1   0.527636047  -0.712568427   0.129348297
 1   4.668165711   0.508264802   1.925925490
 1   3.994339979   0.033453587   0.554621568
 1   4.607813257   2.028048109   1.429359435
 1   3.933987527   1.553236895   0.058055460
 1   3.215473348   2.661832300   0.960671084
 1   2.602000124   0.667237884   0.085933269
 1   1.859623397   0.173430583   0.101470595
 1   1.919975904  -1.346352619   0.598036702
 1   1.825986319   1.020474588  -0.175288054
```

Table C.1 (cont'd)

```
 1   2.439459544   3.015068952   0.699449815
 1   1.765633655   2.540257789  -0.671854107
 1  -0.284867767   2.762854343   0.258639272
 1   0.433646412   1.654258885  -0.643976353
 1   1.047119584   3.648853248   0.230761570
 1   3.336178361  -0.377734208   1.953803192
 1   2.593801688  -0.871541509   1.969340729
 1   1.261814391  -1.757540415   1.997218378
 1  -0.130525360  -1.123756170   1.528529920
 1  -0.906539375  -0.770519413   1.267308758
 6  -0.738528256   1.475564720   2.646170533
 6   0.349649249   2.482833384   2.544070724
 1  -1.714907573   1.862492725   2.942973572
 1  -0.482821103   0.623656709   3.287681044
 1   1.138669938   2.358963789   3.291406861
 1   0.002528091   3.515671251   2.560404161
ENDCART
ATOMLABELS
"Ni1"
"Ni2"
"Ni3"
"Ni4"
"H1"
"H2"
"H3"
"H4"
"H5"
"H6"
"H7"
"H8"
"H9"
"H10"
"H11"
"H12"
"H13"
"H14"
"H15"
"H16"
"H17"
"H18"
"H19"
"H20"
```

Table C.1 (cont'd)

```
"H21"
"H22"
"H23"
"H24"
"H25"
"H26"
"C1"
"C2"
"H27"
"H28"
"H29"
"H30"
ENDATOMLABELS
FROZEN
   1    2    3    4    5    6    7    8    9   10   11   12
  13   14   15   16   17   18   19   20   21   22   23   24
  25   26   27   28   29   30
ENDFROZEN
HESSIAN
   0    0    0    0   13   13   13   13   13   13   13   13
  13   13   13   13   13   13   13   13   13   13   13   13
  13   13   13   13   13   13    0    0   13   13   13   13
   2    3    1
   1    3    1
   1    2    1
   2    4    1
   4    3    1
   1   14    1
   1   12    1
   1   26    1
   1   16    1
   3   28    1
   3   29    1
   3   27    1
   3   18    1
   3   19    1
   3   11    1
   4    7    1
   4    5    1
   4   30    1
   4    8    1
   2   21    1
```

Table C.1 (cont'd)

```
  2   25    1
  2   23    1
  2   24    1
  2   20    1
  2   22    1
  1   15    1
  1   13    1
  1   17    1
  4    9    1
  4   10    1
  4    6    1
 32   31    2
 32   35    1
 31   34    1
 31   33    1
 32   36    1
ENDHESS
BEGINPROPIN

ENDPROPIN
```

Table C.2 SPARTAN'02 output file for equilibrium geometry calculation of ethylene adsorption on Ni(111)

```
Spartan '02 Mechanics Program:  (PC/x86)
Release  115B

 Run Type            :       Frequency
 Method              :          MMFF94 (with extensions)
 Stoichiometry       :      C2 H30 Ni4
 Number of Atoms     :              36
 Point Group         :              C1
 Degrees of Freedom  :             102

Cycle    E           Gmax    maxDist   MaxTors
   0    4.09936e+3   2.96e+3

  Reason for exit: Successful completion
  Mechanics CPU Time : 000:00:00.2
  Mechanics Wall Time: 000:00:00.2
Spartan '02 Quantum Mechanics Program:  (PC/x86)
Release  115B

Job type: Geometry optimization.
Method: RB3LYP
Basis set: 6-31G**
Number of shells: 126
Number of basis functions: 296

SCF model:
 A restricted hybrid HF-DFT SCF calculation will be
 performed using Pulay DIIS extrapolation
          ... 1   -6128.556727741      7.09E-002
          ... 2   -6125.263121512      6.16E-003
          ... 3   -6098.679137773      5.34E-002
          ... 4   -6123.443612898      1.65E-002
          ... 5   -6125.378826505      6.50E-003
          ... 6   -6125.179356326      1.02E-002
          ... 7   -6125.655798502      3.62E-003
          ... 8   -6125.710362168      1.91E-003
          ... 9   -6125.730555333      5.34E-004
          ...10   -6125.725247337      1.19E-003
          ...11   -6125.732310169      4.87E-004
          ...12   -6125.734354081      9.15E-005
          ...13   -6125.734511736      2.80E-005
          ...14   -6125.734567306      3.24E-005
          ...15   -6125.734587132      1.81E-005
          ...16   -6125.734593300      1.07E-005
          ...17   -6125.734599708      3.63E-006
          ...18   -6125.734599026      1.62E-006
          ...19   -6125.734602590      7.27E-007
          ...20   -6125.734594148      3.34E-007
          ...21   -6125.734591119      1.31E-007
```

Table C.2 (cont'd)

```
Optimization:
         Step      Energy          Max Grad.      Max Dist.
            1   -6125.7345943       0.002994       0.009310   2
          ... 1   -6125.734705855      4.00E-005
          ... 2   -6125.734594495      9.74E-006
          ... 3   -6125.734572573      6.41E-005
          ... 4   -6125.734599123      4.71E-006
          ... 5   -6125.734595414      4.92E-006
          ... 6   -6125.734601315      2.88E-006
          ... 7   -6125.734601841      8.91E-007
          ... 8   -6125.734601502      1.08E-006
          ... 9   -6125.734601227      5.16E-007
          ...10   -6125.734593061      5.23E-007
          ...11   -6125.734589593      1.06E-007
            2   -6125.7345818       0.002692       0.228398   1
          ... 1   -6125.726698050      1.14E-003
          ... 2   -6125.730951636      3.59E-004
          ... 3   -6125.697766072      2.47E-003
          ... 4   -6125.731205025      3.40E-004
          ... 5   -6125.731948017      2.53E-004
          ... 6   -6125.732307723      3.74E-005
          ... 7   -6125.732308021      5.06E-005
          ... 8   -6125.732318527      4.05E-005
          ... 9   -6125.732326266      6.83E-006
          ...10   -6125.732322293      5.14E-006
          ...11   -6125.732320541      6.77E-006
          ...12   -6125.732322167      2.86E-006
          ...13   -6125.732320468      7.56E-007
          ...14   -6125.732321483      3.70E-007
          ...15   -6125.732316766      2.73E-007
          ...16   -6125.732331515      1.13E-007
            3   -6125.7323351       0.014897       0.152717
          ... 1   -6125.736256321      7.84E-004
          ... 2   -6125.733899716      2.14E-004
          ... 3   -6125.722982377      1.39E-003
          ... 4   -6125.734058742      1.88E-004
          ... 5   -6125.734316133      1.55E-004
          ... 6   -6125.734438784      2.95E-005
          ... 7   -6125.734427846      5.91E-005
          ... 8   -6125.734444106      1.80E-005
          ... 9   -6125.734445567      1.00E-005
          ...10   -6125.734445074      1.18E-005
          ...11   -6125.734450228      2.17E-006
          ...12   -6125.734449045      1.27E-006
          ...13   -6125.734455883      4.89E-007
          ...14   -6125.734451597      1.95E-007
          ...15   -6125.734454046      2.26E-007
            4   -6125.7344488       0.003697       0.048042
          ... 1   -6125.734926820      2.64E-004
          ... 2   -6125.734588421      4.42E-005
          ... 3   -6125.734118274      2.88E-004
          ... 4   -6125.734600204      3.71E-005
```

Table C.2 (cont'd)

```
... 5   -6125.734618815      1.33E-005
... 6   -6125.734617487      1.61E-005
... 7   -6125.734620553      6.95E-006
... 8   -6125.734619782      8.09E-006
... 9   -6125.734623613      2.08E-006
...10   -6125.734629956      1.19E-006
...11   -6125.734631357      1.39E-006
...12   -6125.734625333      5.08E-007
...13   -6125.734620368      1.82E-007
  5   -6125.7346132        0.001381       0.055695
... 1   -6125.734616683      1.52E-004
... 2   -6125.734618258      3.87E-005
... 3   -6125.734184367      2.88E-004
... 4   -6125.734630186      1.74E-005
... 5   -6125.734629182      1.74E-005
... 6   -6125.734633410      6.54E-006
... 7   -6125.734622555      7.54E-006
... 8   -6125.734625735      1.42E-006
... 9   -6125.734625323      1.08E-006
...10   -6125.734622722      1.17E-006
...11   -6125.734624909      2.82E-007
...12   -6125.734622991      1.19E-007
  6   -6125.7346209        0.001017       0.056069
... 1   -6125.734835732      1.73E-004
... 2   -6125.734642855      3.47E-005
... 3   -6125.734272682      2.63E-004
... 4   -6125.734648294      1.62E-005
... 5   -6125.734651845      9.11E-006
... 6   -6125.734653295      1.20E-005
... 7   -6125.734654668      5.53E-006
... 8   -6125.734655676      2.94E-006
... 9   -6125.734656364      7.90E-007
...10   -6125.734658289      7.73E-007
...11   -6125.734655577      8.16E-007
...12   -6125.734652442      2.56E-007
  7   -6125.7346514        0.000981       0.010925
... 1   -6125.734356911      4.39E-005
... 2   -6125.734652827      1.19E-005
... 3   -6125.734630711      6.94E-005
... 4   -6125.734655650      1.07E-005
... 5   -6125.734659978      6.26E-006
... 6   -6125.734664725      1.66E-006
... 7   -6125.734668588      1.70E-006
... 8   -6125.734662337      6.58E-007
... 9   -6125.734662470      3.34E-007
...10   -6125.734662572      4.60E-007
  8   -6125.7346606        0.000499       0.007554
... 1   -6125.734414849      2.16E-005
... 2   -6125.734652953      3.14E-006
... 3   -6125.734650485      1.56E-005
... 4   -6125.734651945      4.46E-006
... 5   -6125.734652662      2.23E-006
```

Table C.2 (cont'd)

```
... 6   -6125.734655476      1.41E-006
... 7   -6125.734648029      3.77E-007
... 8   -6125.734640676      5.82E-007
... 9   -6125.734640858      1.61E-007
  9   -6125.7346445       0.000435       0.002598
... 1   -6125.734700604      3.32E-005
... 2   -6125.734653296      1.13E-005
... 3   -6125.734633705      6.51E-005
... 4   -6125.734652710      9.60E-006
... 5   -6125.734646209      4.82E-006
... 6   -6125.734646794      1.16E-006
... 7   -6125.734650982      9.33E-007
... 8   -6125.734650862      4.79E-007
... 9   -6125.734650004      2.13E-007
...10   -6125.734649899      3.43E-007
 10   -6125.7346488       0.000291       0.004570
... 1   -6125.734645352      3.28E-005
... 2   -6125.734653992      9.87E-006
... 3   -6125.734635725      6.34E-005
... 4   -6125.734654599      7.08E-006
... 5   -6125.734650459      3.54E-006
... 6   -6125.734649867      1.14E-006
... 7   -6125.734660099      1.36E-006
... 8   -6125.734656396      3.74E-007
... 9   -6125.734658072      2.01E-007
...10   -6125.734656411      2.58E-007
 11   -6125.7346556       0.000093       0.001504
... 1   -6125.734626345      9.00E-006
... 2   -6125.734653978      2.92E-006
... 3   -6125.734657384      1.95E-005
... 4   -6125.734657403      1.59E-006
... 5   -6125.734658841      9.25E-007
... 6   -6125.734652501      3.44E-007
... 7   -6125.734651626      3.99E-007
... 8   -6125.734646030      1.07E-007
 12   -6125.7346537       0.000029       0.001219
... 1   -6125.734646932      3.85E-006
... 2   -6125.734653575      7.70E-007
... 3   -6125.734659662      5.28E-006
... 4   -6125.734660362      4.14E-007
... 5   -6125.734657974      2.63E-007
... 6   -6125.734653181      2.76E-007
 13   -6125.7346519       0.000019       0.001648
... 1   -6125.734631991      3.85E-006
... 2   -6125.734653091      9.22E-007
... 3   -6125.734647702      5.57E-006
... 4   -6125.734650192      8.45E-007
... 5   -6125.734644751      4.57E-007
... 6   -6125.734638359      1.68E-007
... 7   -6125.734632690      2.16E-007
 14   -6125.7346247       0.000022       0.001039
```

Table C.2 (cont'd)

```
  Reason for exit: Sucessful completion
  Quantum Mechanics Program CPU Time : 010:30:41.5
  Quantum Mechanics Program Wall Time: 004:22:01.5

Spartan '02 Properties Program:  (PC/x86)
Release  115B
  Reason for exit: Successful completion
  Properties Program CPU Time : 000:00:01.9
  Properties Program Wall Time: 000:00:02.0
```

Table C.3 PQS log-output file for equilibrium geometry calculation of Ni_{13} nanocluster

```
================================================================================
  PQS  Ab Initio Program Package running on n1
 Date= Mon Jul 11 06:27:15 2005 Time= Mon Jul 11 06:27:15 2005
 Executable : /usr/local/share/PQS/pqs_pvm.x
================================================================================
  Master process on: n1
   4 slaves working on your job
  Slave on: n2
  Slave on: n1
  Slave on: n2
  Slave on: n1
%MEM=200

GEOM=TX92 CHARGE=0 MULT=9
ni   4.943734754   3.122097264  -1.045258458
ni   3.971264599   5.281331800  -1.382954054
ni   2.696827552   3.400313888  -1.268033094
ni   1.446858892   3.131656348   0.613728441
ni   1.422390506   1.519295975  -1.153112134
ni   1.810076471   5.287239638  -0.357643763
ni   0.449920351   3.678530511  -1.490807730
ni   2.004655358   5.019816061  -2.736351644
ni   3.388999747   1.780811715   0.200285456
ni   3.623169314   4.122242022   0.680385678
ni   3.583578634   1.513388138  -2.178422425
ni   3.946796213   3.668971428  -3.149794629
ni   1.770485791   2.678385753  -3.216451866
BASIS=6-31G*
GUESS=HUCKEL
SCF DFTP=B3LYP ITER=7 FACTOR=2
BASIS=m6-31G*
GUESS=READ
SCF DFTP=B3LYP ITER=7 FACTOR=2
BASIS=m6-31G**
OPTIM optc=500 gtol=0.001 dtol=0.01
GUESS=READ
INTE route=2
SCF DFTP=B3LYP THRE=4 ITER=1000 FACTOR=2
FORCE
JUMP

 Empirical Formula: Ni13

    Cartesian Coordinates in Standard Orientation
                 Coordinates (Angstroms)
   ATOM          X         Y         Z
  1  ni       1.935231  -0.628795  -1.017411
  2  ni       1.196038  -1.646205   1.017411
  3  ni       0.000000   0.000000   0.000000
  4  ni      -1.935231  -0.628795  -1.017411
  5  ni      -1.196038   1.646205  -1.017411
  6  ni      -1.196038  -1.646205   1.017411
  7  ni      -1.935231   0.628795   1.017411
  8  ni       0.000000   0.000000   2.293000
```

Table C.3 (cont'd)

```
 9  ni        0.000000    0.000000   -2.293000
10  ni        0.000000   -2.034822   -1.017411
11  ni        1.196038    1.646205   -1.017411
12  ni        1.935231    0.628795    1.017411
13  ni        0.000000    2.034822    1.017411
 Point Group: D5d   Number of degrees of freedom:   3

 Charge:   0  Multiplicity:   9
 Wavefunction:  UDFT                XC potential: b3lyp
 Basis set: m6-31g-dp
 Number of contracted basis functions:   468

** Cycle   1  Energy -19605.366292387   RMSG  0.02752   RMSD  0.17321 **

** Cycle   1  Energy -19605.366292387   RMSG  0.01481   RMSD  0.01597 **

** Cycle   2  Energy -19605.374002027   RMSG  0.01189   RMSD  0.21213 **

** Cycle   3  Energy -19605.389676809   RMSG  0.00478   RMSD  0.11187 **

** Cycle   4  Energy -19605.392963041   RMSG  0.00052   RMSD  0.01316 **

                CONVERGED GEOMETRY
              Coordinates (Angstroms)
              X                Y                Z
ni        2.01154775860037  -0.65359148668241  -1.05901403885244
ni        1.24320488480870  -1.71112472689214   1.05901403885244
ni        0.00000000000000   0.00000000000000   0.00000000000000
ni       -2.01154775860037  -0.65359148668241  -1.05901403885244
ni       -1.24320488480870   1.71112472689214  -1.05901403885244
ni       -1.24320488480870  -1.71112472689214   1.05901403885244
ni       -2.01154775860037   0.65359148668241   1.05901403885244
ni        0.00000000000000   0.00000000000000   2.37753456512288
ni        0.00000000000000   0.00000000000000  -2.37753456512288
ni        0.00000000000000  -2.11506648041945  -1.05901403885244
ni        1.24320488480870   1.71112472689214  -1.05901403885244
ni        2.01154775860037   0.65359148668241   1.05901403885244
ni        0.00000000000000   2.11506648041945   1.05901403885244

 dipole/D =     0.000000  0.000000  0.000000  total=  0.000000
 Expectation value of S**2: 20.4840553  Multiplicity:  9.1069326


 Charge:   0  Multiplicity:   9
 Wavefunction:  UDFT                XC potential: b3lyp
 Basis set: m6-31g-dp
 Number of contracted basis functions:   468

 Energy is:     -19605.392963041 au

 dipole/D =     0.000000  0.000000  0.000000  total=  0.000000
 Expectation value of S**2: 20.4840553  Multiplicity:  9.1069326

================================================================================
Total master CPU time =      6.48 Elapsed =    268.98 min
Termination on Mon Jul 11 10:56:14 2005
================================================================================
```

Table C.4 PQS normal output file for equilibrium geometry calculation of Ni_{13} nanocluster

```
================================================================================
 PQS  Ab Initio Program Package running on n1
 Date= Mon Jul 11 06:27:15 2005 Time= Mon Jul 11 06:27:15 2005
 Executable : /usr/local/share/PQS/pqs_pvm.x
================================================================================

  This program is Copyright 2004 by Parallel Quantum Solutions.
  PQS manufactures high-performance, low-cost parallel supercomputers,
  complete with software, for ab initio molecular modeling

  Web: www.pqs-chem.com  Ph: (479) 521-5118  email: sales@pqs-chem.com

  This software is provided under written license and may be used,
  copied, transmitted or stored only in accord with that license.

  Cite this work as:  PQS version 3.1, Parallel Quantum Solutions,
  2013 Green Acres Road,  Fayetteville,  Arkansas  72703
**********************************************************************
*  WARNING: This program takes advantage of Large-File Handling and  *
*  is capable of writing files of size in excess of 2 GB.  Multiple  *
*  file capability  (formerly in the MP2 energy routines)  has been  *
*  removed. If your operating system is out of date and is limited   *
*  to files no bigger than 2 GB then you will be UNABLE to run large *
*  MP2 energy or MP2 gradient calculations with this executable.     *
*  You should either upgrade your O/S or use an earlier version of   *
*  PQS (version 3.0 or lower) to run these jobs wherever possible.   *
**********************************************************************

  Master process on: n1
    4 slaves working on your job
  Slave on: n2
  Slave on: n1
  Slave on: n2
  Slave on: n1
============================== PQS input ==============================
%MEM=200

GEOM=TX92 CHARGE=0 MULT=9
ni   4.943734754   3.122097264  -1.045258458
ni   3.971264599   5.281331800  -1.382954054
ni   2.696827552   3.400313888  -1.268033094
ni   1.446858892   3.131656348   0.613728441
ni   1.422390506   1.519295975  -1.153112134
ni   1.810076471   5.287239638  -0.357643763
ni   0.449920351   3.678530511  -1.490807730
ni   2.004655358   5.019816061  -2.736351644
ni   3.388999747   1.780811715   0.200285456
ni   3.623169314   4.122242022   0.680385678
ni   3.583578634   1.513388138  -2.178422425
ni   3.946796213   3.668971428  -3.149794629
ni   1.770485791   2.678385753  -3.216451866
BASIS=6-31G*
GUESS=HUCKEL
SCF DFTP=B3LYP ITER=7 FACTOR=2
BASIS=m6-31G*
```

Table C.4 (cont'd)

GUESS=READ
SCF DFTP=B3LYP ITER=7 FACTOR=2
BASIS=m6-31G**
OPTIM optc=500 gtol=0.001 dtol=0.01
GUESS=READ
INTE route=2
SCF DFTP=B3LYP THRE=4 ITER=1000 FACTOR=2
FORCE
JUMP

Empirical Formula: Ni13
nuclear repulsion energy is 11139.580732890 au

Cartesian Coordinates in Standard Orientation

		Coordinates (Angstroms)		
ATOM		X	Y	Z
1	ni	1.935231	-0.628795	-1.017411
2	ni	1.196038	-1.646205	1.017411
3	ni	0.000000	0.000000	0.000000
4	ni	-1.935231	-0.628795	-1.017411
5	ni	-1.196038	1.646205	-1.017411
6	ni	-1.196038	-1.646205	1.017411
7	ni	-1.935231	0.628795	1.017411
8	ni	0.000000	0.000000	2.293000
9	ni	0.000000	0.000000	-2.293000
10	ni	0.000000	-2.034822	-1.017411
11	ni	1.196038	1.646205	-1.017411
12	ni	1.935231	0.628795	1.017411
13	ni	0.000000	2.034822	1.017411

Point Group: D5d Number of degrees of freedom: 3

Largest Abelian subgroup of the molecular point group is C2h
Basis set 6-31g-d from library

1313 gaussians 351 shells 468 contr. gaussians 104 contr. shells
6022147131. integrals (less symmetry or neglect)

Basis may be numerically unstable - integral stability switched on
****CAUTION****
For Huckel Guess: First Row Transition Metals are not
well tested. Use with caution.
Extended Huckel Guess

ALPHA SPIN
orbital symmetries and energies
occupied orbitals

1	Ag	? (E)	? (E)	Bu	Ag
-303.55896		-303.55839	-303.55839	-303.55820	-303.55489
6	? (E)	? (E)	? (E)	? (E)	Ag
-303.55340		-303.55340	-303.55340	-303.55340	-303.55336
11	? (E)	? (E)	Bu (E)	Ag	? (E)
-303.55282		-303.55282	-303.55281	-38.28939	-38.27818
16	? (E)	Bu	? (E)	? (E)	Ag
-38.27818		-38.27812	-38.27543	-38.27543	-38.27532
21	Bu	Ag	? (E)	? (E)	? (E)
-38.27529		-38.27331	-38.27330	-38.27330	-38.27330

Table C.4 (cont'd)

26 ? (E)	Ag	? (E)	? (E)	Bu (E)
-38.27330	-32.69356	-32.69113	-32.69113	-32.69112
31 ? (E)	? (E)	? (E)	? (E)	Ag
-32.69110	-32.69110	-32.69109	-32.69109	-32.69108
36 ? (E)	? (E)	Bu	? (E)	? (E)
-32.69054	-32.69054	-32.69052	-32.69006	-32.69006
41 Bu (E)	Bg (E)	? (E)	? (E)	Au (E)
-32.69006	-32.69003	-32.69003	-32.69003	-32.69000
46 ? (E)	? (E)	? (E)	? (E)	? (E)
-32.69000	-32.69000	-32.69000	-32.69000	-32.68998
51 ? (E)	? (E)	? (E)	? (E)	? (E)
-32.68998	-32.68998	-32.68998	-32.68996	-32.68996
56 Ag (E)	? (E)	? (E)	? (E)	? (E)
-32.68996	-32.68996	-32.68996	-32.68992	-32.68992
61 ? (E)	? (E)	Bu (E)	? (E)	? (E)
-32.68992	-32.68992	-32.68992	-32.68991	-32.68991
66 Ag	? (E)	? (E)	Bu	Ag
-5.51343	-5.43082	-5.43082	-5.43028	-5.38000
71 ? (E)	? (E)	? (E)	? (E)	Ag
-5.37957	-5.37957	-5.37957	-5.37957	-5.36543
76 Bu	? (E)	? (E)	? (E)	? (E)
-5.36538	-5.36520	-5.36520	-3.61595	-3.61595
81 Bu	Bg	? (E)	? (E)	Au (E)
-3.61550	-3.61042	-3.61028	-3.61028	-3.60790
86 ? (E)	? (E)	? (E)	? (E)	? (E)
-3.60790	-3.60790	-3.60783	-3.60783	-3.60776
91 ? (E)	Bu (E)	? (E)	? (E)	? (E)
-3.60776	-3.60776	-3.60772	-3.60772	-3.60761
96 ? (E)	Ag (E)	? (E)	? (E)	Bu
-3.60761	-3.60761	-3.60740	-3.60740	-3.60725
101 ? (E)	? (E)	Bg (E)	Ag (E)	Ag
-3.60559	-3.60559	-3.60557	-3.60557	-3.60104
106 ? (E)	? (E)	? (E)	? (E)	Ag
-3.60040	-3.60040	-3.60039	-3.60039	-3.60026
111 Au (E)	Bu (E)	? (E)	? (E)	Bu
-3.60021	-3.60021	-3.60021	-3.60021	-3.59247
116 ? (E)	? (E)	Ag	Ag	? (E)
-3.59192	-3.59192	-0.63435	-0.56566	-0.56556
121 ? (E)	? (E)	? (E)	Bu	? (E)
-0.56556	-0.56555	-0.56555	-0.56410	-0.56397
126 ? (E)	? (E)	? (E)	? (E)	? (E)
-0.56397	-0.56332	-0.56332	-0.56328	-0.56328
131 Ag	? (E)	? (E)	? (E)	? (E)
-0.56311	-0.56295	-0.56295	-0.56290	-0.56290
136 Bu	Ag	? (E)	? (E)	? (E)
-0.56285	-0.56272	-0.56268	-0.56268	-0.56255
141 ? (E)	? (E)	? (E)	Bu (E)	Au (E)
-0.56255	-0.56250	-0.56250	-0.56233	-0.56233
146 Ag	? (E)	? (E)	? (E)	? (E)
-0.56232	-0.56219	-0.56219	-0.56218	-0.56218
151 Au	? (E)	? (E)	Bu	? (E)
-0.56216	-0.56212	-0.56212	-0.56155	-0.56128
156 ? (E)	Bu	? (E)	? (E)	? (E)
-0.56128	-0.56087	-0.56067	-0.56067	-0.55975
161 ? (E)	? (E)	? (E)	? (E)	? (E)
-0.55975	-0.55975	-0.55975	-0.55969	-0.55969
166 ? (E)	? (E)	? (E)	? (E)	Au (E)

Table C.4 (cont'd)

```
   -0.55963    -0.55963    -0.55958    -0.55958    -0.55951
171   Bu (E)      Bg          ? (E)       ? (E)       Au
   -0.55951    -0.55945    -0.55939    -0.55939    -0.55933
176    ? (E)       ? (E)       Bg          Ag          ? (E)
   -0.55922    -0.55922    -0.55905    -0.55754    -0.55691
181    ? (E)       ? (E)       ? (E)       Bu          ? (E)
   -0.55691    -0.55688    -0.55688    -0.48751    -0.48593
186    ? (E)
   -0.48593
Summary occupancy  Ag    Au    Bg    Bu    ?
              22     7     5    22   130

 BETA SPIN
  orbital symmetries and energies
  occupied orbitals
  1   Ag          ? (E)       ? (E)       Bu          Ag
 -303.55896  -303.55839  -303.55839  -303.55820  -303.55489
  6    ? (E)       ? (E)       ? (E)       ? (E)       Ag
 -303.55340  -303.55340  -303.55340  -303.55340  -303.55336
 11    ? (E)       ? (E)       Bu (E)      Ag          ? (E)
 -303.55282  -303.55282  -303.55281   -38.28939   -38.27818
 16    ? (E)       Bu          ? (E)       ? (E)       Ag
  -38.27818   -38.27812   -38.27543   -38.27543   -38.27532
 21   Bu          Ag          ? (E)       ? (E)       ? (E)
  -38.27529   -38.27331   -38.27330   -38.27330   -38.27330
 26    ? (E)       Ag          ? (E)       ? (E)       Bu (E)
  -38.27330   -32.69356   -32.69113   -32.69113   -32.69112
 31    ? (E)       ? (E)       ? (E)       ? (E)       Ag
  -32.69110   -32.69110   -32.69109   -32.69109   -32.69108
 36    ? (E)       ? (E)       Bu          ? (E)       ? (E)
  -32.69054   -32.69054   -32.69052   -32.69006   -32.69006
 41   Bu (E)      Bg (E)      ? (E)       ? (E)       Au (E)
  -32.69006   -32.69003   -32.69003   -32.69003   -32.69000
 46    ? (E)       ? (E)       ? (E)       ? (E)       ? (E)
  -32.69000   -32.69000   -32.69000   -32.69000   -32.68998
 51    ? (E)       ? (E)       ? (E)       ? (E)       ? (E)
  -32.68998   -32.68998   -32.68998   -32.68996   -32.68996
 56   Ag (E)      ? (E)       ? (E)       ? (E)       ? (E)
  -32.68996   -32.68996   -32.68996   -32.68992   -32.68992
 61    ? (E)       ? (E)       Bu (E)      ? (E)       ? (E)
  -32.68992   -32.68992   -32.68992   -32.68991   -32.68991
 66   Ag          ? (E)       ? (E)       Bu          Ag
   -5.51343    -5.43082    -5.43082    -5.43028    -5.38000
 71    ? (E)       ? (E)       ? (E)       ? (E)       Ag
   -5.37957    -5.37957    -5.37957    -5.37957    -5.36543
 76   Bu          ? (E)       ? (E)       ? (E)       ? (E)
   -5.36538    -5.36520    -5.36520    -3.61595    -3.61595
 81   Bu          Bg          ? (E)       ? (E)       Au (E)
   -3.61550    -3.61042    -3.61028    -3.61028    -3.60790
 86    ? (E)       ? (E)       ? (E)       ? (E)       ? (E)
   -3.60790    -3.60790    -3.60783    -3.60783    -3.60776
 91    ? (E)       Bu (E)      ? (E)       ? (E)       ? (E)
   -3.60776    -3.60776    -3.60772    -3.60772    -3.60761
 96    ? (E)       Ag (E)      ? (E)       ? (E)       Bu
   -3.60761    -3.60761    -3.60740    -3.60740    -3.60725
101    ? (E)       ? (E)       Bg (E)      Ag (E)      Ag
   -3.60559    -3.60559    -3.60557    -3.60557    -3.60104
```

Table C.4 (cont'd)

```
106    ? (E)       ? (E)       ? (E)       ? (E)       Ag
   -3.60040    -3.60040    -3.60039    -3.60039    -3.60026
111   Au (E)      Bu (E)       ? (E)       ? (E)       Bu
   -3.60021    -3.60021    -3.60021    -3.60021    -3.59247
116    ? (E)       ? (E)      Ag          Ag          ? (E)
   -3.59192    -3.59192    -0.63435    -0.56566    -0.56556
121    ? (E)       ? (E)       ? (E)       Bu          ? (E)
   -0.56556    -0.56555    -0.56555    -0.56410    -0.56397
126    ? (E)       ? (E)       ? (E)       ? (E)       ? (E)
   -0.56397    -0.56332    -0.56332    -0.56328    -0.56328
131   Ag          ? (E)       ? (E)       ? (E)       ? (E)
   -0.56311    -0.56295    -0.56295    -0.56290    -0.56290
136   Bu          Ag          ? (E)       ? (E)       ? (E)
   -0.56285    -0.56272    -0.56268    -0.56268    -0.56255
141    ? (E)       ? (E)       ? (E)       Bu (E)      Au (E)
   -0.56255    -0.56250    -0.56250    -0.56233    -0.56233
146   Ag          ? (E)       ? (E)       ? (E)       ? (E)
   -0.56232    -0.56219    -0.56219    -0.56218    -0.56218
151   Au          ? (E)       ? (E)       Bu          ? (E)
   -0.56216    -0.56212    -0.56212    -0.56155    -0.56128
156    ? (E)      Bu          ? (E)       ? (E)       ? (E)
   -0.56128    -0.56087    -0.56067    -0.56067    -0.55975
161    ? (E)       ? (E)       ? (E)       ? (E)       ? (E)
   -0.55975    -0.55975    -0.55975    -0.55969    -0.55969
166    ? (E)       ? (E)       ? (E)       ? (E)       Au (E)
   -0.55963    -0.55963    -0.55958    -0.55958    -0.55951
171   Bu (E)      Bg          ? (E)       ? (E)       Au
   -0.55951    -0.55945    -0.55939    -0.55939    -0.55933
176    ? (E)       ? (E)       Bg
   -0.55922    -0.55922    -0.55905
Summary occupancy  Ag    Au    Bg    Bu    ?
                   21     7     5    21   124
DFT exchange-correlation potential=b3lyp
Lowest eigenvalue of the overlap matrix  0.223572E-04
Integral thresholds are: Final=  0.1000E-09 Initial=  0.2236E-07
SCF parameters:
wave function type             =  uhf
charge                      = 0.00
number of electrons            =  364
number of alpha electrons      =  186
number of beta electrons       =  178
print level                 =    0
threshold for linear dependency = 0.100E-04
SCF threshold                  = 0.100E-04
diis switch-on                 =   2.00000
initial level shift            =   1.000
minimum level shift            =   0.300
Elapsed time before SCF (min)  =      0.07
                                                                  timing/min
SCFiter    etot          e2     Brillouin Delta-dens Errsq     cpu   elapsed
 1-19590.779028684 19169.661548 0.109E+01 6.98035 0.918E+02    0.12    2.00 D
 2-19596.105151650 18669.221544 0.495E+00 25.37009 0.252E+02    0.17    3.88 D
 3-19602.164698849 18924.510675 0.406E+00 26.49721 0.595E+01    0.22    5.71 D
 4-19604.437736027 18868.945866 0.346E+00  5.72954 0.156E+01    0.27    7.47 D
 5-19605.197534514 18758.915822 0.750E-01  6.07748 0.547E+00    0.32    9.18 D
 6-19605.481726334 18794.516765 0.178E-01  1.91604 0.380E-01    0.37   10.83 D
 7-19605.553043032 18786.778919 0.164E-01  1.10138 0.152E-01    0.42   12.44 D
Attention: NO CONVERGENCE
```

Table C.4 (cont'd)

```
 No convergence in    7 steps, Energy=   -19605.553043032 Eh
   Brillouin= 0.16397E-01

 Expectation value of S**2 and multiplicity= 20.0616765  9.0136955
 natural occupation numbers between 0.005 and 1.995
  178    1.992894
  179    1.000000
  180    1.000000
  181    1.000000
  182    1.000000
  183    1.000000
  184    1.000000
  185    1.000000
  186    1.000000
  187    0.007106

======================== SCF RESULTS ==========================

   Total Energy =   -19605.553043032 Eh
   nuclear ener.=    11139.580720653
   one-el.ener. =   -49531.912682851
   two-el.ener. =    18786.778919166
   kinetic ener.=    19572.321332743
   virial coeff.=          1.001698

   dipole/au=     0.000000   0.000000   0.000000  total=   0.000000 au
   dipole/D =     0.000000   0.000000   0.000000  total=   0.000000 D
   quadrupole/    XX=  -180.9563 YY=  -180.9557 ZZ=  -179.3090
   (Debye*Ang)    XY=     0.0000 XZ=     0.0000 YZ=    -0.0001
-------------------------------------------------------------
    Total Energy in different units :

   -85475.274604aJ   -51474378.813kJ/mol   -12302671.801kcal/mol
   -533494.46769eV  -6190908581.55K -0.128998342E+19Hz


======================== SCF RESULTS ==========================

  Alpha spin
   orbital symmetries and energies
   occupied orbitals. . . . . .
  Beta spin
   orbital symmetries and energies
   occupied orbitals. . . . . .
=============================================================
                JOB INFORMATION

 Time for SCF and total time=      0.54      0.56 min

 Master timings in minutes:
 1-el=         0.07  2-el=         0.02  DFT=          0.01
 misc=         0.44  elapsed=     12.57
 Memory status:
 request number=   4 memory marks=  0 last used address=     4642
 high water=  2914809 total available memory=200000001
 SCFMAIN
 **WARNING** Incomplete SCF convergence
```

Table C.4 (cont'd)

```
================================================================================
Program step = scf  Master CPU time =      0.54 Elapsed time =     12.55
Total CPU time =     46.54        Efficiency =   3.710 on   4 processors
0.016

================================================================================

 Basis set m6-31g-d from library

  1313 gaussians  351 shells  468 contr. gaussians  104 contr. shells
    6022147131. integrals (less symmetry or neglect)

 Basis may be numerically unstable - integral stability switched on
 SCF Guess from Previous Calculation
 DFT exchange-correlation potential=b3lyp
 Lowest eigenvalue of the overlap matrix  0.162729E-04
 Integral thresholds are: Final=  0.1000E-09 Initial=  0.1627E-07
 SCF parameters:
 wave function type             =  uhf
 charge                      = 0.00
 number of electrons            =  364
 number of alpha electrons      =  186
 number of beta electrons       =  178
 print level                 =    0
 threshold for linear dependency = 0.100E-04
 SCF threshold                  = 0.100E-04
 diis switch-on                 =   2.00000
 initial level shift            =   1.000
 minimum level shift            =   0.300
 Elapsed time before SCF (min)  =     12.64
                                                                    timing/min
SCFiter    etot          e2     Brillouin  Delta-dens  Errsq     cpu   elapsed
  1-19605.029325955 18823.782149 0.121E+00 27.30687 0.928E+00    0.12   14.84 D
  2-19605.184088540 18733.212334 0.710E-01 16.85643 0.320E+00    0.17   16.80 D
  3-19605.277546767 18812.045352 0.623E-01  2.85387 0.129E+00    0.22   18.74 D
  4-19605.311760859 18786.720206 0.305E-01  0.60997 0.624E-01    0.27   20.55 D
  5-19605.340186636 18783.470620 0.469E-02  0.23073 0.140E-02    0.32   22.31 D
  6-19605.343853126 18785.280144 0.869E-02  0.34567 0.222E-02    0.37   24.01 D
  7-19605.345960694 18786.258131 0.334E-02  0.06093 0.447E-03    0.42   25.62 D
 Attention: NO CONVERGENCE
 No convergence in    7 steps, Energy=   -19605.345960694 Eh
    Brillouin= 0.33431E-02
 Expectation value of S**2 and multiplicity= 20.1292711  9.0286812
 natural occupation numbers between 0.005 and 1.995
  176    1.994873
  177    1.994871
  178    1.983633
  179    1.000000
  180    1.000000
  181    1.000000
  182    1.000000
  183    1.000000
  184    1.000000
  185    1.000000
  186    1.000000
  187    0.016367
  188    0.005129
  189    0.005127
```

Table C.4 (cont'd)

```
========================= SCF RESULTS ==========================

  Total Energy =   -19605.345960694 Eh
  nuclear ener.=    11139.580720653
  one-el.ener. =   -49531.184812273
  two-el.ener. =    18786.258130925
  kinetic ener.=    19566.010754213
  virial coeff.=          1.002010

  dipole/au=     0.000000   0.000000   0.000000  total=   0.000000 au
  dipole/D =     0.000000   0.000000   0.000000  total=   0.000000 D
  quadrupole/    XX=  -169.6084 YY=  -169.6093 ZZ=  -169.4103
  (Debye*Ang)    XY=     0.0000 XZ=     0.0000 YZ=    -0.0004
---------------------------------------------------------------


Total Energy in different units:

  -85474.371777aJ   -51473835.119kJ/mol   -12302541.854kcal/mol
  -533488.83269eV  -6190843190.49K -0.128996979E+19Hz

========================= SCF RESULTS ==========================

 Alpha spin
  orbital symmetries and energies
  occupied orbitals. . . . . .
 Beta spin
  orbital symmetries and energies
  occupied orbitals. . . . . .

================================================================
                JOB INFORMATION

 Time for SCF and total time=      0.55      1.14 min

 Master timings in minutes:
 1-el=         0.07  2-el=         0.02  DFT=          0.01
 misc=         0.45  elapsed=     25.74

 Memory status:
 request number=   5 memory marks=  0 last used address=     9205
 high water=  2920095 total available memory=200000001
 SCFMAIN
 **WARNING** Incomplete SCF convergence

================================================================================
Program step = scf  Master CPU time =      0.55 Elapsed time =     13.15
Total CPU time =     48.75        Efficiency =   3.708 on   4 processors
Time lost due to imbalance =      0.44        Reduce =   0.015
================================================================================


Basis set m6-31g-dp from library

  1313 gaussians  351 shells  468 contr. gaussians  104 contr. shells
   6022147131. integrals (less symmetry or neglect)
```

Table C.4 (cont'd)

```
 Basis may be numerically unstable - integral stability switched on

** GENERATION OF INTERNAL COORDINATES **

 OPTIMIZATION WILL USE DELOCALIZED INTERNAL COORDINATES

 Optimize memory status:
 memory needed= 30238028 high water= 30251796 total available memory=200000001

================================================================================
Program step = opti Master CPU time =      0.23 Elapsed time =      0.23
================================================================================

 SCF Guess from Previous Calculation
 DFT exchange-correlation potential=b3lyp
 Lowest eigenvalue of the overlap matrix  0.162729E-04
 Integral thresholds are: Final=  0.1000E-09 Initial=  0.1627E-07
 SCF parameters:
 wave function type            =  uhf
 charge                    = 0.00
 number of electrons           =  364
 number of alpha electrons     =  186
 number of beta electrons      =  178
 print level                   =    0
 threshold for linear dependency = 0.100E-04
 SCF threshold                 = 0.100E-03
 diis switch-on                =   2.00000
 initial level shift           =   1.000
 minimum level shift           =   0.300
 Elapsed time before SCF (min)  =     26.02
                                                                      timing/min
SCFiter    etot          e2     Brillouin Delta-dens  Errsq     cpu   elapsed
  1-19605.346139395 18783.830607 0.104E-01  6.90503 0.220E-02    0.11   28.22 D
  2-19605.345995224 18786.855032 0.176E-01  0.26304 0.512E-02    0.16   29.86 D
  3-19605.349213971 18785.852019 0.299E-02  0.24165 0.340E-03    0.21   31.47 D
  4-19605.350884866 18784.538585 0.126E-02  0.02388 0.223E-03    0.26   33.05 D
  5-19605.353252431 18784.543071 0.907E-03  0.04811 0.129E-03    0.31   34.67 D
 Switching to Full Fock Evaluation  Integral Threshold:   0.1000E-09
  6-19605.358499121 18784.037074 0.164E-01  6.83908 0.138E-01    0.36   37.96 D
  7-19605.359078588 18784.060990 0.705E-02  0.31534 0.185E-02    0.41   40.91 D
  8-19605.355299971 18782.738625 0.182E-01  0.18414 0.127E-01    0.45   43.80 D
  9-19605.361183902 18783.977427 0.192E-02  0.12162 0.181E-03    0.50   46.65 D
 10-19605.361396832 18783.784876 0.952E-03  0.01155 0.895E-04    0.55   49.26 D
 11-19605.361646899 18783.726143 0.966E-03  0.00383 0.936E-04    0.61   51.85 D
 12-19605.360490991 18783.612990 0.947E-03  0.02492 0.105E-03    0.66   54.60 D
 13-19605.360304965 18783.666970 0.942E-03  0.01916 0.807E-04    0.71   57.36 D
 14-19605.363493457 18783.052122 0.537E-03  0.15061 0.381E-04    0.76   60.29 D
 Switching to Full Fock Evaluation  Integral Threshold:   0.1000E-09
 15-19605.365422935 18782.036797 0.893E-03  6.44309 0.438E-04    0.81   63.57 D
 16-19605.365725307 18781.844940 0.491E-03  0.02544 0.222E-04    0.86   66.36 D
 17-19605.365887266 18781.720980 0.375E-03  0.01436 0.119E-04    0.92   69.11 D
 18-19605.366140583 18781.447597 0.406E-03  0.03572 0.703E-05    0.97   71.91 D
 19-19605.366242981 18781.339232 0.287E-03  0.00728 0.387E-05    1.02   74.65 D
 20-19605.366276578 18781.299196 0.673E-04  0.00590 0.652E-06    1.08   77.33 D
 Switching to Full Fock Evaluation  Integral Threshold:   0.1000E-09
 21-19605.366281797 18781.281984 0.139E-03  6.35925 0.150E-05    1.13   80.60 D
 22-19605.366283478 18781.288653 0.150E-03  0.00152 0.221E-05    1.18   83.14 D
 23-19605.366304208 18781.261545 0.137E-03  0.00884 0.120E-05    1.24   85.78 D
 24-19605.366303885 18781.261766 0.141E-03  0.00005 0.124E-05    1.29   87.95 D
 25-19605.366299025 18781.258709 0.105E-03  0.00193 0.809E-06    1.35   90.41 D
```

Table C.4 (cont'd)

```
26-19605.366292387 18781.254196 0.715E-04  0.00169 0.421E-06    1.40   92.96 D

 Expectation value of S**2 and multiplicity= 20.3477019  9.0769382
 natural occupation numbers between 0.005 and 1.995
  169    1.995000
  170    1.992586
  171    1.992583
  172    1.992570
  173    1.992565
  174    1.992369

  175    1.979551
  176    1.979539
  177    1.979486
  178    1.957439
  179    1.000000
  180    1.000000
  181    1.000000
  182    1.000000
  183    1.000000
  184    1.000000
  185    1.000000
  186    1.000000
  187    0.042561
  188    0.020514
  189    0.020461
  190    0.020449
  191    0.007631
  192    0.007435
  193    0.007430
  194    0.007417
  195    0.007414
  196    0.005000

========== SCF RESULTS ==========

   Total Energy =   -19605.366292387 Eh
   nuclear ener.=    11139.580720653
   one-el.ener. =   -49526.201208887
   two-el.ener. =    18781.254195846
   kinetic ener.=    19566.177254224
   virial coeff.=          1.002003

   dipole/au=     0.000000   0.000000   0.000000  total=   0.000000 au
   dipole/D =     0.000000   0.000000   0.000000  total=   0.000000 D
   quadrupole/    XX=  -172.1657 YY=  -172.1567 ZZ=  -171.3963
   (Debye*Ang)    XY=     0.0000 XZ=     0.0000 YZ=     0.0009
------------------------------------------------------------------
    Total Energy in different units :

   -85474.460418aJ   -51473888.500kJ/mol   -12302554.613kcal/mol
   -533489.38595eV  -6190849610.70K -0.128997113E+19Hz



========== SCF RESULTS ==========
```

Table C.4 (cont'd)

```
 Alpha spin
  orbital symmetries and energies
  occupied orbitals. . . . . .


 Beta spin
  orbital symmetries and energies
  occupied orbitals. . . . . .


============================================================
                JOB INFORMATION

 Time for SCF and total time=      1.52      2.91 min

 Master timings in minutes:
 1-el=         0.05  2-el=         0.06  DFT=          0.05
 misc=         1.35  elapsed=     93.08

 Memory status:
 request number=   6 memory marks=  0 last used address=    13768
 high water= 30251796 total available memory=200000001

============================================================================
Program step = scf  Master CPU time =      1.52 Elapsed time =     67.09
Total CPU time =    248.17        Efficiency =   3.699 on   4 processors
Time lost due to imbalance =       2.79        Reduce =   0.057
============================================================================


============================================================================
             The Analytical Forces Module

                    UHF/DFT

Master CPU time for 1e part of gradient =     0.12 Elapsed =      0.12 min
   L-shells have been segmented for forces

Master CPU time for 2e part of gradient =     0.00 Elapsed =      7.30 min
Master CPU time for XC part of gradient =     0.01 Elapsed =      5.24 min

 Number of electrons over grid:     363.999975
Atom  Name       force-x    force-y    force-z

 1     ni     0.0227690 -0.0074070 -0.0123694
 2     ni     0.0141099 -0.0193825  0.0123738
 3     ni     0.0000000  0.0000000  0.0000000
 4     ni    -0.0227690 -0.0074070 -0.0123694
 5     ni    -0.0141099  0.0193825 -0.0123738
 6     ni    -0.0141099 -0.0193825  0.0123738
 7     ni    -0.0227690  0.0074070  0.0123694
 8     ni     0.0000000 -0.0000337  0.0253091
 9     ni     0.0000000  0.0000337 -0.0253091
```

Table C.4 (cont'd)

```
 10     ni     0.0000000 -0.0240104 -0.0123587
 11     ni     0.0141099  0.0193825 -0.0123738
 12     ni     0.0227690  0.0074070  0.0123694
 13     ni     0.0000000  0.0240104  0.0123587
Sum or total torque of the forces does not vanish
Sum= 0.0000000 0.0000000 0.0000000 Torque=-0.0000737 0.0000000 0.0000000

 Maximum Cartesian force component=   0.0253091 Eh/a0 on atom    8
--------------------------------------------------------------------------------
 Memory status:       end of forces
 request number=   6 memory marks=  0 last used address=    13768
 high water= 30251796 total available memory=200000001
--------------------------------------------------------------------------------

================================================================================
Program step = forc Master CPU time =      0.23 Elapsed time =     12.76
Total CPU time =     46.96        Efficiency =   3.679 on   4 processors
Time lost due to imbalance =      0.70        Reduce =   0.005
================================================================================


** GEOMETRY OPTIMIZATION IN DELOCALIZED INTERNAL COORDINATES **
  Searching for a Minimum

  Optimization Cycle:   1

                  Coordinates (Angstroms)
   ATOM          X          Y          Z
  1  ni       1.935231  -0.628795  -1.017411
  2  ni       1.196038  -1.646205   1.017411
  3  ni       0.000000   0.000000   0.000000
  4  ni      -1.935231  -0.628795  -1.017411
  5  ni      -1.196038   1.646205  -1.017411
  6  ni      -1.196038  -1.646205   1.017411
  7  ni      -1.935231   0.628795   1.017411
  8  ni       0.000000   0.000000   2.293000
  9  ni       0.000000   0.000000  -2.293000
 10  ni       0.000000  -2.034822  -1.017411
 11  ni       1.196038   1.646205  -1.017411
 12  ni       1.935231   0.628795   1.017411
 13  ni       0.000000   2.034822   1.017411
  Point Group: D5d   Number of degrees of freedom:   3


  Energy is -19605.366292387

 gradient converged in  1 cycles

 3 Hessian modes will be used to form the next step
 Hessian Eigenvalues:
   0.064822    0.077627    0.126889

 Minimum Search - Taking Simple RFO Step
 Searching for Lambda that Minimizes Along All modes
 Value Taken    Lambda =  -0.01591150
```

Table C.4 (cont'd)

```
Calculated Step too Large.  Step scaled by  0.898728
Step Taken.  Stepsize is  0.300000

                    Maximum     Tolerance    Cnvgd?
      Gradient          0.047661      0.001000      NO
      Displacement      0.299951      0.010000      NO
      Energy change     *********     0.000001      NO


New Cartesian Coordinates Obtained by Inverse Iteration

 ***ERROR*** Exceeded allowed number of iterative cycles in GetCART
**WARNING** Problems with Internal Coordinates
 Switching to Cartesian Coordinates

Translations and Rotations Projected Out of Hessian

33 Hessian modes will be used to form the next step
 Hessian Eigenvalues:
   1.000000   1.000000   1.000000   1.000000   1.000000   1.000000
   1.000000   1.000000   1.000000   1.000000   1.000000   1.000000
   1.000000   1.000000   1.000000   1.000000   1.000000   1.000000
   1.000000   1.000000   1.000000   1.000000   1.000000   1.000000
   1.000000   1.000000   1.000000   1.000000   1.000000   1.000000
   1.000000   1.000000   1.000000

Minimum Search - Taking Simple RFO Step
Searching for Lambda that Minimizes Along All modes
Value Taken    Lambda =  -0.00848429
Step Taken.  Stepsize is  0.091722

                    Maximum     Tolerance    Cnvgd?
      Gradient          0.025309      0.001000      NO
      Displacement      0.025096      0.010000      NO
      Energy change     *********     0.000001      NO


Optimize memory status:
memory needed= 30238028 high water= 30251796 total available memory=200000001
SCF Guess from Previous Calculation
DFT exchange-correlation potential=b3lyp
Lowest eigenvalue of the overlap matrix  0.167616E-04
Integral thresholds are: Final=  0.1000E-09 Initial=  0.1676E-07
SCF parameters:
wave function type            =  uhf
charge                      = 0.00
number of electrons           =  364
number of alpha electrons     =  186
number of beta electrons      =  178
print level                 =    0
threshold for linear dependency = 0.100E-04
SCF threshold               = 0.100E-03
diis switch-on              =   2.00000
initial level shift         =   1.000
minimum level shift         =   0.300
Elapsed time before SCF (min)   =    105.90
```

Table C.4 (cont'd)

						timing/min	
SCFiter	etot	e2	Brillouin	Delta-dens	Errsq	cpu	elapsed
1-	-19605.372890437	18711.855497	0.271E-01	6.32730	0.503E-01	0.11	108.01 D
2-	-19605.373741209	18714.250866	0.164E-02	0.27096	0.306E-03	0.16	109.69 D
3-	-19605.373785575	18711.895926	0.339E-02	0.08712	0.811E-03	0.21	111.28 D
4-	-19605.374110243	18713.347767	0.306E-02	0.05583	0.166E-03	0.26	112.81 D
5-	-19605.374295224	18713.956814	0.786E-03	0.03567	0.291E-04	0.31	114.22 D
Switching to Full Fock Evaluation Integral Threshold: 0.1000E-09							
6-	-19605.373747478	18713.501008	0.158E-01	6.31426	0.128E-01	0.36	117.40 D
7-	-19605.373941542	18713.539432	0.128E-03	0.31010	0.264E-05	0.41	120.23 D
8-	-19605.373955337	18713.484004	0.341E-03	0.02633	0.686E-05	0.46	122.85 D
9-	-19605.373961990	18713.479779	0.856E-04	0.00679	0.128E-05	0.51	125.32 D
Switching to Full Fock Evaluation Integral Threshold: 0.1000E-09							
10-	-19605.373979372	18713.526975	0.360E-03	6.33473	0.528E-05	0.56	128.50 D
11-	-19605.373968565	18713.462380	0.135E-03	0.00463	0.159E-05	0.61	131.00 D
12-	-19605.374002027	18713.455360	0.833E-04	0.01378	0.813E-06	0.66	133.57 D

Expectation value of S**2 and multiplicity= 20.3576866 9.0791380
natural occupation numbers between 0.005 and 1.995

168	1.994926
169	1.994918
170	1.992440
171	1.992431
172	1.992427
173	1.992422
174	1.992186
175	1.979067
176	1.978802
177	1.978779
178	1.955332
179	1.000000
180	1.000000
181	1.000000
182	1.000000
183	1.000000
184	1.000000
185	1.000000
186	1.000000
187	0.044668
188	0.021221
189	0.021198
190	0.020933
191	0.007814
192	0.007578
193	0.007573
194	0.007569
195	0.007560
196	0.005082
197	0.005074

========== SCF RESULTS ==========

Total Energy = -19605.374002027 Eh
nuclear ener.= 11071.503552883
one-el.ener. = -49390.332914487
two-el.ener. = 18713.455359576
kinetic ener.= 19565.975766261
virial coeff.= 1.002014

Table C.4 (cont'd)

```
  dipole/au=     0.000000   0.000000   0.000000  total=   0.000000 au
  dipole/D =     0.000000   0.000000   0.000000  total=   0.000000 D
  quadrupole/    XX=  -172.3089 YY=  -172.2773 ZZ=  -171.4520
  (Debye*Ang)    XY=     0.0000 XZ=     0.0000 YZ=     0.0050
---------------------------------------------------------------
   Total Energy in different units :

  -85474.494030aJ   -51473908.741kJ/mol   -12302559.451kcal/mol
  -533489.59574eV  -6190852045.19K -0.128997164E+19Hz

========================= SCF RESULTS ==========================

 Alpha spin
  orbital symmetries and energies
  occupied orbitals. . . . . .
 Beta spin
  orbital symmetries and energies
  occupied orbitals. . . . . .
  ============================================================
               JOB INFORMATION

 Time for SCF and total time=      0.78      3.94 min

 Master timings in minutes:
 1-el=         0.05  2-el=         0.03  DFT=          0.02
 misc=         0.67  elapsed=    133.69

 Memory status:
 request number=   6 memory marks=  0 last used address=    13768
 high water= 30251796 total available memory=200000001

================================================================================
Program step = scf  Master CPU time =      0.78 Elapsed time =     27.83
Total CPU time =    102.67        Efficiency =   3.690 on   4 processors
Time lost due to imbalance =      1.12        Reduce =   0.024
================================================================================
              The Analytical Forces Module

                    UHF/DFT

Master CPU time for 1e part of gradient =    0.12 Elapsed =     0.12 min
   L-shells have been segmented for forces

Master CPU time for 2e part of gradient =    0.00 Elapsed =     7.17 min
Master CPU time for XC part of gradient =    0.01 Elapsed =     5.09 min

 Number of electrons over grid:     363.999975
Atom  Name       force-x    force-y    force-z

  1     ni     0.0182366 -0.0058986 -0.0099732
  2     ni     0.0113087 -0.0155696  0.0099450
  3     ni     0.0000000  0.0000000  0.0000000
  4     ni    -0.0182366 -0.0058986 -0.0099732
  5     ni    -0.0113087  0.0155696 -0.0099450
  6     ni    -0.0113087 -0.0155696  0.0099450
  7     ni    -0.0182366  0.0058986  0.0099732
  8     ni     0.0000000  0.0000034  0.0203165
```

Table C.4 (cont'd)

```
 9    ni    0.0000000 -0.0000034 -0.0203165
10    ni    0.0000000 -0.0193175 -0.0099139
11    ni    0.0113087  0.0155696 -0.0099450
12    ni    0.0182366  0.0058986  0.0099732
13    ni    0.0000000  0.0193175  0.0099139

 Maximum Cartesian force component=   0.0203165 Eh/a0 on atom    8
--------------------------------------------------------------------------------
 Memory status:       end of forces
 request number=   6 memory marks=  0 last used address=    13768
 high water= 30251796 total available memory=200000001
--------------------------------------------------------------------------------

================================================================================
Program step = forc Master CPU time =      0.23 Elapsed time =     12.48
Total CPU time =     46.03        Efficiency =   3.688 on   4 processors
Time lost due to imbalance =      0.67        Reduce =   0.005
================================================================================


 Cartesian Hessian Update
 Hessian Updated using BFGS Update


** GEOMETRY OPTIMIZATION IN CARTESIAN COORDINATES **
  Searching for a Minimum

  Optimization Cycle:   2

                    Coordinates (Angstroms)
   ATOM          X         Y         Z
  1  ni       1.947192  -0.632681  -1.023901
  2  ni       1.203431  -1.656381   1.023901
  3  ni       0.000000   0.000000   0.000000
  4  ni      -1.947192  -0.632681  -1.023901
  5  ni      -1.203431   1.656381  -1.023901
  6  ni      -1.203431  -1.656381   1.023901
  7  ni      -1.947192   0.632681   1.023901
  8  ni       0.000000   0.000000   2.306280
  9  ni       0.000000   0.000000  -2.306280
 10  ni       0.000000  -2.047399  -1.023901
 11  ni       1.203431   1.656381  -1.023901
 12  ni       1.947192   0.632681   1.023901
 13  ni       0.000000   2.047399   1.023901
  Point Group: D5d   Number of degrees of freedom:   3


  Energy is -19605.374002027


 Translations and Rotations Projected Out of Hessian

 2 Hessian modes will be used to form the next step
 Hessian Eigenvalues:
   0.199012    1.000005
```

Table C.4 (cont'd)

```
Minimum Search - Taking Simple RFO Step
Searching for Lambda that Minimizes Along All modes
Value Taken    Lambda =  -0.02464695
Calculated Step too Large.  Step scaled by  0.903718
Step Taken.  Stepsize is  0.300000

                    Maximum     Tolerance    Cnvgd?
      Gradient        0.020316    0.001000     NO
      Displacement    0.082091    0.010000     NO
      Energy change  -0.007710    0.000001     NO


Optimize memory status:
memory needed= 30238028 high water= 30251796 total available memory=200000001
SCF Guess from Previous Calculation
DFT exchange-correlation potential=b3lyp
Lowest eigenvalue of the overlap matrix  0.184692E-04
Integral thresholds are: Final=  0.1000E-09 Initial=  0.1847E-07
SCF parameters:
wave function type            =  uhf
charge                     = 0.00
number of electrons           =  364
number of alpha electrons     =  186
number of beta electrons      =  178
print level                =    0
threshold for linear dependency = 0.100E-04
SCF threshold                 = 0.100E-03
diis switch-on                =   2.00000
initial level shift           =   1.000
minimum level shift           =   0.300
Elapsed time before SCF (min)   =    146.21
                                                                        timing/min
SCFiter    etot          e2     Brillouin Delta-dens Errsq     cpu   elapsed
 1-19605.378123483 18492.250050 0.875E-01 6.23824 0.402E+00    0.10  148.21 D
 2-19605.385440976 18499.795377 0.526E-02 0.32331 0.314E-02    0.14  149.84 D
 3-19605.384068124 18492.616068 0.129E-01 0.27677 0.896E-02    0.18  151.42 D
 4-19605.387314285 18496.772379 0.105E-01 0.19633 0.189E-02    0.21  152.96 D
 5-19605.388251549 18498.948659 0.231E-02 0.09943 0.291E-03    0.25  154.37 D
 6-19605.388991759 18497.462243 0.559E-03 0.08183 0.287E-04    0.29  155.83 D
Switching to Full Fock Evaluation  Integral Threshold:   0.1000E-09
 7-19605.388342350 18497.643483 0.169E-01 6.17448 0.148E-01    0.32  158.87 D
 8-19605.388699322 18497.339389 0.169E-02 0.29810 0.681E-04    0.36  161.58 D
 9-19605.388581924 18498.026836 0.655E-02 0.03480 0.744E-03    0.40  164.15 D
10-19605.388915991 18497.466218 0.263E-03 0.04556 0.916E-05    0.43  166.62 D
11-19605.389077888 18497.414525 0.359E-03 0.00980 0.136E-04    0.47  169.08 D
12-19605.389257830 18497.329195 0.259E-03 0.01353 0.737E-05    0.51  171.56 D
13-19605.389455535 18497.271856 0.268E-03 0.01337 0.718E-05    0.54  174.02 D
14-19605.389423023 18497.269816 0.257E-03 0.00142 0.720E-05    0.58  176.34 D
15-19605.389411602 18497.400423 0.252E-03 0.01098 0.786E-05    0.62  178.78 D
Switching to Full Fock Evaluation  Integral Threshold:   0.1000E-09
16-19605.389598787 18497.039178 0.170E-03 6.13155 0.501E-05    0.66  181.81 D
17-19605.389736833 18496.885439 0.296E-03 0.01507 0.106E-04    0.70  184.34 D
18-19605.389851716 18496.802593 0.135E-03 0.01654 0.209E-05    0.74  186.87 D
19-19605.389912792 18496.753521 0.123E-03 0.01060 0.123E-05    0.78  189.35 D
20-19605.389917658 18496.751409 0.122E-03 0.00052 0.124E-05    0.82  191.57 D
21-19605.389877985 18496.745124 0.139E-03 0.00218 0.148E-05    0.86  193.97 D
22-19605.389863901 18496.733569 0.157E-03 0.00368 0.165E-05    0.90  196.35 D
23-19605.389860977 18496.714374 0.113E-03 0.00602 0.784E-06    0.94  198.77 D
24-19605.389874157 18496.712063 0.114E-03 0.00068 0.715E-06    0.98  201.09 D
25-19605.389825837 18496.719820 0.994E-04 0.00704 0.664E-06    1.02  203.52 D
```

Table C.4 (cont'd)

```
 Switching to Full Fock Evaluation  Integral Threshold:   0.1000E-09

26-19605.389837270 18496.702086 0.111E-03  6.08642 0.730E-06    1.06  206.54 D
27-19605.389676809 18496.689368 0.512E-04  0.01096 0.414E-06    1.10  209.12 D

 Expectation value of S**2 and multiplicity= 20.4433129  9.0979806
 natural occupation numbers between 0.005 and 1.995
  170    1.991891
  171    1.991843
  172    1.991842
  173    1.991750
  174    1.991747
  175    1.969369
  176    1.969345
  177    1.968876
  178    1.941600
  179    1.000000
  180    1.000000
  181    1.000000
  182    1.000000
  183    1.000000
  184    1.000000
  185    1.000000
  186    1.000000
  187    0.058400
  188    0.031124
  189    0.030655
  190    0.030631
  191    0.008253
  192    0.008250
  193    0.008158
  194    0.008157
  195    0.008109

========================= SCF RESULTS ==========================

   Total Energy =   -19605.389676809 Eh
   nuclear ener.=    10854.540789904
   one-el.ener. =   -48956.619834904
   two-el.ener. =    18496.689368192
   kinetic ener.=    19565.577542063
   virial coeff.=          1.002035

   dipole/au=     0.000000   0.000000   0.000000  total=   0.000000 au
   dipole/D =     0.000000   0.000000   0.000000  total=   0.000000 D
   quadrupole/    XX=  -173.2042 YY=  -173.2039 ZZ=  -172.4520
   (Debye*Ang)    XY=     0.0000 XZ=     0.0000 YZ=     0.0090
-------------------------------------------------------------
    Total Energy in different units :

   -85474.562368aJ   -51473949.895kJ/mol   -12302569.287kcal/mol
   -533490.02227eV  -6190856994.87K -0.128997267E+19Hz
========================= SCF RESULTS ==========================

  Alpha spin
   orbital symmetries and energies
   occupied orbitals. . . . . .
```

Table C.4 (cont'd)

```
 Beta spin
  orbital symmetries and energies
  occupied orbitals. . . . . .
================================================================
                JOB INFORMATION

 Time for SCF and total time=      1.21      5.38 min

 Master timings in minutes:
 1-el=         0.05  2-el=         0.07  DFT=          0.05
 misc=         1.03  elapsed=    209.23

 Memory status:
 request number=   6 memory marks=  0 last used address=    13768
 high water= 30251796 total available memory=200000001

================================================================================
Program step = scf  Master CPU time =      1.21 Elapsed time =     63.05
Total CPU time =    233.82        Efficiency =   3.709 on   4 processors
Time lost due to imbalance =      3.05        Reduce =   0.052
================================================================================

================================================================================
              The Analytical Forces Module

                     UHF/DFT

Master CPU time for 1e part of gradient =    0.12 Elapsed =     0.12 min
   L-shells have been segmented for forces


Master CPU time for 2e part of gradient =    0.00 Elapsed =     6.85 min
Master CPU time for XC part of gradient =    0.01 Elapsed =     5.03 min

 Number of electrons over grid:     363.999978
Atom  Name       force-x    force-y    force-z
  1     ni     0.0073329 -0.0024107 -0.0041069
  2     ni     0.0045580 -0.0062249  0.0040847
  3     ni     0.0000000  0.0000000  0.0000000
  4     ni    -0.0073329 -0.0024107 -0.0041069
  5     ni    -0.0045580  0.0062249 -0.0040847
  6     ni    -0.0045580 -0.0062249  0.0040847
  7     ni    -0.0073329  0.0024107  0.0041069
  8     ni     0.0000000  0.0000010  0.0078769
  9     ni     0.0000000 -0.0000010 -0.0078769
 10     ni     0.0000000 -0.0077492 -0.0041482
 11     ni     0.0045580  0.0062249 -0.0040847
 12     ni     0.0073329  0.0024107  0.0041069
 13     ni     0.0000000  0.0077492  0.0041482
Sum or total torque of the forces does not vanish
Sum= 0.0000000 0.0000000 0.0000000 Torque= 0.0001232 0.0000000 0.0000000
Maximum Cartesian force component=   0.0078769 Eh/a0 on atom    8
--------------------------------------------------------------------------------
 Memory status:       end of forces
 request number=   6 memory marks=  0 last used address=    13768
 high water= 30251796 total available memory=200000001
--------------------------------------------------------------------------------
```

Table C.4 (cont'd)

```
================================================================================
Program step = forc Master CPU time =      0.22 Elapsed time =     12.09
Total CPU time =     44.57       Efficiency =   3.687 on   4 processors
Time lost due to imbalance =      0.68       Reduce =   0.005
================================================================================


 Cartesian Hessian Update
 Hessian Updated using BFGS Update


** GEOMETRY OPTIMIZATION IN CARTESIAN COORDINATES **
   Searching for a Minimum

   Optimization Cycle:   3

                  Coordinates (Angstroms)
    ATOM          X          Y          Z
   1  ni       1.986292  -0.645385  -1.045177
   2  ni       1.227596  -1.689641   1.045177
   3  ni       0.000000   0.000000   0.000000
   4  ni      -1.986292  -0.645385  -1.045177
   5  ni      -1.227596   1.689641  -1.045177
   6  ni      -1.227596  -1.689641   1.045177
   7  ni      -1.986292   0.645385   1.045177
   8  ni       0.000000   0.000000   2.349721
   9  ni       0.000000   0.000000  -2.349721
  10  ni       0.000000  -2.088511  -1.045177
  11  ni       1.227596   1.689641  -1.045177
  12  ni       1.986292   0.645385   1.045177
  13  ni       0.000000   2.088511   1.045177
   Point Group: D5d   Number of degrees of freedom:   3


   Energy is -19605.389676809


 Translations and Rotations Projected Out of Hessian

  3 Hessian modes will be used to form the next step
  Hessian Eigenvalues:
    0.148100    1.000003    1.000026

 Minimum Search - Taking Simple RFO Step
 Searching for Lambda that Minimizes Along All modes
 Value Taken    Lambda =  -0.00577758
 Step Taken.  Stepsize is  0.193766

                     Maximum     Tolerance    Cnvgd?
       Gradient        0.007877      0.001000      NO
       Displacement    0.052560      0.010000      NO
       Energy change  -0.015675      0.000001      NO

 Optimize memory status:
 memory needed= 30238028 high water= 30251796 total available memory=200000001
 SCF Guess from Previous Calculation
 DFT exchange-correlation potential=b3lyp
```

Table C.4 (cont'd)

```
Lowest eigenvalue of the overlap matrix  0.196835E-04
Integral thresholds are: Final=  0.1000E-09 Initial=  0.1000E-09
SCF parameters:
wave function type            =  uhf
charge                     = 0.00
number of electrons           =  364
number of alpha electrons     =  186
number of beta electrons      =  178
print level                =    0
threshold for linear dependency = 0.100E-04
SCF threshold                 = 0.100E-03
diis switch-on                =   2.00000
initial level shift           =   1.000
minimum level shift           =   0.300
Elapsed time before SCF (min)  =    221.36
                                                                                    timing/min
SCFiter    etot          e2     Brillouin  Delta-dens  Errsq     cpu   elapsed
 1-19605.388784933 18358.511773 0.564E-01  6.01545 0.145E+00    0.10  224.42 D
 2-19605.391490195 18362.961830 0.326E-02  0.16897 0.120E-02    0.13  227.04 D
 3-19605.390787052 18358.968679 0.941E-02  0.18071 0.364E-02    0.16  229.64 D
 4-19605.392109629 18361.066996 0.685E-02  0.13152 0.777E-03    0.20  232.20 D
 5-19605.392461916 18362.601171 0.130E-02  0.06266 0.115E-03    0.23  234.64 D
 6-19605.392629327 18361.687923 0.364E-03  0.05064 0.899E-05    0.26  237.11 D
 7-19605.392696508 18361.793866 0.240E-03  0.00629 0.583E-05    0.30  239.49 D
 8-19605.392770596 18361.685025 0.174E-03  0.00465 0.350E-05    0.33  241.87 D
 9-19605.392802323 18361.659793 0.208E-03  0.00572 0.314E-05    0.37  244.18 D
Switching to Full Fock Evaluation  Integral Threshold:   0.1000E-09
10-19605.392886928 18361.605857 0.102E-03  5.97847 0.164E-05    0.40  247.13 D
11-19605.392971569 18361.506981 0.101E-03  0.01693 0.150E-05    0.44  249.55 D
12-19605.392964527 18361.508206 0.969E-04  0.00074 0.149E-05    0.47  251.73 D
Switching to Full Fock Evaluation  Integral Threshold:   0.1000E-09
13-19605.392987515 18361.535526 0.227E-03  5.96366 0.280E-05    0.50  254.67 D
14-19605.392963041 18361.508426 0.918E-04  0.00306 0.134E-05    0.54  256.98 D

Expectation value of S**2 and multiplicity= 20.4840553  9.1069326
natural occupation numbers between 0.005 and 1.995
 170    1.991453
 171    1.991451
 172    1.991349
 173    1.991275
 174    1.991256
 175    1.965285
 176    1.965110
 177    1.964946
 178    1.934784
 179    1.000000
 180    1.000000
 181    1.000000
 182    1.000000
 183    1.000000
 184    1.000000
 185    1.000000
 186    1.000000
 187    0.065216
 188    0.035054
 189    0.034890
 190    0.034715
 191    0.008744
 192    0.008725
```

Table C.4 (cont'd)

```
 193    0.008651
 194    0.008549
 195    0.008547

========================= SCF RESULTS ==========================

  Total Energy =   -19605.392963041 Eh
  nuclear ener.=    10718.888097161
  one-el.ener. =   -48685.789486374
  two-el.ener. =    18361.508426172
  kinetic ener.=    19565.332914168
  virial coeff.=          1.002048

  dipole/au=     0.000000   0.000000   0.000000  total=   0.000000 au
  dipole/D =     0.000000   0.000000   0.000000  total=   0.000000 D
  quadrupole/    XX=  -173.5450 YY=  -173.5555 ZZ=  -172.8513
  (Debye*Ang)    XY=     0.0000 XZ=     0.0000 YZ=     0.0687
---------------------------------------------------------------
   Total Energy in different units :

  -85474.576695aJ   -51473958.523kJ/mol   -12302571.349kcal/mol
  -533490.11169eV  -6190858032.57K -0.128997289E+19Hz

================================================================
                JOB INFORMATION

 Time for SCF and total time=      0.64      6.26 min

 Master timings in minutes:

 1-el=         0.05  2-el=         0.04  DFT=          0.03
 misc=         0.52  elapsed=    257.08

 Memory status:
 request number=   6 memory marks=  0 last used address=    13768
 high water= 30251796 total available memory=200000001

================================================================================
Program step = scf  Master CPU time =      0.64 Elapsed time =     35.75
Total CPU time =    132.59        Efficiency =   3.709 on   4 processors
Time lost due to imbalance =       1.74        Reduce =   0.030
================================================================================

================================================================================
              The Analytical Forces Module

                    UHF/DFT

Master CPU time for 1e part of gradient =    0.12 Elapsed =     0.12 min
   L-shells have been segmented for forces

Master CPU time for 2e part of gradient =    0.00 Elapsed =     6.68 min
Master CPU time for XC part of gradient =    0.01 Elapsed =     5.01 min

 Number of electrons over grid:     363.999979
Atom  Name       force-x    force-y    force-z
```

Table C.4 (cont'd)

```
 1    ni     0.0008548 -0.0003450 -0.0005452
 2    ni     0.0004210 -0.0005965  0.0004828
 3    ni     0.0000000  0.0000000  0.0000000
 4    ni    -0.0008548 -0.0003450 -0.0005452
 5    ni    -0.0004210  0.0005965 -0.0004828
 6    ni    -0.0004210 -0.0005965  0.0004828
 7    ni    -0.0008548  0.0003450  0.0005452
 8    ni     0.0000000  0.0000634  0.0002822
 9    ni     0.0000000 -0.0000634 -0.0002822
10    ni     0.0000000 -0.0009921 -0.0007560
11    ni     0.0004210  0.0005965 -0.0004828
12    ni     0.0008548  0.0003450  0.0005452
13    ni     0.0000000  0.0009921  0.0007560

 Maximum Cartesian force component=   0.0009921 Eh/a0 on atom   13
--------------------------------------------------------------------------------
 Memory status:       end of forces
 request number=   6 memory marks=  0 last used address=    13768
 high water= 30251796 total available memory=200000001
--------------------------------------------------------------------------------

================================================================================
Program step = forc Master CPU time =      0.22 Elapsed time =     11.89
Total CPU time =     43.48        Efficiency =   3.656 on   4 processors
Time lost due to imbalance =      0.69        Reduce =   0.005
================================================================================


 Cartesian Hessian Update
 Hessian Updated using BFGS Update

** GEOMETRY OPTIMIZATION IN CARTESIAN COORDINATES **
   Searching for a Minimum

   Optimization Cycle:   4

                    Coordinates (Angstroms)
    ATOM          X         Y         Z
   1  ni        2.011548  -0.653591  -1.059014
   2  ni        1.243205  -1.711125   1.059014
   3  ni        0.000000   0.000000   0.000000
   4  ni       -2.011548  -0.653591  -1.059014
   5  ni       -1.243205   1.711125  -1.059014
   6  ni       -1.243205  -1.711125   1.059014
   7  ni       -2.011548   0.653591   1.059014
   8  ni        0.000000   0.000000   2.377535
   9  ni        0.000000   0.000000  -2.377535
  10  ni        0.000000  -2.115066  -1.059014
  11  ni        1.243205   1.711125  -1.059014
  12  ni        2.011548   0.653591   1.059014
  13  ni        0.000000   2.115066   1.059014
   Point Group: D5d   Number of degrees of freedom:   3

   Energy is -19605.392963041

 Translations and Rotations Projected Out of Hessian
```

Table C.4 (cont'd)

```
 3 Hessian modes will be used to form the next step
 Hessian Eigenvalues:
   0.137695    1.000003    1.000062

Minimum Search - Taking Simple RFO Step
Searching for Lambda that Minimizes Along All modes
Value Taken    Lambda =  -0.00007231
Step Taken.  Stepsize is  0.022795

                    Maximum     Tolerance    Cnvgd?
      Gradient          0.000858      0.001000     YES
      Displacement      0.005950      0.010000     YES
      Energy change    -0.003286      0.000001      NO


 Optimize memory status:
 memory needed= 30238028 high water= 30251796 total available memory=200000001
 unidentified card= linu
================================================================================
Memory status:
request number=   6 memory marks=  0
high water= 30251796 total available memory=200000001
Total master CPU time =      6.48 Elapsed =    268.98 min
      Total CPU time =    993.93 Efficiency =   3.695 on   4 processors
Termination on Mon Jul 11 10:56:14 2005
================================================================================
```